

**This dissertation has been  
microfilmed exactly as received**

**66-11,786**

**BREIG, Edward Louis, 1932-**

**A STUDY OF VIBRATIONAL EXCITATION OF  
MOLECULES AND TRANSITIONS BETWEEN THE  
SPIN-MULTIPLETS OF ATOMIC OXYGEN IN-  
DUCED BY ELECTRON COLLISION.**

**The University of Oklahoma, Ph.D., 1966  
Physics, general**

**University Microfilms, Inc., Ann Arbor, Michigan**

THE UNIVERSITY OF OKLAHOMA  
GRADUATE COLLEGE

A STUDY OF VIBRATIONAL EXCITATION OF MOLECULES AND TRANSITIONS  
BETWEEN THE SPIN-MULTIPLETS OF ATOMIC OXYGEN  
INDUCED BY ELECTRON COLLISION

A DISSERTATION  
SUBMITTED TO THE GRADUATE FACULTY  
in partial fulfillment of the requirements for the  
degree of  
DOCTOR OF PHILOSOPHY

BY  
EDWARD LOUIS BREIG  
Norman, Oklahoma  
1966

A STUDY OF VIBRATIONAL EXCITATION OF MOLECULES AND TRANSITIONS  
BETWEEN THE SPIN-MULTIPLETS OF ATOMIC OXYGEN  
INDUCED BY ELECTRON COLLISION

APPROVED BY

*W. C. Fowler*  
*W. Fowler*  
*Ch. L. Critchfield*  
*J. M. Canfield*  
*E. E. Snider*

DISSERTATION COMMITTEE

## ACKNOWLEDGMENTS

The author wishes to express his appreciation to his research director, Professor Chun C. Lin, for the expert technical assistance rendered, and to Dr. K. Takayanagi, U. of Tokyo, Tokyo, Japan, for his continued interest in this work.

Sincere thanks must also be extended to Barbra Lafon for her assistance with the numerical analysis and the computer programs, and to Dave Ashbaucher of the O. U. Computing Laboratory for his help with the computing phases of the problem. The author is especially indebted to Dr. J. B. Harvill, Miss P. Stauffer and Marshall Turser of the S. M. U. Computing Laboratory for the use of their computing facilities and the many special favors granted. The efforts of Betty Bellis in typing the manuscript are also highly appreciated.

Finally, acknowledgment must be made of the personal financial assistance afforded by the generous Science-Engineering Fellowship grants received from Mr. F. G. Rizzardi and North American Aviation, Inc.

# TABLE OF CONTENTS

	Page
LIST OF TABLES. . . . .	vi
LIST OF ILLUSTRATIONS . . . . .	viii
PART I. VIBRATIONAL EXCITATION OF DIATOMIC MOLECULES BY ELECTRON IMPACT	
Chapter	
I. INTRODUCTION. . . . .	1
II. FORMULATION OF THE COLLISION PROBLEM. . . . .	7
Calculation of $Q^0(0 \rightarrow 1)$ . . . . .	15
Calculation of $Q^1(0 \rightarrow 1)$ . . . . .	21
III. APPLICATION TO HYDROGEN MOLECULE. . . . .	23
Molecular Constants and Selection of Cut-Off Parameter	23
Numerical Results. . . . .	26
Comparison with Experiment . . . . .	30
IV. EXTENSION TO OTHER DIATOMIC MOLECULES . . . . .	34
Application to Nitrogen Molecule . . . . .	34
Application to Polar Molecules - CO. . . . .	35
V. GENERAL DISCUSSION OF RESULTS . . . . .	40
PART II. EXCITATION BY ELECTRON IMPACT OF THE SPIN-MULTIPLETS OF THE GROUND STATE OF THE NEUTRAL OXYGEN ATOM	
VI. INTRODUCTION. . . . .	44
Importance of the Spin-Multiplet Transitions . . . . .	47
VII. PROPERTIES OF THE NEUTRAL OXYGEN ATOM . . . . .	50
Problems Concerning the P-wave . . . . .	52
Difficulties with S-wave . . . . .	59
VIII. BASIC FORMULATION . . . . .	62
IX. FORMULATION IN TERMS OF THE COMPOSITE REPRESENTATION. . .	67

# TABLE OF CONTENTS--Continued

Chapter	Page
X. SPECIAL APPROXIMATIONS AND PROCEDURES. . . . .	78
Radial Potential Functions. . . . .	82
XI. CROSS SECTIONS FOR EXCITATION. . . . .	85
The Scattering and Related Matrices . . . . .	85
Born Approximation. . . . .	89
Distorted Wave Approximation. . . . .	91
XII. COLLISION STRENGTHS FOR S-WAVE . . . . .	94
Effect of Energy Differences. . . . .	106
XIII. COLLISION STRENGTHS FOR D-WAVE . . . . .	109
XIV. COLLISION STRENGTHS FOR P-WAVE, STRONG COUPLING METHODS. .	114
The Basic Transformation. . . . .	119
Application of Basic Transformation to Equations for $J_T = 1/2, 3/2$ . . . . .	125
XV. COLLISION STRENGTHS FOR P-WAVE, SPECIAL REFINEMENTS. . . .	141
Exact Solutions for $J_T = 5/2$ Equations. . . . .	141
Application of the Method of Distorted Waves. . . . .	143
Validity of Approximations. . . . .	151
Allowance for Energy Differences. . . . .	156
XVI. NUMERICAL METHODS. . . . .	163
XVII. POLARIZATION INTERACTION . . . . .	171
XVIII. SUMMARY OF COLLISION STRENGTHS FOR THE SPIN-MULTIPLETS OF OI . . . . .	178
Appendices	
I. Wave Functions for the Atomic Spin-Multiplet States, and for the Free Electron. . . . .	187
II. Atomic Radial Wave Functions for OI. . . . .	192
III. Potential Functions for OI . . . . .	195
IV. Hartree-Fock Differential Equations for Bound-State Functions of OI. . . . .	197
BIBLIOGRAPHY . . . . .	199

# LIST OF TABLES

Table	Page
I. Treatment of Polarization--Bibliography . . . . .	17
II. Molecular Parameters for $H_2$ Molecule. . . . .	23
III. Cut-Off Parameters. . . . .	25
IV. $Q^0(0 \rightarrow 1)$ for $H_2$ ; A Comparison of Selected Models for $V^0$ at 2 eV . . . . .	27
V. Comparison of the Calculated Values of $Q^1(0 \rightarrow 1)$ and $Q^0(0 \rightarrow 1)$ for $H_2$ . . . . .	29
VI. Vibrational Excitation Cross Section for $H_2$ . . . . .	33
VII. Vibrational Excitation Cross Section for $N_2$ . . . . .	36
VIII. Vibrational Excitation Cross Section for CO . . . . .	38
IX. Energies of Interest for Projectile Electron. . . . .	53
X. Composite States for Values of $l \leq 2$ . . . . .	69
XI. Selected Composite State Wave Functions for $M_T = J_T$ . . . .	74
XII. Coefficients in the Potential and Exchange Matrix Elements for S-wave . . . . .	96
XIII. R-matrix Elements for S-wave with the Exact Resonance Approximation . . . . .	101
XIV. Computed Phases for S-wave Functions Under Exact Resonance . . . . .	104
XV. Collision Strengths for S-wave. . . . .	105
XVI. Matrix Element Coefficients for Potential Coupling Terms, D-wave . . . . .	111
XVII. Collision Strengths for D-wave, Born Approximation. . . .	113

# LIST OF TABLES--Continued

Table	Page
XVIII. Coefficients in the Potential and Exchange Matrix Elements for P-wave . . . . .	116
XIX. Coefficients and Coupling Terms for $\Lambda_1(PG_1)$ Parameters. . . . .	132
XX. Elements of R-matrix for States Connected Under the "Basic Transformation". . . . .	136
XXI. Computed Phases for Modified Equations of $J_T = 1/2$ . . . . .	138
XXII. Computed Phases for Modified Equations of $J_T = 3/2$ . . . . .	139
XXIII. Elements of R-matrix for $J_T = 5/2$ . . . . .	144
XXIV. Computed Phases for $J_T = 5/2$ . . . . .	145
XXV. Comparison of Distorted Wave and "Exact" Collision Strengths, $J_T = 5/2$ . . . . .	148
XXVI. Components of Distorted Wave Integrals. . . . .	149
XXVII. Post-Prior Discrepancies Under Distorted Wave Method. . . . .	150
XXVIII. Comparison of Approximate and Exact Methods . . . . .	155
XXIX. Analysis and Summary of Collision Strengths for P-wave Under Exact Resonance . . . . .	157
XXX. Comparison of Different Methods of Allowing for Energy Differences, $J_T = 5/2$ . . . . .	159
XXXI. P-wave Collision Strengths with Allowance for Energy Differences . . . . .	162
XXXII. Comparison of Associated Collision Strengths for OI and OIII. . . . .	181
XXXIII. Final Summary of the Collision Strengths for the Spin- Multiplets of OI. . . . .	183



## LIST OF ILLUSTRATIONS

Figure	Page
1. The Collision of an Electron with a Diatomic Molecule. . .	7
2. Characteristic Profiles for Various Choices of $g(r)$ . . . .	20
3. The Spin-Multiplets of $^3P$ in $(1s)^2 (2s)^2 (2p)^4$ Ground Configuration of OI . . . . .	51
4. Effective Potentials for $\ell = 0, 1, 2$ Incident Partial Waves. . . . .	55
5. Comparison of Bound P Wave Function with Free and Potential Distorted P-waves. . . . .	57
6. Comparison of Bound P Wave Function with P-waves which Display the Effects of Exchange Distortion and Orthogonality. . . . .	58
7. Effect of Different Polarization Cut-Off Parameters upon S-wave Cross Sections. . . . .	175
8. A Comparison of the Ground Configuration Energy Levels of OI and OIII . . . . .	180

## LIST OF ILLUSTRATIONS

Figure	Page
1. The Collision of an Electron with a Diatomic Molecule. . .	7
2. Characteristic Profiles for Various Choices of $g(r)$ . . . .	20
3. The Spin-Multiplets of $^3P$ in $(1s)^2 (2s)^2 (2p)^4$ Ground Configuration of OI . . . . .	51
4. Effective Potentials for $l = 0, 1, 2$ Incident Partial Waves. . . . .	55
5. Comparison of Bound P Wave Function with Free and Potential Distorted P-waves. . . . .	57
6. Comparison of Bound P Wave Function with P-waves which Display the Effects of Exchange Distortion and Orthogonality. . . . .	58
7. Effect of Different Polarization Cut-Off Parameters upon S-wave Cross Sections. . . . .	175
8. A Comparison of the Ground Configuration Energy Levels of OI and OIII . . . . .	180

A STUDY OF VIBRATIONAL EXCITATION OF MOLECULES AND TRANSITIONS  
BETWEEN THE SPIN-MULTIPLETS OF ATOMIC OXYGEN  
INDUCED BY ELECTRON COLLISION

PART I. VIBRATIONAL EXCITATION OF DIATOMIC MOLECULES  
BY ELECTRON IMPACT

CHAPTER I

INTRODUCTION

The excitations of molecular rotation and vibration are important energy loss mechanisms for slow electrons in molecular gas. These excitation processes find special application in gaseous discharges and upper atmosphere physics. The present work is directed toward the particular study of the vibrational excitation of a molecule upon collision with slow electrons.

Until the past decade, very little reliable experimental data was available on the vibrational excitation of molecules by electron impact, even for the very simple cases. Early experimenters relied exclusively on either the diffusion method, or the so-called "swarm" experiments. In the latter procedure, a swarm of electrons with a widely-spaced velocity distribution was allowed to drift through the gas under the influence of a uniform d. c. electric field. Ramien<sup>1</sup> and

Harries<sup>2</sup> applied the diffusion method to  $H_2$  and  $N_2$ , respectively, and were able to deduce from their observations an estimate of the probability for the excitation of one vibrational quantum. Results of the swarm experiments are expressed in terms of a parameter which is to represent the fractional total energy loss per collision for the electrons. This parameter is a "composite" quantity, being a mixture of contributions from many different loss mechanisms, and no detailed information on the vibrational portion can be estimated with any degree of accuracy without a complete knowledge of the remaining cross sections.

Interest in the vibrational excitation of molecules has grown in recent years, encouraged in part by the excellent experimental work of Schulz<sup>3,4,5</sup> with beam techniques. The "trapped-electron" method, and the subsequent development of the electrostatic analyzer, have allowed a determination of considerable detail and structure in the vibrational excitation curves, in addition to providing accurate values for the magnitudes of the cross sections. Schulz has studied, among other molecules,  $H_2$ ,  $N_2$ , and CO; the results are discussed later in this work where they are compared with current theoretical calculations. However, it is appropriate to point out at this time some significant qualitative features of Schulz's curves, especially those for  $N_2$  and CO. The data show a series of sharp and well-defined peaks that have been interpreted as originating through an intermediate negative ion state. The theory of such states is currently under intensive investigation; Chen and Magee<sup>6</sup> have predicted a resonance peak in the  $H_2$  spectrum, but none has yet been observed experimentally. However, these theories do not account for the magnitudes of the cross sections in the non-resonant energy

regions, and it is toward these latter cross sections that the attention is to be directed in this presentation.

Phelps and co-workers<sup>7,8</sup> have succeeded in contributing another technique for establishing the vibrational excitation cross sections for the simpler molecules. These authors have performed a detailed analysis of transport coefficients that were obtained experimentally for electrons in such gases as  $H_2$ ,  $N_2$ , etc. In conjunction with the various other loss mechanisms, they were able to deduce curves representative of the cross sections for vibrational excitation. For certain molecules (notably  $H_2$ ), their published findings differ considerably from the curves of Schulz in selected portions of the energy spectrum, and their analyses have yielded no information on the above-mentioned resonance peaks. This method of approach, although displaying a considerable refinement of procedure, appears to bear the same limitations that were inherent in the earlier swarm experiments.

One of the first comprehensive theoretical treatments of the vibrational excitation of a molecule by electron collision was that of Wu.<sup>9</sup> For symmetric top molecules which possess a permanent dipole moment, Wu considered the interaction to be solely that between a point-charge and point-dipole. The Born approximation was assumed valid, and the results were applied to vibrational transitions in CO gas. However, the formulas can be readily applied to any polar diatomic molecule.

The solution of the general set of differential equations which describe the scattering of an electron by a non-polar diatomic molecule is complicated by the lack of spherical symmetry of the interaction potential, providing, of course, that the latter can be accurately

represented. Wu also considered electron collisions with  $H_2$ , a homonuclear diatomic molecule having no long-range dipole interactions. For even this simplest of cases, the detailed interaction is complicated and not subject to ready accurate algebraic simplification. Wu averaged the detailed interaction potential over all molecular orientations, and essentially chose for his model that of a central force field with a fixed effective charge and a single pole at the center of the molecule. Hence, there was no really accurate representation of the true molecular field. The Distorted Wave method was selected for the theoretical development of the scattering equations, however various simplifications were introduced into the analysis to decrease the reliability of this approximation.


Morse<sup>10</sup> applied the Born approximation to the problem of electron scattering from  $H_2$ , and decomposed the potential field of the homonuclear diatomic molecule into the sum of two equal parts, each centered about one of the nuclei. The integrals which involve these two potential functions were found to differ only by a phase factor. Expressions for the effective cross sections were derived, but Morse only compared the total rotation-vibration-translation energy loss with the single loss due to translation alone, and gave no numerical values for the magnitudes of the cross sections.

Carson<sup>11</sup> adopted the Born approximation and the same scheme for the decomposition of the potential as Morse, the belief being that this form was the most accurate representation available for the molecular field. However, an additional allowance was made for the variation of the effective nuclear charge with the internuclear distance. This

refinement was found to alter the vibrational excitation cross section for  $H_2$  by a significant amount, especially in the low-energy region where a sharp peak was predicted around 1 eV. The results of Carson are found to be somewhat larger than those of Wu for the  $H_2$  molecule.

A comparison of the theoretical cross sections for  $H_2$  with the experimental results quickly illustrates the important fact that even the most refined calculation is at least two orders of magnitude below experiment. Wu, Morse, and Carson considered in their work only the short-range electrostatic interactions. It is obvious that these forces alone are insufficient to account for the large observed cross sections for vibrational excitation in non-polar gases. A similar conclusion may be drawn for the polar gases, but for these molecules the discrepancies are not found to be so serious. However, in both cases a re-examination of the theory is certainly most desirable.

As the short-range forces do not appear to be important, it is necessary to examine the effects of the longer-range interactions. Recent theoretical works on electron-atom collisions (see references for Table I) have pointed out the important contribution from the polarization interaction to the cross sections. This is an interaction between the incident electron and the corresponding induced dipole moment of the molecule. The exact nature of this interaction is not known. The polarization potential behaves as  $r^{-4}$  at large interparticle separation, but the potential close to the molecule is expected to deviate considerably from this simple form. In electron-atom collisions, the customary procedure has been to choose some empirical form for this interaction, and to adjust parameters to achieve a good fit with experiment. In some cases,



the  $r^{-4}$  dependence has been retained for distances near the molecule but arbitrarily cut off at a certain distance to prevent divergence difficulties at the origin. A discussion of the different cut-off methods and their effects upon the cross sections will be presented in this work.



## CHAPTER II

### FORMULATION OF THE COLLISION PROBLEM

The problem to be considered is the collision of an electron with a diatomic molecule, the electron being scattered inelastically with the molecule acquiring excitation to a higher vibrational state. The projectile electron has position coordinate given by  $\vec{r}$  ( $r, \theta, \phi$ ), the coordinate origin is chosen at the center of mass of the molecule with the  $\hat{z}$  axis in the direction of the electron's initial incident motion, and  $\vec{\xi}(\xi, \Theta, \Phi)$  describes the motion of the nuclei of the target molecule. The collision process and coordinate are illustrated in Figure 1.

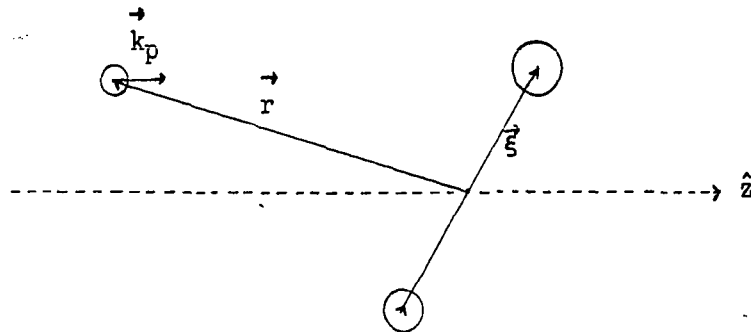


Figure 1. The Collision of an Electron with a Diatomic Molecule.

The time-independent formalism has been adopted for the presentation of the basic equations. A continuous parallel stream of electrons is assumed incident upon the target molecule providing the conditions necessary for a steady state to exist. If the time of observation is much greater than the time interval involved in the collision process, the Schrodinger equation describing the system of electrons + molecule will have the time-independent form:

$$H \Psi = E \Psi \quad . \quad (2.1)$$

If the motion of the center of mass of the system is assumed to have been separated out, Eq. (2.1) represents a description of the internal state of the molecule plus the motion of an electron relative to the molecule. The Hamiltonian,  $H$ , can be decomposed into a part representing the motion of the molecular constituents, a part describing the relative motion of molecule and electron, and an interaction potential:

$$H = H_m(\vec{\xi}) + H_e(\vec{r}) + V(\vec{r}, \vec{\xi}). \quad (2.2)$$

The wave function describing the state of a diatomic molecule (i.e., an eigenfunction of  $H_m(\vec{\xi})$ ) can be approximated as:

$$\chi_{n,v,J,M} = G_n(\vec{r}_i, \xi, \Theta, \Phi) \chi_v(\xi) \psi_{J,M}(\Theta, \Phi) \quad (2.3)$$

where  $\psi_{J,M}(\Theta, \Phi)$  describes the rotation of the nuclei,  $\chi_v(\xi)$  pertains to the vibration of the nuclei, and  $G_n(\vec{r}_i, \xi, \Theta, \Phi)$  is the wave function for the electronic motion ( $\vec{r}_i$  being the position vector for the  $i$ -th electron).

The major concern here is in the vibrational excitation of the molecule with no change in the corresponding electronic state quantum numbers; consequently, in the analysis to follow, the electronic portion of the wave function will always integrate to unity. Hence, this part of the wave function is hereafter ignored, and the molecular states will be described by the index,  $p$ , representing the set of quantum numbers  $(v, J, M)$ . Thus, a linear vibrating rotor is chosen as a model for the molecule. For a diatomic molecule, the rotation can be described by the normalized spherical harmonics, i.e.,  $\Psi_{J,M}(\Theta, \Phi) = Y_{J,M}(\Theta, \Phi)$ .

If the Born approximation can be assumed to be valid, the cross section for excitation from the state  $p$  to the state  $p'$  by electron impact will have the form:<sup>12</sup>

$$Q(p \rightarrow p') = \frac{k_{p'}}{k_p} \int_0^{2\pi} \int_0^{\pi} |f_{p',p}(\theta, \phi)|^2 \sin \theta \, d\theta \, d\phi \quad (2.4)$$

The incident and scattered propagation vectors for the electron at  $\vec{r}(r, \theta, \phi)$  are denoted by  $\vec{k}_p$  and  $\vec{k}_{p'}$ , respectively. In the above expression:

$$f_{p',p}(\theta, \phi) = -\frac{1}{4\pi} \left[ \frac{2m}{\hbar^2} \right] \int e^{i(\vec{k}_p - \vec{k}_{p'}) \cdot \vec{r}_1} V_{p',p}(\vec{r}_1) d\vec{r}_1 \quad (2.5)$$

where

$$V_{p',p}(\vec{r}) = \langle v', J', M' | V(\vec{r}, \vec{\xi}) | v, J, M \rangle \quad (2.6)$$

is the matrix element of the interaction potential between the two molecular states and " $m$ " is the mass of the electron. It is customary to simplify calculations by introducing the relative momentum coordinate,  $\vec{K} = \vec{k}_p - \vec{k}_{p'}$ , in lieu of the scattering angle,  $\theta$ . ( $K^2 = k_p^2 + k_{p'}^2$

-  $2k_p k_{p'} \cos \theta$ .) With this change of variable, Eq. (2.4) may be written:

$$Q(p \rightarrow p') = \frac{1}{k_p^2} \int_0^{2\pi} \int_{|k_p - k_{p'}|}^{k_p + k_{p'}} |f_{p,p}(K, \phi)|^2 K dK d\phi \quad (2.7)$$

The interaction of an electron with a non-polar diatomic molecule can be written in the form:

$$V(\vec{r}, \vec{\xi}) = -\frac{1}{2} e^2 \alpha r^{-4} - \frac{1}{2} e^2 r^{-4} (\alpha' + r \mathcal{Q}) P_2(\hat{r} \cdot \hat{\xi}) + V_s \quad (2.8)$$

where  $\alpha$  and  $\alpha'$  represent respectively the spherically-symmetric and angular-dependent parts of the polarizability of the molecule. These quantities are related to  $\alpha_{||}$  (the polarizability parallel to the internuclear axis) and  $\alpha_{\perp}$  (that perpendicular to this same axis) by the relations:

$$\alpha = \frac{1}{3} (\alpha_{||} + 2\alpha_{\perp}), \quad \alpha' = \frac{2}{3} (\alpha_{||} - \alpha_{\perp}). \quad (2.9)$$

The molecular quadrupole moment,  $\mathcal{Q}$ , is defined as:

$$\mathcal{Q} = \int \rho(x', y', z') (3z'^2 - r'^2) d\tau' / e \quad (2.10)$$

where  $\rho$  is the charge density of the molecule. In Eq. (2.8) above,  $P_2(\hat{r} \cdot \hat{\xi})$  is the usual Legendre Polynomial. The term  $V_s$  has been included to represent the influence of short-range interactions and must include terms to cancel out the singularities at the origin due to the polarization and quadrupole terms. The exact nature of this term is not known, and as the vibrational excitation is dictated primarily by the longer-range interactions, the direct effect of  $V_s$  will be neglected here.

To investigate the effects of the polarization and quadrupole terms in the interaction potential, it is convenient to write Eq. (2.8) in the following form:

$$V(\vec{r}, \vec{\xi}) = V'_s + V^0 + V^1 = V'_s + V^P \quad (2.11)$$

where:

$$V^0 = -\frac{e^2 \alpha}{2} g(r) \quad (2.12)$$

$$V^1 = -\frac{e^2}{2} \left[ \alpha' g(r) + \mathcal{Q} f(r) \right] P_2(\hat{r} \cdot \hat{\xi}). \quad (2.13)$$

The functions,  $g(r)$  and  $f(r)$ , are to remain unspecified for the moment, except that they must be well-behaved at the origin and approach  $r^{-4}$  and  $r^{-3}$ , respectively, for large values of  $r$ . The term  $V'_s$  is intended to include the remainder of the short-range interactions, and its contribution will be considered as negligible.

The addition theorem for spherical harmonics permits an expansion of  $P_2(\hat{r} \cdot \hat{\xi})$  in terms of the harmonics related to  $\theta, \phi$  of the electron and  $\Theta, \Phi$  of the molecule. Vibrational excitation by this mechanism is possible only if the quantities,  $\alpha$ ,  $\alpha'$ , and  $\mathcal{Q}$ , are considered as functions of  $\xi$ . The matrix element between two molecular states for the polarization and quadrupole interaction is:

$$V_{p'p}^P = V_{p'p}^0 + V_{p'p}^1 \quad (2.14)$$

$$V_{p'p}^0 = -\frac{1}{2} e^2 g(r) \alpha_{v'v} \delta_{J'J} \delta_{M'M} \quad (2.15)$$

$$V_{p'p}^1 = (-1)^{M-M'+1} \frac{e^2}{2} \left[ \frac{4\pi}{5} \right]^{1/2} U_{v'v} C^{(2)}(J'M', JM) Y_{2, M-M'}(\theta, \phi) \quad (2.16)$$

with

$$C^{(2)}(J'M', JM) = \left[ \frac{4\pi}{5} \right]^{1/2} \int Y_{J'M'}^*(\theta, \phi) Y_{2, M'-M}(\theta, \phi) Y_{JM}(\theta, \phi) \sin \theta \, d\theta \, d\phi \quad (2.17)$$

$$U_{v'v} = \alpha_{v'v} g(r) + \beta_{v'v} f(r) \quad (2.18)$$

$$\alpha_{v'v} = \int \chi_{v'}^* \alpha(\xi) \chi_v \, d\xi, \text{ etc.} \quad (2.19)$$

If Eqs. (2.14), (2.15) and (2.16) are used in conjunction with Eqs. (2.5), (2.6) and (2.7), the excitation cross section  $Q(p \rightarrow p')$  may be calculated. It is readily observed that there will be three terms contributing to this cross section, namely terms which are proportional to the following:

- (a)  $\delta_{J'J} \delta_{M'M}$
- (b)  $|C^{(2)}(J'M', JM)|^2$
- (c)  $C^{(2)}(J'M', JM) \delta_{J'J} \delta_{M'M}$

Integration over  $\phi_1$  in Eq. (2.5) determines the rule  $\Delta M = 0$  for all three of these terms. For terms (a) and (c), the additional rotational selection rule is  $\Delta J = 0$ . From the properties of the spherical harmonics, term (b) is nonzero only for  $J' = J, J \pm 2$  with  $J' \geq 0$  (except for the special case  $J' = J = 0$  which is forbidden).

For the transition between two vibrational states, the cross section is obtained by summing over all final rotational states and averaging over all initial rotational states. The following formulas are valuable in performing the required sums:

$$\sum_M C^{(2)}(JM, JM) = 0$$

$$\frac{1}{2J+1} \sum_M |C^{(2)}(JM, J+2M)|^2 = \frac{3(J+1)(J+2)}{10(2J+3)(2J+1)}$$

$$\frac{1}{2J+1} \sum_M |C^{(2)}(JM, JM)|^2 = \frac{J(J+1)}{5(2J-1)(2J+3)} \quad (2.20)$$

$$\frac{1}{2J+1} \sum_M |C^{(2)}(JM, J-2M)|^2 = \frac{3J(J-1)}{10(2J-1)(2J+1)}$$

$$\frac{1}{2J+1} \sum_{M, J'} |C^{(2)}(JM, J'M)|^2 = \frac{1}{5}$$

After integration of the angular coordinate and the appropriate summations, the vibrational excitation cross section arising from polarization and quadrupole interactions can be written as the sum of the independent contributions from  $V^0$  and  $V^1$ :

$$Q^P(v \rightarrow v') = Q^0(v \rightarrow v') + Q^1(v \rightarrow v') \quad (2.21)$$

$$Q^0(v \rightarrow v') = 2\pi (m e^2 \alpha_{v'v} / \hbar^2 k_p)^2 \int_{|k_p - k_{p'}|}^{k_p + k_{p'}} N^2 K^3 dK \quad (2.22)$$

$$Q^1(v \rightarrow v') = \frac{2\pi}{5} (m e^2 / \hbar^2 k_p)^2 \int_{|k_p - k_{p'}|}^{k_p + k_{p'}} \eta^2 K dK \quad (2.23)$$

In the above formulas, the following convenient notation has been employed:

$$N = K^{-2} \int_0^\infty r_1 \sin(Kr_1) g(r_1) dr_1 \quad (2.24)$$

$$\eta = K^{-3} \int_0^{\infty} \{ [(Kr_1)^2 - 3] \sin(Kr_1) + 3(Kr_1) \cos(Kr_1) \} \\ \times [\alpha'_{v,v} g(r_1) + \alpha_{v,v} f(r_1)] r_1^{-1} dr_1 \quad (2.25)$$

For small vibrations, it is within the present order of approximation to assume the wave functions which describe the vibrational motion to be those of a simple one-dimensional harmonic oscillator. The molecular parameters  $\alpha(\xi)$ ,  $\alpha'(\xi)$ , and  $\alpha_2(\xi)$  may be expanded in a Taylor series about the equilibrium separation  $\xi_0$  of the nuclei, e. g.,

$$\alpha(\xi) = \alpha_0 + (\partial \alpha / \partial \xi)_0 (\xi - \xi_0) + \dots \quad (2.26)$$

where the subscript  $0$  denotes evaluation at the equilibrium separation. If the second- and higher-order terms in this expansion are neglected, the matrix element connecting the ground and first vibrational levels has the simple form

$$\alpha_{10} = (2\beta)^{-1/2} (\partial \alpha / \partial \xi)_0, \quad \beta = 2\pi \mathcal{M} \nu_0 / \hbar, \quad (2.27)$$

where  $\mathcal{M}$  is the reduced mass of the molecule and  $\nu_0$  is the characteristic vibrational frequency. Expressions for  $\alpha'_{10}$  and  $\alpha_{210}$  have forms similar to Eq. (2.27). The only unknowns are  $(\partial \alpha / \partial \xi)_0$ ,  $(\partial \alpha' / \partial \xi)_0$ , and  $(\partial \alpha_2 / \partial \xi)_0$ , the first two of which can be readily estimated from experimental data of the intensities of Raman spectra. This data is currently available for a limited number of the simpler diatomic molecules which are of interest here. Theoretical calculations for all three of the above quantities have also been made for the hydrogen molecule,<sup>13,14</sup> but Raman data are used in this work wherever available.



The two cross sections  $Q^0(0 \rightarrow 1)$  and  $Q^1(0 \rightarrow 1)$  are now examined separately to determine the magnitude and relative importance of their contributions to the total vibrational cross section.

### Calculation of $Q^0(0 \rightarrow 1)$

In general, numerical integration is necessary to evaluate the integrals in Eqs. (2.22) through (2.25). For calculations with a computer, it has been found to be very efficient to select a value,  $r = d$ , above which  $g(r)$  is proportional to  $r^{-4}$ , and to evaluate this portion of  $N$  in a semi-closed form. For the proper choice of  $d$ ,

$$N = K^{-2} \int_0^d r_1 \sin(Kr_1) g(r_1) dr_1 + \frac{1}{2} (Kd)^{-2} \times [\sin(Kd) + (Kd) \cos(Kd)] + \frac{1}{2} [Si(Kd) - \frac{\pi}{2}], \quad (2.28)$$

where

$$Si(Kd) = \int_0^{Kd} y^{-1} \sin y dy, \quad (2.29)$$

the latter having a converging power series representation.

In the absence of rigorous calculations, the choice of  $g(r)$  is necessarily somewhat arbitrary. Several different expressions have found limited success in the application of polarization to atomic problems. The polarization interaction is proportional to  $r^{-4}$  only at large distances from the molecule; this dependence certainly does not hold for  $r$  less than the size of the molecule, and its validity in the near field is likewise highly questionable. The net result of most prior applications has been to choose some particular parametric model for the

near-field interaction which is valid in the far field and finite at the origin, and to select the parameters to give reasonable agreement with experiment.

There are four specific models which warrant consideration and are to be identified as follows (see Table I for appropriate references):

1. Model A - Bates formula:

$$g(r) = (r^2 + a^2)^{-2} \quad (2.30)$$

2. Model B - Step-function formula:

$$\begin{aligned} g(r) &= r^{-4} & a \leq r \\ &= a^{-4} & r \leq a \end{aligned} \quad (2.31)$$

3. Model C - Zero step-function formula:

$$\begin{aligned} g(r) &= r^{-4} & a \leq r \\ &= 0 & r < a \end{aligned} \quad (2.32)$$

4. Model D - Analytic formula:

$$g(r) = r^{-4} \left[ 1 - \exp(-r^n/a^n) \right] \quad (2.33)$$

In each of these expressions, "a" denotes an adjustable parameter which is related in some manner to the size of the scattering center. Figure 2 presents a rough sketch of the general behavior of these various models.

Information and comments relating to prior successful applications of the different models are summarized in Table I. In particular, Models A and B assume the maximum interaction to occur for  $r \leq a$  with non-zero values at the origin, while Models C and D attempt to minimize the effects

TABLE I  
TREATMENT OF POLARIZATION - BIBLIOGRAPHY

Application	Reference	Selection of Cut-Off Parameter	Comments
<u>Model A: Bates Formula</u>			
Photo-Ionization cross section of atomic Potassium.	Bates (15)	Atomic radius	Results were not sensitive to particular choice of "a".
Elastic scattering by atomic Hydrogen.	Bransden, Dalgarno, John and Seaton(16)	a=1.5 au. gave best fit to data for p-wave	
Elastic scattering by CsI atoms.	Robinson (17)	$a^2 = \sum_{i=1}^N \frac{1}{r_i^2}$	Reproduces shape of experimental curve, but there is poor agreement with its magnitude. (See Garrett and Mann below.)
<u>Model B: Step-Function Formula</u>			
Calculation of energy levels for Si <sup>13+</sup> from observed spectra.	Douglas (18)		Three regions about nucleus were considered, and parameters were determined to give the best fit with observed data.
Vibrational excitation of H <sub>2</sub> due to slow electrons.	Takayanagi (19)		Results were found to be very sensitive to the choice of "a". (Only a preliminary investigation.)

TABLE I--Continued

Application	Reference	Selection of Cut-Off Parameter	Comments
<u>Model B: Continued</u>			
Rotational excitation of $H_2$ due to slow electrons.	Takayanagi and Geltman (20)	Parameter selected to give general agreement with low-energy elastic scattering experimental data.	For $H_2$ , calculations were performed with $a=1.2$ and $1.3$ au. $N_2$ required $a=1.75$ and $1.8$ au. Authors considered the Distorted Wave approximation for the rotational transitions; the sensitivity to the choice of " $a$ " is approximately that encountered in the present work on vibration.
<u>Model D: Analytic Polarization Formula</u>			
Calculation of wave functions for CaII.	Biermann and Trefftz (21)	Atomic radius	Assumed $n = 8$
Calculation of oscillator strengths in the spectrum of NaI, KI, and MgII.	Biermann (22)	Order of atomic core	Assumed $n = 5$
Elastic scattering of low energy electrons from NI, OI, and ArI atoms.	Lenander (23)	For $r > a$ , net atomic charge per electron required to be less than $0.01$ au.	Author considered electrostatic and exchange effects for $r < a$ . In the absence of these latter terms in the Hamiltonian, it appears feasible to relax the rather stringent restrictions upon the choice of " $a$ ". Author assumed $n = 8$ .

TABLE I--Continued

Application	Reference	Selection of Cut-Off Parameter	Comments
<u>Model D: Continued</u>			
Elastic scattering of slow electrons by CsI atoms.	Garrett and Mann (24)	Last maximum in valence electron wave function, and varied up to 10 per cent to best fit the data.	Assumed $n = 8$ . The low-energy cross section was found to be highly sensitive to the choice of "a", but there was only a slight sensitivity at energies above 11 eV where good agree- ment was obtained with experi- ment. (See Robinson above.)
Elastic scattering of slow electrons by NaI and KI atoms.	Garrett and Mann (25)	As above, but only a 5 per cent varia- tion needed to fit the data.	Same general conclusions as above. Polarization was found to yield the major contribution to the cross section.

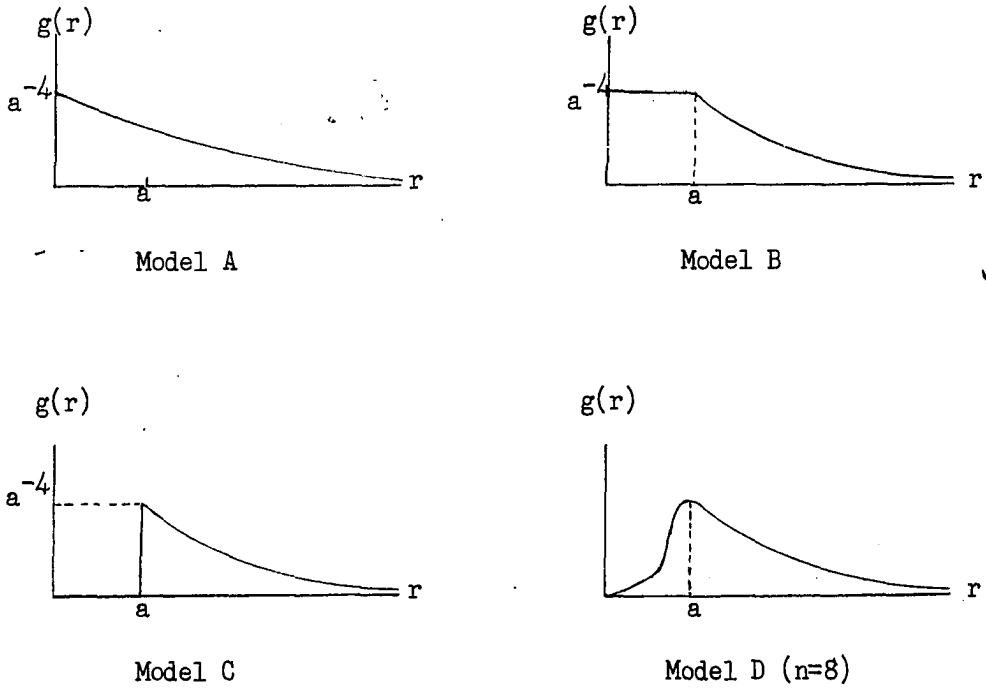


Figure 2. Characteristic Profiles for Various Choices of  $g(r)$ .

of this interior region and to concentrate the major contribution into some neighborhood about  $r = a$ .

For the four models, the integrals required in the calculation of the cross sections assume the following forms:

Model A:

$$\begin{aligned}
 \int_{|k_p - k_{p'}|}^{k_p + k_{p'}} N^2 K^3 dK &= \frac{1}{2} \left[ \frac{\pi e^{-ak_p}}{4a^2} \right]^2 [(2ak_p + 1) \sinh(2ak_{p'}) \\
 &\quad - 2ak_{p'} \cosh(2ak_{p'})] \quad (2.34)
 \end{aligned}$$

Model B:

$$N = \frac{1}{2} \left[ \frac{[2 + (Ka)^2] \sin(Ka)}{(Ka)^4} - \frac{[2 - (Ka)^2] \cos(Ka)}{(Ka)^3} + \text{Si}(Ka) - \frac{\pi}{2} \right] \quad (2.35)$$

Model C:

$$N = \frac{\sin(Ka) + (Ka) \cos(Ka)}{2 (Ka)^2} + \frac{1}{2} \left[ \text{Si}(Ka) - \frac{\pi}{2} \right] \quad (2.36)$$

Model D:

$$N = K^{-2} \int_0^d [1 - e^{-(r_1/a)^n}] \sin(Kr_1) r_1^{-3} dr_1 \quad (2.37)$$

$$+ \frac{1}{2} (Kd)^{-2} [\sin(Kd) + (Kd) \cos(Kd)] + \frac{1}{2} [\text{Si}(Kd) - \frac{\pi}{2}] .$$

For Model D above, it has been found sufficient to choose  $d = 1.5a$ .

Model D has found increasing favor in recent years for the treatment of polarization in atomic problems, with "n" usually chosen equal to 8. In a recent detailed calculation for neutral atomic oxygen, Jackson and Garrett<sup>26</sup> have derived a polarization function very similar in form to that obtained with this model.

#### Calculation of $Q^1(0 \rightarrow 1)$

If the far-field formulas for  $g(r)$  and  $f(r)$  are assumed to be valid for the complete range of integration, Eq. (2.25) can be written in the simplified form:

$$\eta = \int_0^\infty y^{-4} [(y^2 - 3) \sin y + 3y \cos y] [K y^{-1} \alpha'_{10} + a_{10}] dy, \quad (2.38)$$

with the change of variable  $y = Kr_1$ . Although this integral does not

present divergence difficulties, it is not to be expected that the given far-field representation of the interaction in Eq. (2.38) will be valid for the interior regions of the molecule. Nevertheless, anticipating the results of succeeding paragraphs, this approximation should yield an estimate of the upper limit to the contributions from  $Q^1(0 \rightarrow 1)$ .

The resulting formulas have the following form:

$$\eta = - \left[ \frac{a_{10}}{3} + \frac{\pi}{16} K \alpha'_{10} \right] \quad (2.39)$$

$$Q^1(0 \rightarrow 1) = \frac{2\pi}{5} \left[ \frac{m e^2}{\hbar^2} \right]^2 \frac{k_{p'}}{k_p} \left[ \frac{2 a_{10}^2}{9} + \frac{\pi}{36} a_{10} \alpha'_{10} (4k_p - \frac{\Delta(k^2)}{k_p}) + \frac{\pi^2 \alpha_{10}'^2}{128} (2k_p^2 - \Delta(k^2)) \right], \quad (2.40)$$

where

$$\Delta(k^2) = k_p^2 - k_{p'}^2. \quad (2.41)$$

Portions of Eq. (2.40) are essentially in agreement with calculations performed by Takayanagi.<sup>19</sup>



## CHAPTER III

### APPLICATION TO HYDROGEN MOLECULE

#### Molecular Constants and Selection of Cut-Off Parameter

For the hydrogen molecule, the molecular constants of special interest for the  $0 \rightarrow 1$  vibrational transition are given in Table II.

TABLE II  
MOLECULAR PARAMETERS FOR  $H_2$  MOLECULE  
(Atomic Units)

$(\partial\alpha/\partial\xi)_0$	$(\partial\alpha'/\partial\xi)_0$	$(\partial^2/\partial\xi^2)_0$	$\alpha_{10}$	$\alpha'_{10}$	$a_{10}$
4.53	2.34	1.13 <sup>(b)</sup>	0.769 <sup>(a)</sup>	0.397 <sup>(a)</sup>	0.192

(a) Experimental data on Raman intensities, Golden and Crawford.<sup>27</sup>

(b) Estimated from theoretical calculations by Kolos and Roothaan.<sup>14</sup>

Ishiguro, et al., have performed theoretical calculations of  $\alpha_{10}$  and  $\alpha'_{10}$  for this molecule and have concluded that the anharmonicity of vibration and the non-linearity of  $\alpha$  and  $\alpha'$  in  $\xi$  contribute significantly to these matrix elements. Their value for the important  $\alpha_{10}$

exceeds that presented in the table by approximately 20%, and Takayanagi<sup>19,20</sup> has used their results in his work. However, Raman intensity data is available for other more complex diatomic molecules and, for consistency, the Raman results have been used in the present calculations. The remaining well-known molecular constants for  $H_2$  can be inserted into Eq. (2.27) to yield expressions of the form:

$$\alpha_{10} = 0.1695 \left[ \frac{\partial \alpha}{\partial \xi} \right]_0 \text{ au.}, \quad (3.1)$$

etc., for the construction of the table.

The criterion for the selection of the cut-off parameter "a" has not been well established. The methods for atomic problems have been summarized in Table I. For an atom, a reasonable choice would be that adopted by Garrett and Mann,<sup>24,25</sup> namely, the outermost maximum in the charge distribution of the outer electronic shell. Indeed, in the recent calculations of Jackson and Garrett<sup>26</sup> the theoretical polarization function for OI was shown to peak in the neighborhood of this point. However, in applying this criterion to a diatomic molecule, additional complications are introduced as the approximate spherical symmetry of the atom is no longer present. The two alternatives which have appeared to be the most feasible are the following:

(1) Let  $r_a$  be the average radius of the outermost maximum in the charge distribution of the outer electronic shell for the constituent atoms. A good estimate of the lower limit of the cross section attributable to polarization may be obtained by selecting the cut-off parameter in terms of a sphere with radius:  $a_1 = r_a + \xi_0/2$ .

(2) The molecular shape may also be approximated as an ellipsoid with a semi-major axis of  $r_a + \xi_0/2$  and semi-minor axes of  $r_a$ . The cut-off parameter,  $a_2$ , is chosen as the radius of a sphere having the equivalent volume of such an ellipsoid. As the spherically-symmetrical portion of the polarization potential will be shown to dominate over the other contributions (see Table V), this model is not completely without merit and may be considered as providing an effective upper bound to the cross section.

The appropriate molecular constants and resulting values of the cut-off parameter for several molecules of interest are presented in Table III. For the  $H_2$  molecule, an alternative approach is available.

TABLE III  
CUT-OFF PARAMETERS  
(Atomic Units)

Molecule	$\xi_0$	$r_a$	$a_1$	$a_2$
$H_2$	1.4	1.0	1.7	1.2
$N_2$	2.07	1.04	2.1	1.3
CO	2.13	1.06 <sup>(a)</sup>	2.1	1.35

(a) This value is the average of the corresponding values for C and O.

With molecular beam techniques, Ramsey<sup>28</sup> has experimentally determined the following molecular charge distribution expectation values for the

hydrogen molecule:

$$\langle x_c^2 \rangle = \langle y_c^2 \rangle = 0.766 \text{ au.}$$

$$\langle z_c^2 \rangle = 1.0604 \text{ au.,}$$

which gives another estimate of the cut-off parameter as

$$a \simeq \left[ \langle x_c^2 \rangle + \langle y_c^2 \rangle + \langle z_c^2 \rangle \right]^{1/2} = 1.61 \text{ au.}$$

This value would also be a suitable choice for the parameter, and indeed is within the bounds established in Table III.

### Numerical Results

With the appropriate values for the constants in Eq. (2.22) and an adjustment of units,  $Q^0(0 \rightarrow 1)$  for the hydrogen molecule may be calculated from:

$$Q^0(0 \rightarrow 1) (\text{cm}^2) = \frac{1.41 \times 10^{-15}}{E(\text{eV})} \left[ \int_{|k_p - k_{p'}|}^{k_p + k_{p'}} N^2 K^3 dK \right]_{\text{au.}}, \quad (3.2)$$

where the required integrals are to be evaluated in atomic units and  $E$  is the incident electron energy in electron volts. This form is particularly useful for comparison with experiment. Calculations were performed with each of the four models for  $g(r)$  which have been presented, and the results are tabulated in Table IV. An incident electron energy of 2 eV was selected for comparison with experiment, and the parameter, "a", was allowed to vary over a limited range of interest to investigate the relative sensitivity of the various models to its selection. As indicated in the table, each of the four models studied shows about the

TABLE IV  
 $Q^0(0 \rightarrow 1)$  FOR  $H_2$ ; A COMPARISON OF SELECTED MODELS  
 FOR  $V^0$  AT 2 eV

(Cross Sections in Units of  $10^{-17} \text{ cm}^2$ )

Cut-off Parameter (au.)	$Q^0(0 \rightarrow 1)$			
	Model A	Model B	Model C	Model D
1.1	3.4	13.8	6.2	7.9
1.2	2.6	11.0	4.8	6.2
1.3	2.1	8.8	3.8	4.9
1.6	1.1	4.9	1.9	2.6
1.7	0.9	4.0	1.6	2.1
1.8	0.7	3.4	1.3	1.8

These cross sections should be compared with the following previous determinations at 2 eV:

1. Schulz (experimental)<sup>3</sup> - 5.5
2. Carson (theoretical)<sup>11</sup> - 0.19
3. Wu (theoretical)<sup>9</sup> - 0.08

same relative sensitivity to the choice of this cut-off parameter; this sensitivity changes only slightly with a variation of the parameter over the range considered. At an incident energy of 2 eV, all of the models yield cross sections which have an order of magnitude comparable with experiment and which show a considerable improvement over calculations that neglect this interaction.

Eq. (2.40) with its corresponding approximation for  $g(r)$  and  $f(r)$  was used in conjunction with the molecular constants of Table II to calculate the contribution of  $Q^1(0 \rightarrow 1)$  to the vibrational excitation cross section for  $H_2$ . Table V displays these results for several incident electron energies and presents a comparison with the experimental findings of Schulz and the theoretical calculation of Carson for  $H_2$ . Values of  $Q^0(0 \rightarrow 1)$  as calculated from Model D for  $a = 1.7$  au. have been included to emphasize the relative importance of the two cross sections. Because of the nature of the approximations concerning the form of the interaction, the values for  $Q^1(0 \rightarrow 1)$  presented in Table V should perhaps be considered only as an upper limit to the correct cross section.

As illustrated in Table V, for the range of energies of interest, it is safe to conclude that the contribution of  $Q^0(0 \rightarrow 1)$  dominates over that of  $Q^1(0 \rightarrow 1)$ . Due to the error involved in the calculation of  $Q^0(0 \rightarrow 1)$  because of the uncertainties in the proper choice of the cut-off parameter (see Table IV), detailed calculations of  $Q^1(0 \rightarrow 1)$  are of limited value in the current problem and are not further considered. However, Table V does emphasize an important additional point, namely that the relative importance of  $Q^1(0 \rightarrow 1)$  does increase with an increase

TABLE V  
COMPARISON OF THE CALCULATED VALUES OF  $Q^1(0 \rightarrow 1)$   
AND  $Q^0(0 \rightarrow 1)$  FOR  $H_2$

Energy (eV)	Cross Section ( $10^{-17} \text{ cm}^2$ )				Percent of $Q^1(0 \rightarrow 1)$ Attributable to Quadrupole Interaction
	$Q^1(0 \rightarrow 1)$	$Q^0(0 \rightarrow 1)^{(a)}$	Experiment (Schulz <sup>3</sup> )	Theory (Carson <sup>11</sup> )	
2	0.06	2.1	5.5	0.19	39%
7	0.13	0.8	1.7	0.09	21%
10	0.16	0.6			17%

(a) For purposes of comparison, the cut-off parameter  $a_1 = 1.7 \text{ au.}$  has been used which corresponds to the estimate of the lower bound established for  $Q^0(0 \rightarrow 1)$ . (See Table IV.) Model D has been selected for purposes of comparison.

in the incident electron energy and this increase may be attributed to an increase in importance of  $\alpha'$  relative to  $\alpha$  in the interaction potential.

### Comparison with Experiment

Recent experimental data concerning vibrational excitation in  $H_2$  show inconsistent results. Schulz<sup>3</sup> has obtained the energy spectrum with a double electrostatic analyzer, and his findings for the  $v = 0$  to  $v = 1$  vibrational transition display the following characteristics:

1. A "delayed onset" in the threshold for vibrational excitation from 0.53 eV to around 1.0 eV which may be interpreted as due to some "compound state" mechanism.
2. The cross section peak occurs around 2 eV.
3. Evidence was present for the excitation of the second vibrational level in the region around 3.4 eV indicating either the existence of some "compound state" mechanism or the importance of anharmonicity of the molecular vibration.

Conflicting results have been reported by Engelhardt and Phelps<sup>7</sup> from an analysis of transport coefficients. These authors confirm the threshold at 0.53 eV, but indicate a peak in their curve at 4.0 eV. Their cross sections considerably exceed those of Schulz in the energy region between 3.0 and 8.0 eV.

Ramien<sup>1</sup> in 1931 reported the percentages of collisions of electrons with hydrogen molecules which had produced excitation of one vibrational quantum. With the tables for the elastic cross sections



given by Massey and Burhop,<sup>29</sup> the following estimates were made:

<u>Energy</u>	<u>% (Ramien)</u>	<u>Approximate Cross Section</u>
3.5 eV	3%	$4.0 \times 10^{-17} \text{ cm}^2$
7.0 eV	2%	$1.7 \times 10^{-17} \text{ cm}^2$

These results agree remarkably well with the curve presented by Schulz.

The non-resonant vibrational excitation of  $\text{H}_2$  has been studied theoretically by Massey,<sup>30</sup> Morse,<sup>10</sup> Wu,<sup>9</sup> and Carson,<sup>11</sup> respectively. These investigators assumed short-range interactions only with no consideration being given to the effects of polarization. In particular, the work of Carson has probably been the most elaborate, with potentials centered around each nucleus and an explicit dependence of the effective nuclear charge upon the internuclear distance. However, in all cases, theoretical calculations neglecting polarization have been one or two orders of magnitude below experiment.

Chen and Magee<sup>6</sup> have predicted that vibrational excitation in  $\text{H}_2$  could proceed through a resonance phenomenon involving the compound state  $\text{H}_2^-$ . This mechanism would produce a sharp narrow peak centered around 7.0 eV. No experimental evidence is available to verify the existence of this peak, and this theory alone does not account for the level of the cross section for off-resonance energies.

The vibrational excitation cross section for  $\text{H}_2$  at selected energies has been computed with the analytic formula for polarization, Model D, and the set of cut-off parameters given in Table III. In accordance with the results presented in Table V concerning  $Q^1(0 \rightarrow 1)$ ,

and if the effects of  $V'_s$  can be assumed negligible, the approximation  $Q(0 \rightarrow 1) \cong Q^0(0 \rightarrow 1)$  should be valid. Hence, the calculations have been performed utilizing Eqs. (3.2) and (2.37). Table VI summarizes these cross sections and presents a comparison with experimental and prior theoretical determinations. The best approximate fit with the experimental data of Schulz has been found for a value of the cut-off parameter in the vicinity of 1.3 au. The calculated cross sections with polarization do agree, in order of magnitude, with the experimental results for the entire range of the values of the cut-off parameter given previously. Furthermore, these theoretical values are much larger than those of Wu and of Carson, indicating the importance of the polarization effect on the vibrational excitation.

TABLE VI  
VIBRATIONAL EXCITATION CROSS SECTION FOR  $H_2$

Energy (eV)	Q(0 → 1) in units of $10^{-17} \text{ cm}^2$						
	Experimental		Previous Theory		Calculated with $Q^0(0 \rightarrow 1)$		
	Schulz <sup>3</sup>	Engelhardt & Phelps <sup>7</sup>	Wu <sup>9</sup>	Carson <sup>11</sup>	$a_1 = 1.7$	$a_2 = 1.2$	$a = 1.3^{(a)}$
0.53	Threshold						
1.5	3.0	2.2	0.07	0.20	2.2	5.3	4.4
2	5.5	4.0	0.08	0.19	2.1	6.2	4.9
5	3.0	7.6	0.07	0.13	1.1	3.8	3.2
7	1.7	5.0	0.06	0.09	0.8	3.0	2.7

(a) Selected as an approximate best fit with the experimental data of Schulz<sup>3</sup>.

## CHAPTER IV

### EXTENSION TO OTHER DIATOMIC MOLECULES

#### Application to Nitrogen Molecule

Schulz<sup>3,5</sup> has recently determined the energy spectrum for the vibrational excitation of  $N_2$  with the electrostatic analyzer. The curves for excitation from the ground to various excited vibrational states display a series of sharp and well-defined peaks of exceptionally large magnitude. These peaks have been interpreted as characteristic of some compound state mechanism, and are not of concern here. The  $v = 0$  to  $v = 1$  curve has a long low-energy tail proceeding from a peak at 2 eV; Engelhardt, Phelps and Risk,<sup>8</sup> in an analysis of transport coefficients, have found this tail to extend down to the threshold at 0.292 eV, and in both cases this tail has been interpreted as the "direct" excitation of the first vibrational state. Portions of this low-energy tail should be of value for comparison with calculations made with the polarization interaction.

The "total" vibrational cross section (i.e., the sum of the individual experimental cross sections from the ground to various excited vibrational states) shows a peak at 2.3 eV. Haas,<sup>31</sup> from swarm experiments, gives a total vibrational cross section of  $3.8 \times 10^{-16} \text{ cm}^2$  at this peak. Schulz's curves were normalized to this peak value, while

Engelhardt, Phelps and Risk found a value of  $5.5 \times 10^{-16} \text{ cm}^2$  was necessary to obtain good agreement with experimental data. Schulz also reports measured values ranging from  $3.3 \times 10^{-16} \text{ cm}^2$  to  $5.8 \times 10^{-16} \text{ cm}^2$  for various angles of scattering. Hence a considerable amount of uncertainty persists as to the actual magnitude of these cross sections.

The vibrational excitation cross section for  $\text{N}_2$  at several energies has been computed with the analytic formula for polarization in a manner similar to that described for  $\text{H}_2$ . The cut-off parameters are those given in Table III, and the approximation  $Q(0 \rightarrow 1) \approx Q^0(0 \rightarrow 1)$  has been extended to this molecule. For  $\text{N}_2$ , Stansbury, Crawford and Welsh<sup>32</sup> have determined  $(\partial\alpha/\partial\xi)_0 = 5.71 \text{ au.}$  from Raman measurements. With the simple-harmonic oscillator approximation,  $\alpha_{10} = 0.344 \text{ au.}$  The cross sections were calculated from Eq. (3.2) by replacing the numerical coefficient with  $2.84 \times 10^{-16}$  and making use of Eq. (2.37). The results are given in Table VII which includes a comparison with the appropriate low-energy experimental data.

#### Application to Polar Molecules - CO

The CO molecule has a permanent dipole moment, and the interaction of the incident electron with this dipole moment can also give rise to vibrational excitation. The Hamiltonian given in Eqs. (2.2) and (2.8) must be modified to include a term of the form

$$V^D = -e\mu r^{-2} P_1(\hat{r} \cdot \hat{\xi}), \quad (4.1)$$

where  $\mu$  is the dipole moment of the molecule. Wu<sup>9</sup> has calculated the vibrational cross section which arises exclusively from this term and

TABLE VII  
VIBRATIONAL EXCITATION CROSS SECTION FOR  $N_2$

Energy (eV)	$Q(0 \rightarrow 1)$ in units of $10^{-17} \text{ cm}^2$				
	Calculated with $Q^0(0 \rightarrow 1)$		Estimated from experimental data <sup>(a)</sup>		
	$a_1 = 2.1$	$a_2 = 1.3$	Schulz <sup>(b),3,5</sup>	Phelps, et al. <sup>(c),8</sup>	Schulz <sup>(d)</sup> (modified)
0.292	Threshold				
1.25	0.29	0.99		0.2	1.0
1.50	0.27	0.91	0.8	1.0	1.1
1.75	0.25	0.87	1.0		
2	0.24	0.85			
5	0.15	0.64			
7	0.12	0.55			

(a) Accuracy is uncertain (see discussion).

(b) Total vibrational cross section was normalized to  $3.8 \times 10^{-16} \text{ cm}^2$  at 2.3 eV.

(c) Total vibrational cross section was normalized to  $5.5 \times 10^{-16} \text{ cm}^2$  at 2.3 eV.

(d) Data obtained by Schulz modified by Phelps, et al., by renormalizing the total vibrational cross section to  $5.5 \times 10^{-16} \text{ cm}^2$  at 2.3 eV.

has found:

$$Q^D(0 \rightarrow 1) = \frac{2\pi}{3k_p^2} \left[ \frac{2me}{\hbar^2} \right]^2 |\mu_{10}|^2 \ln \left[ \frac{k_p + k_{p'}}{k_p - k_{p'}} \right]. \quad (4.2)$$

In the derivation of this formula, the selection rules applicable to transitions between rotational states are found to be  $\Delta M = 0$ ,  $J' = J \pm 1$ ,  $J' \geq 0$ . Upon comparison with the corresponding selection rules pertaining to  $Q^0(0 \rightarrow 1)$  and  $Q^1(0 \rightarrow 1)$ , the cross sections from the different interactions are found to be strictly additive under the Born approximation. Hence, separate calculations of the different cross sections are meaningful and can be combined to yield a final total cross section:

$$Q(0 \rightarrow 1) = Q^0(0 \rightarrow 1) + Q^1(0 \rightarrow 1) + Q^D(0 \rightarrow 1). \quad (4.3)$$

Here again, the contribution of  $V'_S$  has been omitted as negligible.

A good estimate of  $Q^D(0 \rightarrow 1)$  can be obtained with a technique similar to that employed for the evaluation of  $\alpha_{10}$ , etc., in the previous development for nonpolar molecules. The expansion of  $\mu(\xi)$  and the simple-harmonic oscillator approximation yield an expression for  $\mu_{10}$  similar in form to Eq. (2.27). The quantity,  $(\partial \mu / \partial \xi)_0 = 0.654$  au., has been evaluated for CO from infrared intensity measurements,<sup>33</sup> and the resulting matrix element has been found to be  $\mu_{10} = 0.0416$  au. The cross sections for CO obtained with this approximation and Eq. (4.2) are listed in Table VIII.

The polarization contribution to the vibrational cross section for CO has been evaluated in a manner analogous to that described for

TABLE VIII  
VIBRATIONAL EXCITATION CROSS SECTION FOR CO  
(in units of  $10^{-17} \text{ cm}^2$ )

Energy (eV)	$Q^D(0 \rightarrow 1)$	$Q^0(0 \rightarrow 1)$		Calculated $Q(0 \rightarrow 1)$		Experi- ment <sup>(a)</sup>
		$a_1=2.1$	$a_2=1.35$	$a_1=2.1$	$a_2=1.35$	
0.269	Threshold					
0.6	1.8	0.6	1.8	2.4	3.6	5
0.8	1.6	0.6	1.7	2.2	3.3	5
1	1.4	0.6	1.7	2.0	3.1	8
2	0.9	0.5	1.5	1.4	2.4	
3	0.7	0.4	1.3	1.1	2.0	
5	0.5	0.3	1.1	0.8	1.6	

(a) Accuracy is uncertain. Values are estimated from curves obtained by Schulz<sup>3,4</sup> for which the confidence error is claimed to be a factor of two.



$H_2$  and  $N_2$ . Although Raman intensities for this molecule are not available,  $(\partial\alpha/\partial\epsilon)_0$  can be readily estimated from the intensity related to the symmetric vibration of  $CO_2$ . For the latter molecule, Stansbury, Crawford and Welsh<sup>32</sup> have found  $(\partial\alpha/\partial r_{C-O})_0 = 14.98$  au. for the symmetric vibration mode. It is reasonable to assume that half of this value, or 7.49 au., can be attributed to the C-O bond and hence provide a good approximation to the CO molecular constant. With  $\alpha_{10} = 0.476$  au., the remainder of the calculation of  $Q^0(0 \rightarrow 1)$  for CO follows the same general pattern as has been prescribed for  $H_2$  and  $N_2$ . As for these latter molecules, the contribution of  $Q^1(0 \rightarrow 1)$  and the effects of  $V'_s$  have again been neglected in comparison with  $Q^0(0 \rightarrow 1)$ . As is evident from Table VIII,  $Q^0(0 \rightarrow 1)$  and  $Q^D(0 \rightarrow 1)$  must be considered as being of comparable importance in establishing the total vibrational cross section for CO.

Schulz<sup>3,4</sup> has also experimentally ascertained the energy dependence of the vibrational cross section of CO to the first eight vibrational states. The individual curves display the same resonant peak structure that has been described for  $N_2$ ; in like manner, the existence of the low-energy tail to the  $v' = 1$  curve may be ascribed to "direct" excitation and should be of value in the present work. The "direct" excitation cross sections have been estimated from the relevant portions of these curves (Schulz obtained absolute values for the cross sections by assuming isotropic scattering and states the confidence error as a factor of two), and are compared with the calculated results for CO in Table VIII.

## CHAPTER V

### GENERAL DISCUSSION OF RESULTS

Tables VI, VII, and VIII are sufficient to demonstrate the importance of the polarization interaction in determining the magnitude of the vibrational excitation cross section for the simpler molecules. In fact, this contribution alone is sufficient to predict the correct order of magnitude for  $H_2$ ,  $N_2$  and CO as determined by experiment. For  $\sqrt{H_2}$ , the vibrational excitation cross section arising from the spherically-symmetric polarization term is about two orders of magnitude above that established by previous theories which ignored this interaction, while for the polar CO molecule, it is found to have an importance comparable with that derived from the electron-dipole potential. The quadrupole and asymmetric polarization terms were found to be of minor significance for vibrational excitation, but they should be investigated for each molecule and energy range studied. These latter effects are particularly important in the special cases where there are no contributions from the spherically-symmetric term, as, for example, in the rotational excitation of a molecule.

Several forms of the polarization potential have been examined. For the different models considered, the precise form of the near-field interaction was found to be of lesser importance than the choice of the

empirical parameters. The analytic formula for polarization (Model D) was chosen for the majority of the detailed calculations; as mentioned in the discussion, this model has yielded excellent results for electron-atom collisions and a similar profile has recently been derived for OI.<sup>26</sup> The selection of the cut-off parameter must be considered as a critical step in any treatment of polarization, and there is yet no clear-cut theoretical justification for a particular method of selection. In the present analysis, reasonable limits were established for the range of this parameter (and were different for each molecule studied), and although there has been some sensitivity of the cross section to its precise value, the fluctuation has not been sufficient to alter the order of magnitude or qualitative features of the results.

The nature and effects of the polarization interaction are worthy of considerable further investigation. Temkin<sup>34,35,36</sup> and others have obtained good results in electron-atom collisions with polarized orbitals, and this technique may find ultimate application to the electron-molecule problem. However, the asymmetry of even a diatomic molecule is sufficient to add tremendous difficulties to an already complex calculation, and, to be of value for the study of vibrational excitation, an additional dependence upon internuclear separation must be incorporated into the formalism. From a practical viewpoint, the reliability of any refined treatment of polarization should be well established for the very simple systems (such as electron-atom collisions) before an extension is attempted to the electron-molecule vibration problem.

In addition to the above considerations, there are also many inherent errors in the employment of the Born approximation. The

contribution to the cross section from the short-range portion of the polarization interaction could depend rather heavily upon the distortion of the incident and scattered particle waves. Inclusion of this distortion into the scattering equations would be the next logical step in a refinement of the present treatment. However, in light of the uncertainties concerning the proper treatment of polarization, such improvements are of questionable value at the present time.

There is a very significant feature of the present method of calculation which allows it to be easily extended to more complex molecules without a corresponding increase in difficulty. The equations for the cross sections were written explicitly in terms of  $(\partial\alpha/\partial\xi)_0$ , a quantity meant to represent a composition of the detailed behavior of the constituent particles of the molecule. This parameter was evaluated from published data acquired from experimental measurements of the intensity of Raman spectra. With the proper Raman intensity information, the calculation of vibrational excitation cross sections by the method suggested here is not necessarily restricted by the specific molecular complexity. However, at the present time, absolute Raman intensity measurements are still difficult to perform and only a limited amount of experimental data has been made available. This limitation is considered to be only temporary, and should not be allowed to detract from the general usefulness of the technique.

While this work was in progress, papers on vibrational and rotational excitation have appeared by Takayanagi.<sup>19,20</sup> He has examined the polarization effect, and has calculated the vibrational excitation cross section of  $H_2$  by both the Born and Distorted Wave approximations.

He has found the energy dependence of this cross section to vary between the two alternative methods, but the order of magnitude was found to be correctly predicted by Born approximation. He used a cut-off scheme that is equivalent to Model B investigated here, and his overall general approach parallels that of the present work. However, instead of Raman data, he adopted theoretical results for  $(\partial\alpha/\partial\epsilon)_0$  of  $H_2$ .<sup>13</sup> The cut-off parameter was selected to obtain agreement with elastic scattering experimental data; the choice is found to be within the limits established in this analysis. However, the present work has been a much more comprehensive study of the form of the interaction and the cut-off procedure and has included the vibrational excitation of the  $N_2$  and CO molecules as well.

Recently, Bardsley, et al.,<sup>37</sup> have interpreted the vibrational excitation process for  $H_2$  as a resonant one. Although it is possible for the resonance phenomenon to yield a contribution to the observed cross section, it is also impossible to neglect the contribution from the polarization interaction entirely. In spite of the many ambiguities regarding the choice of a cut-off parameter, it should be recognized that the polarization force is of major importance in exciting the vibration of at least the simple molecules.

## PART II

### EXCITATION BY ELECTRON IMPACT OF THE SPIN-MULTIPLETS OF THE GROUND STATE OF THE NEUTRAL OXYGEN ATOM

#### CHAPTER VI

#### INTRODUCTION

Forbidden transitions between the spectral terms of the ground configuration of neutral atomic oxygen give rise to some of the most prominent lines in the spectrum of the aurorae and the night-sky light. The mechanism for the population of these metastable states has been shown to be excitation by electron impact. This important process involves only single atoms, and is also of great importance in other astrophysical problems. Accurate experimental determinations of the various rate coefficients are not available at the present time, hence complete reliance must be placed upon accurate quantum mechanical calculations.

The difficulties associated with accurate determinations of the excitation probabilities for the neutral oxygen atom by electron impact were first encountered by Yamanouchi, Inui and Amemiya<sup>38</sup> in 1940. These authors recognized the peculiar form of the OI potential (to be described in detail in Chapter VII) in their calculations of the excitation and de-excitation cross sections for the different spectral terms,

$^3P$ ,  $^1D$ , and  $^1S$ , of the ground configuration,  $(1s)^2 (2s)^2 (2p)^4$ .

Weak-coupling approximations were considered valid, and calculations were performed with the usual Born-Oppenheimer approximation modified in the following manner:

1. Only potential distortion was considered, with a neglect of all exchange distortion terms.
2. Only the spherically-symmetric potential coupling and distortion terms were retained; likewise for the spherically-symmetric exchange coupling terms.
3. The wave function for the free electron was assumed orthogonal to the bound atomic orbitals.

Under these conditions, the contribution of the p-wave was found to dominate to the extent that all other contributions to the cross sections were negligible.

However, as electron-atom collision theory became more fully developed, it became obvious that the results obtained by the above workers were grossly in error. Bates, et al., (1950)<sup>39</sup> demonstrated from a consideration of charge conservation that these OI cross sections were over-estimated by at least several orders of magnitude. The errors had arisen from the incorrect assumptions regarding weak distortion and weak coupling and the failure to consider the orthogonality requirements.

In an attempt to correct the situation and obtain reliable cross sections for these same transitions in OI, Seaton (1953)<sup>40</sup> formulated the electron-atom collision problem in a manner analogous to the Hartree-Fock method for bound atomic states. Continuous-state Hartree-Fock equations were obtained by adopting an explicitly anti-symmetric

expression for the basis wave functions in the appropriate expansions. Only the p-wave was considered important, but for this interaction the strength of the exchange coupling was found to be so great that the usual weak-coupling approximations could not be relied upon. By retaining only the strong spherically-symmetric exchange terms (both coupling and distortion), and assuming all bound states in the configuration to have equal energies (the Exact-Resonance approximation), the scattering equations were uncoupled by transformation and solved numerically. This, essentially, is the basic framework upon which the present calculation has been performed, and is to be more thoroughly discussed in following chapters. Seaton found that the exchange distortion terms were indeed significant, and that the corrections to the cross sections due to non-orthogonality of the free and bound wave functions were of sign opposite to the other contributions. The latter resulted in cancellations between various contributing interactions, and decreased the cross sections to within the limits established by the conservation theorem. In later papers,<sup>41,42</sup> Seaton employed a modified type of Distorted Wave method and perturbation techniques to correct for the coupling terms which had been omitted in the earlier work; the corrections were considered only minor and emphasized the importance of the symmetric exchange effects. Accuracy of the method is expected to be comparable with that of the Hartree-Fock method for bound-state problems.

The OIII ion with a ground configuration of  $(1s)^2 (2s)^2 (2p)^2$  has the same set of spectral terms as OI. Hebb and Menzel (1940)<sup>43</sup> calculated the transition probabilities between the  $^3P$ ,  $^1D$ , and  $^1S$  terms, and included the cross sections for the different J-components



of the  $3P$  excited level. The latter are the spin-multiplets, the counterpart of which are the subject of the present investigation concerning OI. The cross sections for these transitions in OIII were important in determining the conditions under which the Bowen fluorescent mechanism would operate. The calculations were performed with the Born-Oppenheimer approximation, exchange and potential coupling, and the free plane wave appropriately replaced by the continuous Coulomb wave functions. The resultant target areas were found to be exceptionally large, especially for the spin-multiplet transitions.

Seaton (1955)<sup>42</sup> refined these calculations by using the Distorted Wave Born-Oppenheimer approximation and neglected exchange distortion. The methods employed by Hebb and Menzel were found to have given the wrong sign to the exchange terms; instead of the potential and exchange interactions correctly cancelling to some extent, these prior methods had permitted them to reinforce one another and consequently had over-estimated the cross sections by about an order of magnitude. The work of Seaton has been the last reliable calculation performed for the spin-multiplet transitions of the OIII ion, and has often been utilized to estimate transition probabilities in ions of a similar nature.

#### Importance of the Spin-Multiplet Transitions

The space between stars is occupied by a very rarefied gas. This interstellar matter is not uniformly distributed, with large dense masses scattered throughout the region. Most of these interstellar "clouds" are not directly observable even with a telescope, and other methods are necessary to gain knowledge of their properties. The cloud density is about  $10 \text{ atoms/cm}^3$  and consists chiefly of neutral atomic hydrogen.

Hence, these clouds are sometimes referred to as HI regions or zones. Observation of hydrogen line emission and absorption at 21 cm has established a cloud temperature of around  $125^{\circ}\text{K}$ , although this is known to vary from cloud to cloud.

The intercloud gas has a lower density of around  $.1 \text{ atom/cm}^3$ , is almost completely ionized, and has a typical temperature of  $10,000^{\circ}\text{K}$ . This portion of space has been called the HII region or zone. A problem of considerable current interest is that of explaining the observed temperature of the HI clouds. Typical heating mechanisms that have been considered in an energy balance equation are (1) Ionization of the gas in the cloud by starlight, (2) Cloud-cloud collisions, (3) Heating by conduction from the higher-temperature HII zone (this implies an intermediate transition region across which the temperature drops by two orders of magnitude), (4) Heating by cosmic rays, etc. The possible cooling processes include (1) Cooling by atom-electron and ion-electron collision, (2) Rotational excitation of the  $\text{H}_2$  molecule and similar molecules and (3) Electronic excitation of ions by collision with hydrogen atoms, among many others.

One of the most important of the possible cooling processes is perhaps that listed first, namely the excitation of an atom or ion by electron impact, with subsequent radiation of the transferred energy. Among the relatively abundant atoms in the HI cloud,  $\text{C}^+$ ,  $\text{Si}^+$ ,  $\text{Fe}^+$  and  $\text{OI}$  are the only species which possess low-lying excited electronic energy levels. Seaton<sup>44,45</sup> has investigated the ions in detail and has established their contribution to be of considerable significance. In the normal calculations, the neutral oxygen contribution has always

been neglected because the excitation cross sections for positive ions are much larger than for OI due to the long-range Coulomb attraction. However, Gershberg<sup>46</sup> has recently considered the effects of the low-lying OI levels and has found these excitation cross sections to be within an order of magnitude of those for  $C^+$ . Best estimates show that the number density of OI atoms to be 3 to 6 times larger than that of  $C^+$ , hence the conclusion that the neutral oxygen contribution to the cooling rate may be comparable with the carbon contribution.

The OI levels of interest above are the spin-multiplets of the  $^3P$  multiplet of the ground configuration. As accurate values for these cross sections have not been available, Gershberg was forced to extract them by rough approximation from other data. All transition probabilities between levels of the ground configuration of the OIII ion have been determined with at least some degree of accuracy, as have been cross sections for transitions between the  $^3P$ ,  $^1D$ , and  $^1S$  states of OI. By establishing ratios of corresponding cross sections for OI and OIII, Gershberg was able to deduce order-of-magnitude cross sections for the OI spin-multiplets. These results are discussed further in Chapter XVIII. However, it is well known that ion and neutral atom cross sections behave quite differently at low energy, and the approach taken by Gershberg has been thought to be an over-estimation at the low temperatures being considered.

Hence, a definite need has been established for accurate values for the transition probabilities between the spin-multiplets of neutral atomic oxygen. The calculation of these cross sections is the primary purpose of this analysis.

## CHAPTER VII

### PROPERTIES OF THE NEUTRAL OXYGEN ATOM

The neutral oxygen atom has a ground configuration given by  $(1s)^2 (2s)^2 (2p)^4$  with terms  $^3P$ ,  $^1D$  and  $^1S$ . The  $^3P$  multiplet has the lowest energy, and is characterized by electronic orbital angular momentum,  $L = 1$ , and electronic spin,  $S = 1$ . These two angular momentum vectors can be coupled to form  $\vec{J} = \vec{L} + \vec{S}$ , and a representation chosen wherein  $J$  and  $M_J$  are good quantum numbers. It is found that there are three possible values for  $J$ , namely  $J = 0, 1$  and  $2$ , and each has a  $(2J + 1)$  spatial degeneracy. Spin-orbit coupling is relatively strong for OI; if this contribution is added to the Hamiltonian of the free atom, the  $^3P$  energy level is split into three levels corresponding to these different  $J$  values. These latter levels distinguished by  $J = 0, 1$  and  $2$  are the spin-multiplets which are to be investigated in the present work. Excitation of these levels by electron impact can result in the submillimeter radiation and subsequent cooling effects which are of current interest to astrophysicists.

An energy level diagram for the  $^3P$  spin-multiplets of OI is shown in Figure 3. Unless explicit indications are to the contrary, Hartree atomic units are adopted throughout this discussion. If the projectile electron has a propagation vector denoted by  $\vec{k}$ , its energy

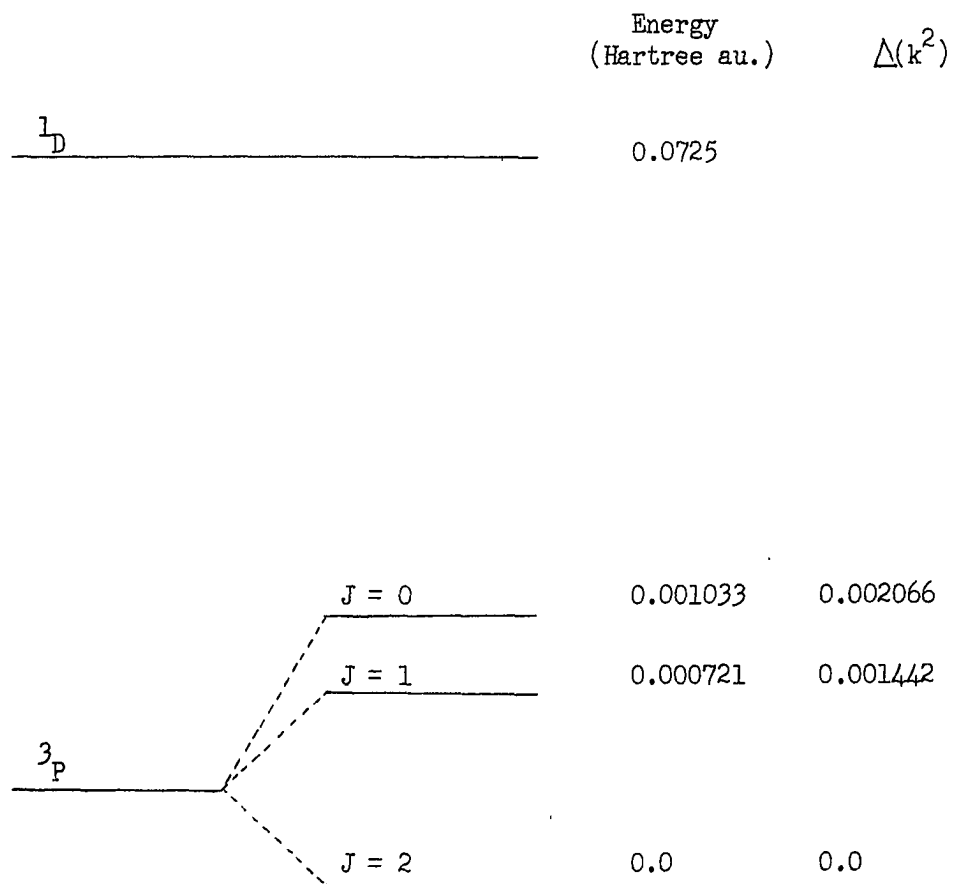


Figure 3. The Spin-Multiplets of  $3P$  in the  $(1s)^2 (2s)^2 (2p)^4$  Ground Configuration of OI. (Drawing is not to scale.)

can be expressed very simply as  $E = k^2/2$ . Calculations have been performed over the energy range of current interest in astrophysical studies; these energies are listed in Table IX. Although these energies appear rather low as compared to those generally considered in collision problems, it should be observed that those listed are generally well in excess of the minima required for excitation of the OI spin-multiplet states. Hence, a useful and highly valid initial approximation of the various transition probabilities can be obtained by ignoring the energy differences between these states (the Exact-Resonance approximation). It should also be noted that all electron energies which are considered are also well below the requirement for excitation of the  $^1D$  multiplet, and the latter level can be treated as energetically inaccessible.

#### Problems Concerning the P-wave

In the analysis that is to follow, the various cross sections are decomposed into contributions from incident electrons having different values of the relative orbital angular momentum. In addition to encountering the force field of the atom, these particles are restricted in their motion by limits imposed by the conservation theorems on angular momentum. The effects of the latter appear as repulsive-type terms in the scattering differential equations, and play a role comparable to that of the spherically-symmetric potential terms. The combination of these two quantities is often referred to as an "Effective Potential" and is to be defined here as follows:

TABLE IX  
ENERGIES OF INTEREST FOR PROJECTILE ELECTRON

Energy		$k^2$
$^{\circ}\text{K}$	Hartree au.	
500	0.001584	0.003168
1,000	0.003168	0.006336
5,000	0.01584	0.03168
10,000	0.03168	0.06336

$$U^0 = \frac{\ell(\ell+1)}{2r^2} + U, \quad (7.1)$$

where  $U$  is the combined effect of the attractive nuclear charge and the spherically-symmetric repulsion of the bound atomic electrons. The quantity,  $U$ , is formally defined by Eq. (10.7); the notation and methods of evaluation are discussed in Chapter X. Figure 4 illustrates the profile of the "Effective Potential" curves for  $\ell = 0, 1$ , and  $2$ .

The concern at the moment is with the shape of the curve for the p-wave with  $\ell = 1$ . As shown in the figure, as the interparticle separation decreases, this curve rises very slowly, has a broad peak centered around  $r = 1.6$ , quickly decreases to a deep minimum in the neighborhood of  $r = 0.25$ , and finally rises again sharply as the  $\frac{\ell(\ell+1)}{2r^2}$  term begins to dominate in the vicinity of the origin. The broad peak has a value of approximately 0.25 au. (corresponding to  $k^2 = 0.5$ ). Yamanouchi, et al.,<sup>38</sup> state that this maximum, along with the depth of the well and the necessary modifications of the potential to be consistent with a  $(2p)^5$  configuration, makes possible the existence of one discrete level of the negative ion,  $O^-$ . Classically, for  $k^2 < 0.5$ , the electron cannot penetrate the barrier, but the "tunneling effect" of quantum mechanics allows a penetration of the barrier at energies well below the peak value. Hence, there exists a finite probability for a low-energy incident p-electron to become entrapped in the interior of the well, to spend a considerable amount of time in the vicinity of the bound atomic electrons, and hence to be very effective in inducing electronic excitation. It is to be expected that the wave function which describes the incident p-electron should display at least a very small



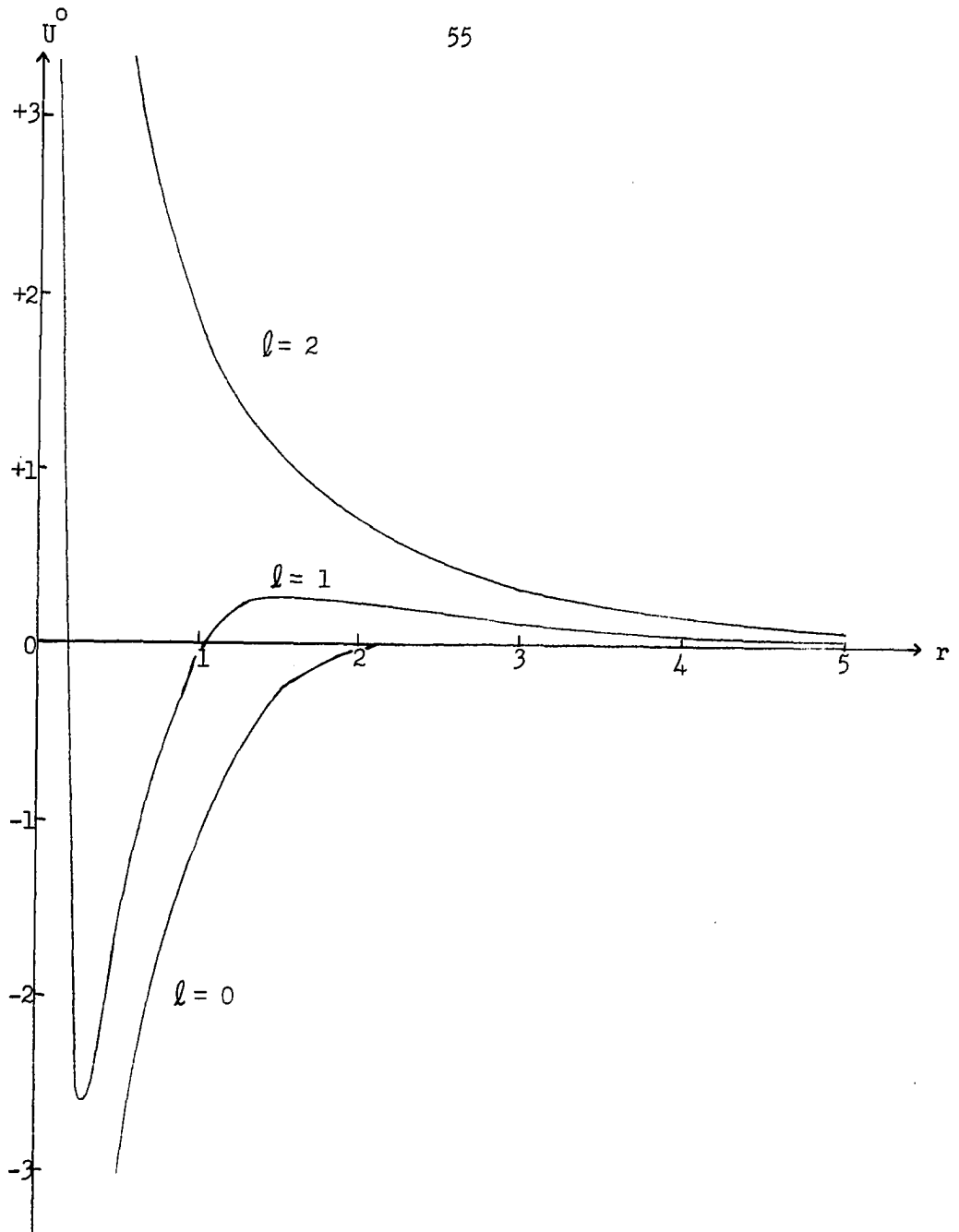


Figure 4. Effective Potentials for  $l = 0, 1, 2$  Incident Partial Waves.

peak in the vicinity of the interior well. Hence, considerable distortion should occur for this wave function, as compared to that for a similar free particle.

Of course, the above effect is of major importance for incident electron energies immediately below the peak value. The limits to this energy interval of importance have not been established. In the present calculation, the highest energy corresponds to  $k^2 = 0.06336$ ; it is not too unrealistic to believe the influence of this effect to extend down to this value. The effects are manifested indirectly through an importance of short-range exchange forces and corresponding requirements upon orthogonality. Indeed, these contributions were found to completely dominate the cross sections in previous studies of  $OI^{40}$  (however, generally the energies were much higher than those now being considered). In any case, the inner well and barrier should cause sufficient distortion in the p-wave function to warrant more than a casual consideration.

At least a qualitative justification of the preceding ideas can be established through an examination of the curves presented in Figures 5 and 6. The radial wave function for a bound (2p) orbital is denoted by P. (This function is formally defined and described in later chapters.) Figure 5 compares this bound wave function with that of a free particle having angular momentum  $\ell = 1$ . Included also is the wave function for a similar particle in the Coulomb field of a neutral oxygen atom. The distortion of the wave function due to the Coulomb potential is certainly noticeable, but these deviations are not considered as extreme. It is clear from Figure 5 that the P function is not orthogonal to the other two functions. In several of the earlier

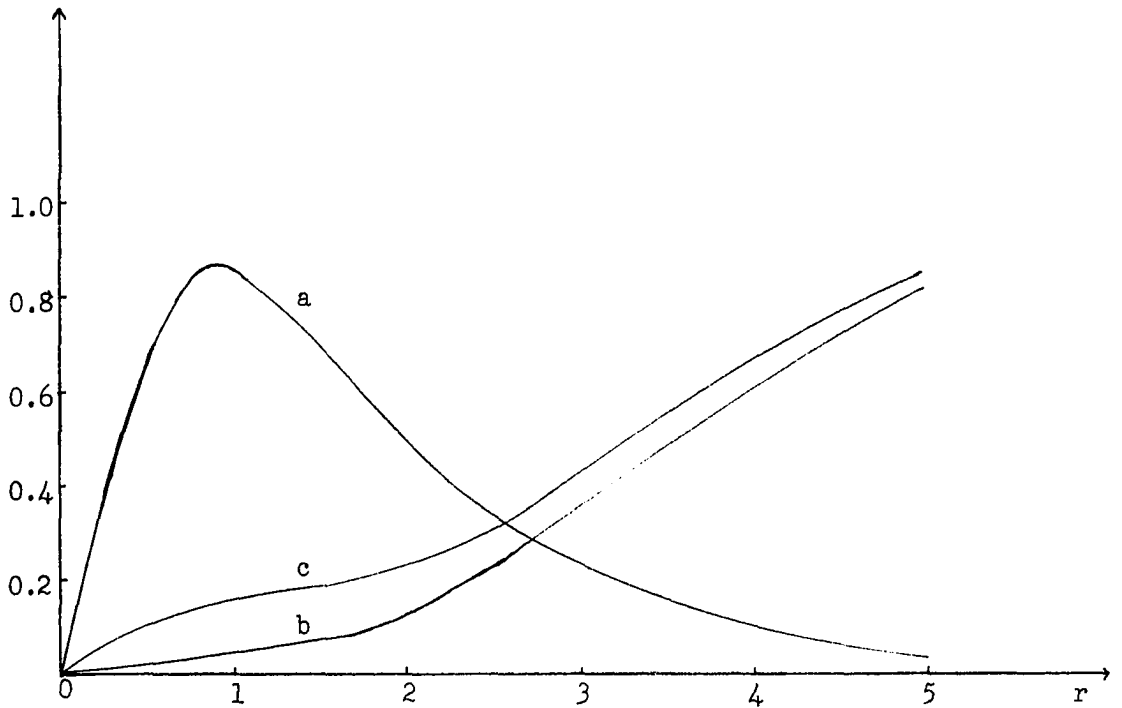


Figure 5. Comparison of Bound P Wave Function with Free and Potential Distorted P-waves.

Curve a. The bound state radial wave function for (2p) orbital.

Curve b. Free particle wave function, p-wave,  $k^2 = .06336$ , asymptotic amplitude =  $k^{-1/2}$ .

Curve c. Same as (b), but with allowance for potential distortion.

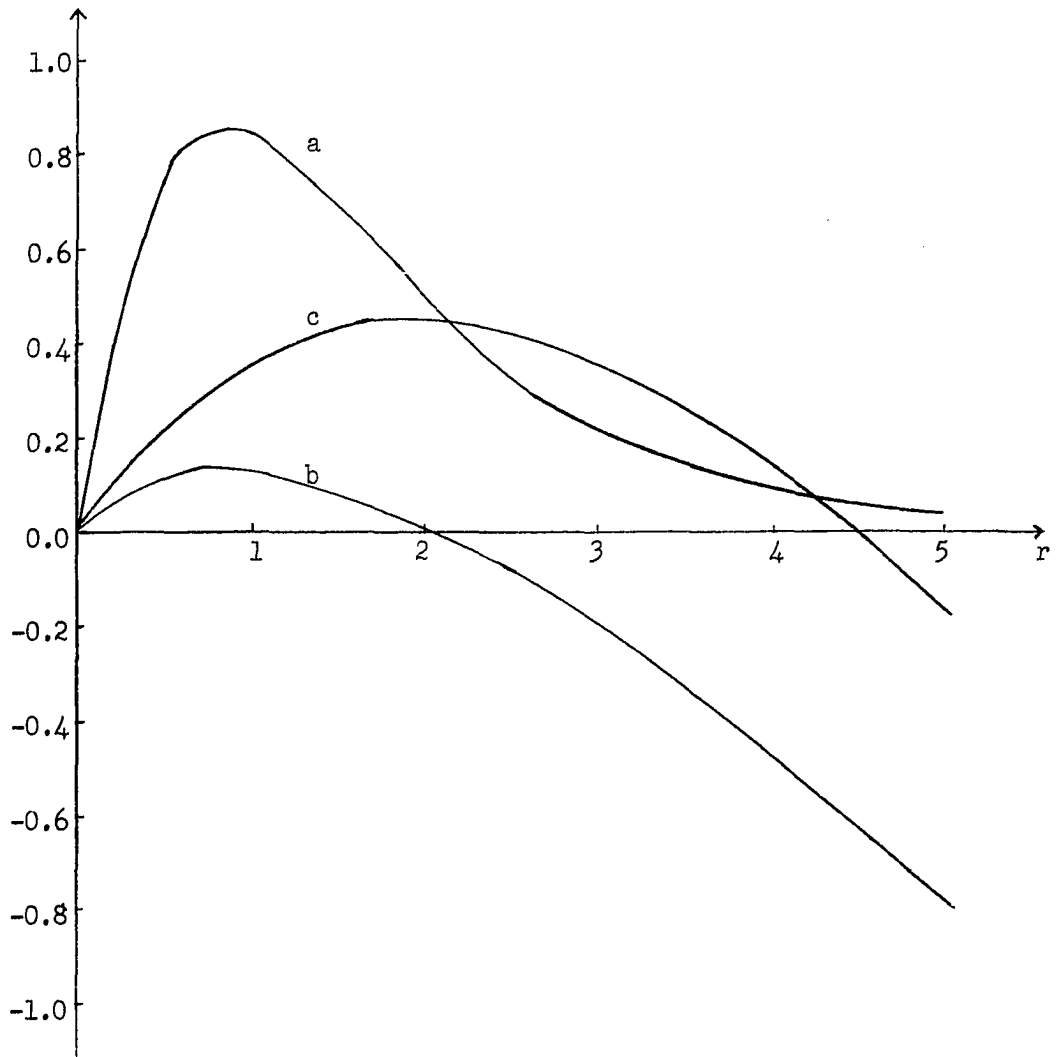


Figure 6. Comparison of Bound P Wave Function with P-waves Which Display the Effects of Exchange Distortion and Orthogonality.

Curve a. The bound-state radial wave function for (2p) orbital.

Curve b.  $S^1$ -type function for p-wave, exchange distortion,  $k^2 = .06336$ , asymptotic amplitude =  $k^{-1/2}$ .

Curve c.  $S^2$ -type function for p-wave, exchange distortion,  $k^2 = .06336$ , asymptotic amplitude =  $k^{-1/2}$ .

investigations of OI transition probabilities, serious error was introduced into the calculations by an incorrect consideration of this requirement.

Figure 6 displays the effects of including the spherically-symmetric exchange terms in the distortion, and of modifying the wave functions to achieve orthogonality. The two functions, labeled  $\mathcal{P}$ -type and  $\mathcal{Q}$ -type, are treated at length in Chapters XIV and XV; the chosen curves are introduced here to emphasize the importance of these phases of the analysis. The  $\mathcal{P}$ -type function is orthogonal to the P function, while the  $\mathcal{Q}$ -type is not (although attempts have been made to partially correct for this deficiency). The significance of exchange distortion and orthogonality should be evident from the two graphs. As will be demonstrated, the exchange coupling terms are extremely important in establishing the OI transition probabilities; these terms depend rather heavily upon the amount of free wave-bound wave overlap. The functions described in Figure 5 are certainly expected to over-estimate the magnitudes of these terms, while those in Figure 6 should provide more accurate results. However, the latter in turn should display a high degree of sensitivity to the short-range distortion terms and the corresponding shape of the wave function for small values of  $r$ .

#### Difficulties with S-wave

The calculation of the various transition probabilities for OI is further complicated by the possibility of resonance effects for the s-wave with  $\ell = 0$ . There is, at present, strong evidence for the existence of a  $(2p)^4 (3s)$  excited bound state of  $O^-$  with near-zero

binding energy.<sup>47</sup> If this state is in fact a reality, the magnitudes of the cross sections should be tremendously increased in the lower energy range.

Employing purely empirical methods, Bates<sup>48</sup> has found that for the negative ion,  $O^-$ , the  $(2p)^4 (3s)$  configuration should lie about 2.0 eV higher than the  $(2p)^5$  ground configuration. As the most probable value for the electron affinity is approximately 2.2 eV, a stable excited state of the negative ion may exist very close to the continuum. There is also good experimental evidence supporting this possibility. In separate experiments whereby  $O_2$ , CO, and NO, respectively, were bombarded with electrons,  $O^-$  ions were observed which were believed to be in stable excited states within 0.2 eV of the continuum.<sup>47</sup> Evidence has not been complete in any of the individual cases, but the combination is strongly suggestive of the existence of such a state.

Attempts to provide a detailed theory for this phenomenon have generally proven unsuccessful. Bates and Massey<sup>49</sup> have attempted to obtain a stable  $(2p)^4 (3s)$  orbital for  $O^-$  by allowing for the increased long-range field acting on the  $(3s)$  electron due to the polarization of the OI neutral atom. However, it was found that the polarization required to give a stable level was far in excess of the most probable theoretical and experimental value. Other effects arising from the perturbation of the neutral atom would have to be taken into account to permit such a stable excited state.

Different numerical calculations of the OI elastic cross section have shown widely inconsistent results, especially in the low-energy region below 1 eV. The major disagreements can be traced to different

treatments and approximations concerning polarization, an interaction of utmost significance in the formation of the excited negative ion state. All of the calculated elastic cross sections are found to approach non-zero values as  $k^2 \rightarrow 0$ , but the behavior of the various curves near this point varies considerably. The curves of Bates and Massey,<sup>49</sup> Temkin,<sup>36</sup> Lenander,<sup>23</sup> Cooper and Martin,<sup>50</sup> Klein and Brueckner,<sup>51</sup> and others show a slow but definite decrease in value near zero incident energy, while the results of Robinson,<sup>52</sup> and more recently of Jackson and Garrett,<sup>26</sup> show a sharp, narrow rise of exceptional magnitude in this part of the energy spectrum. The latter would be more indicative than the former of a resonance effect of the type that has been described for s-wave. However, the proper treatment of polarization must be considerably clarified before ultimate conclusions can be derived from these curves. In the present work, excitation cross sections which originate from s-wave interactions are first obtained with a total neglect of polarization effects, but possible corrections are presented later as derivable from an accepted empirical form for the polarization potential.

## CHAPTER VIII

### BASIC FORMULATION

For a system consisting of an  $(N + 1)$ -electron atom (in essence, a neutral atom designated as the atomic core with nuclear charge  $Z$  and  $N$  electrons, and one external or free (denoted by  $i$ ) electron), the Hamiltonian may be written as:

$$H = H_i + H(i^{-1}) + \sum_{\substack{j=1 \\ (j \neq i)}}^{N+1} \frac{1}{r_{ij}} \quad (8.1)$$

where

$$H_i = -\frac{1}{2} \nabla_i^2 - \frac{Z}{r_i} \quad (8.2)$$

is the Hamiltonian for the  $i$ -electron in the field of a charge  $Z$ , and

$$H(i^{-1}) = \sum_{\substack{j=1 \\ (j \neq i)}}^{N+1} \left[ H_j + \sum_{\substack{k > j \\ (k \neq i)}}^{N+1} \frac{1}{r_{jk}} \right] \quad (8.3)$$

represents the Hamiltonian for the remainder of the  $(N + 1)$  electrons excluding all interactions with the  $i$ -electron. The wave functions for the atomic core,  $\Psi_n(i^{-1})$ , form a complete orthonormal set and satisfy the differential equation:



$$H(i^{-1}) \Psi_n(i^{-1}) = E_n \Psi_n(i^{-1}) \quad (8.4)$$

The subscript,  $n$ , represents a series of quantum numbers which specify a particular quantum state of the neutral atom.

The Schroedinger equation for the  $(N + 1)$ -electron system may be written in the form

$$[H - E] \Psi = 0 \quad (8.5)$$

wherein advantage has been taken of the time-independent, steady-state formulation of the scattering problem. The first step in the solution of Eq. (8.5) is generally to perform an infinite expansion of  $\Psi$  in terms of the orthonormal set,  $\Psi_n(i^{-1})$ , with the coefficients in the expansion carrying the dependence upon the coordinates of the  $i$ -electron. This expansion is generally understood to be a summation over the bound states and an integration over the states in the continuum. However, in practical calculations, it is necessary to neglect part of the summation, cut off the expansion after  $n_0$  terms, and thereby obtain only an approximate solution to Eq. (8.5). The approximation is usually made to include only the states within the particular configuration of interest, or alternatively, to include only the states which are energetically accessible. (In the present problem the latter procedure has been followed, namely an inclusion only of the states belonging to the set of spin-multiplets for the  $^3P$  ground state of OI with the  $^1D$  and  $^1S$  states of the  $(2p)^4$  configuration inaccessible for the energies of interest.) Terms in the scattering equations which arise from the consideration of energetically inaccessible states can be interpreted as yielding a polarization correction.

For results which are to be physically significant, the complete wave function,  $\Psi$ , must be antisymmetric in the interchange of the coordinates of the  $i$ -electron with any other electron. This requirement is best incorporated into the problem by explicitly antisymmetrizing the individual functional terms in the expansion for  $\Psi$  thereby guaranteeing the antisymmetry of the total wave function. (Determinantal wave functions are used for  $\Psi_n(i^{-1})$ , thus there is antisymmetry with respect to the interchange of coordinates of any of these electrons.) With these considerations in mind, the required expansion takes the following form:

$$\Psi = \sum_{n=1}^{n_0} A \phi_n(i) \Psi_n(i^{-1}). \quad (8.6)$$

If Eq. (8.5) is multiplied on the left by  $\Psi_m^*(1^{-1})$  and integrated over all coordinates except those of  $l$ -electron, and if use is made of Eqs. (8.4) and (8.6), the result is a set of coupled integro-differential equations for the wave function of the free electron (now carrying the index  $l$ ).

$$\left[ H_l - \frac{k_m^2}{2} \right] \phi_m(l) + \sum_{n=1}^{n_0} [V_{mn}(l) \phi_n(l) - W_{mn}(l)] = 0 \quad (8.7)$$

$$V_{mn}(l) = \int \Psi_m^*(1^{-1}) \left[ \sum_{j \neq l} \frac{1}{r_{lj}} \right] \Psi_n(1^{-1}) dx_1^{-1} \quad (8.8)$$

$$W_{mn}(l) = N \int \Psi_m^*(1^{-1}) [H - E] \Psi_n(2^{-1}) \phi_n(2) dx_1^{-1} \quad (8.9)$$

The notation in Eqs. (8.8) and (8.9) indicates that the integration is

to be performed over all coordinates except those of l-electron. The term  $k_m^2/2$  represents the energy of l-electron at infinite separation from the atom, the latter being in the state "m" with energy  $E_m$ . By conservation of energy:

$$E - E_m = \frac{k_m^2}{2}. \quad (8.10)$$

Eqs. (8.8) and (8.9) are referred to as the potential and exchange integrals, respectively, and give rise to transitions between the various atomic states.

Eq. (8.9) can be simplified into either of two forms:

$$W_{mn}(1) = N \int \Psi_m^* (1^{-1}) \left[ H_2 - \frac{k_n^2}{2} + \sum_{j \neq 2} \frac{1}{r_{j2}} \right] \Psi_n(2^{-1}) \phi_n(2) dx_1^{-1} \quad (8.11)$$

$$W_{mn}(1) = N \int \Psi_m^* (1^{-1}) \left[ H_1 - \frac{k_m^2}{2} + \sum_{j \neq 1} \frac{1}{r_{j1}} \right] \Psi_n(2^{-1}) \phi_n(2) dx_1^{-1} \quad (8.12)$$

Eq. (8.11) follows directly from the above-described procedure, while Eq. (8.12) results from the Hermitean property of  $H(1^{-1})$ . Eqs. (8.9), (8.11) and (8.12) can be shown to be equivalent when exact wave functions are used; in numerical work a choice must be made between Eq. (8.11) and Eq. (8.12), and, as only approximate wave functions are available, the final cross sections will vary depending upon the particular selection. Eq. (8.11) is referred to as "prior" interaction, and Eq. (8.12) as "post" interaction. Post-prior discrepancy is a problem that always presents difficulties where exchange interaction is important in establishing the total cross section. Such is the case for

OI, and although Eq. (8.11) was used in developing the scattering equations, the formalism adopted allows a ready determination of the difference between the two alternative approaches.

The function representing the motion and spin of the free electron may be further expanded in terms of partial waves:

$$\begin{aligned} \phi_n(1) = & \sum_{\ell, m_\ell, m_s} [4\pi(2\ell + 1)]^{1/2} i^\ell \delta(m_s) Y_\ell^{m_\ell}(\theta_1, \phi_1) \\ & \times \frac{F_n(m_\ell m_s k \ell | r_1)}{r_1} \end{aligned} \quad (8.13)$$

where  $\delta(m_s)$  denotes the electron's spin function and  $Y_\ell^{m_\ell}(\theta_1, \phi_1)$  is a spherical harmonic describing the partial wave with relative orbital angular momentum  $\ell$  and space projection  $m_\ell$ . Eq. (8.13) may be inserted into Eq. (8.7) to yield a set of differential equations for the radial functions  $F_m(m_\ell m_s k \ell | r_1)$ . However, instead of presenting this set of equations for solution, it is appropriate to describe an alternative approach which results in a considerable simplification in the final set of coupled equations.

## CHAPTER IX

### FORMULATION IN TERMS OF THE COMPOSITE REPRESENTATION

The expansion, Eq. (8.13), is basically one in terms of products of the spatial and spin functions of the external, free electron. The spatial factor has orbital angular momentum  $\vec{l}$ , and the spin portion is representative of the vector  $\vec{s}$ . Let  $\vec{j} = \vec{l} + \vec{s}$ ; under standard methods for vector coupling, a simple transformation will yield a set of basis functions which are linear combinations of the above functions, and which are characterized by the set of quantum numbers  $(j, m_j, l, s = 1/2)$ . The functions which are of importance in the present work are listed in Appendix I in terms of a slightly more general notation. These selected functions are written,  $\Phi_j^{m_j}(l)$ .

The current analysis is oriented toward the determination of the excitation cross sections for the states of the various spin-multiplets of the  $^3P$  multiplet of neutral atomic oxygen. Basically, these different states arise from the  $(2p)^4$  configuration with an inner core of  $(1s)^2 (2s)^2$ , and have wave functions which are best described using linear combinations of determinantal functions. Appendix I describes the calculation of these wave functions along with a summary of the functions for the various states. A particular state in this set is distinguished by the quantum numbers  $J$  and  $M$  (representing the total and  $\hat{z}$  component, respectively, of the total atomic electronic

angular momentum), and has a wave function referred to by the notation,  $\Psi_J^M$ .

It is advantageous to perform another stage of vector-coupling, to couple the  $\vec{J}$  of the neutral atom with  $\vec{j}$  of the free electron to form the total angular momentum of the system,  $\vec{J}_T = \vec{J} + \vec{j}$ . The basis functions in this representation are constructed, as before, from linear combinations of the form:

$$\begin{aligned} X(J_T, M_T, J, j, L=1, S=1, \ell, s=1/2, \ell_i=1, s_i=1/2) \\ = \sum_{M+m_j=M_T} (J M j m_j | J j J_T M_T) \Psi_J^M \Phi_j^{m_j}(\ell) \end{aligned} \quad (9.1)$$

where  $(J M j m_j | J j J_T M_T)$  is the Clebsch-Gordan (or vector-coupling) coefficient. Table X presents the available composite states (ignoring  $M_T$  labeling) for values of  $\ell$  up to and including  $\ell = 2$ . The wave functions which are required in the present work are listed in Table XI at the latter part of this chapter.

The total wave function for the system may be expanded in terms of these new composite basis functions:

$$\Psi = \sum_{n=1}^{n_0} A_n X_n \quad (9.2)$$

The index,  $n$ , now represents the array of quantum numbers given in Eq. (9.1) to describe the composite state. The differential equations for the radial functions,  $F_m(r_1)$ , are obtained by simplifying the expression:

TABLE X  
COMPOSITE STATES FOR VALUES OF  $\ell \leq 2$

$J_T$	$J$	$j$	$\ell$	State Designation ( $M_T = J_T$ )
1/2	1	1/2	0	a
	0	1/2	0	b
	2	3/2	1	c
	1	3/2	1	d
	1	1/2	1	e
	0	1/2	1	f
	2	5/2	2	g
	2	3/2	2	h
	1	3/2	2	p
3/2	2	1/2	0	1
	1	1/2	0	2
	2	3/2	1	3
	1	3/2	1	4
	0	3/2	1	5
	2	1/2	1	6
	1	1/2	1	7

TABLE X--Continued

$J_T$	$J$	$j$	$\ell$	State Designation ( $M_T = J_T$ )
$3/2$	2	$5/2$	2	8
	1	$5/2$	2	9
	2	$3/2$	2	10
	1	$3/2$	2	11
	0	$3/2$	2	12
$5/2$	2	$1/2$	0	A
	2	$3/2$	1	B
	1	$3/2$	1	C
	2	$1/2$	1	D
	2	$5/2$	2	E
	1	$5/2$	2	F
	0	$5/2$	2	G
	2	$3/2$	2	H
	1	$3/2$	2	P
$7/2$	2	$3/2$	1	I
	2	$5/2$	2	II
	1	$5/2$	2	III
	2	$3/2$	2	IV



$$\int \frac{X_{(1),m}^*}{F_m(r_1)/r_1} [H - E] \sum_n [X_{(1),n} - NX_{(2),n}] dr_1^{-1} = 0 \quad (9.3)$$

wherein the notation  $X_{(i),n}$  implies that the  $i$ -electron is to be treated as the free electron. It should be noted that the integration in Eq. (9.3) is to be performed over all coordinates except  $r_1$ .

The resulting set of coupled radial differential equations may be written in the following form:

$$\mathcal{L}_m^l F_m(r_1) + \sum_n [\mathcal{V}_{mn} F_n(r_1) - r_1 \mathcal{W}_{mn}] = 0. \quad (9.4)$$

The radial differential operator has been defined:

$$\mathcal{L}_m^l = -\frac{1}{2} \frac{d^2}{dr^2} + \frac{l(l+1)}{2r^2} - \frac{Z}{r} - \frac{k_m^2}{2}. \quad (9.5)$$

The matrix elements,  $\mathcal{V}_{mn}$  and  $\mathcal{W}_{mn}$ , are to be interpreted in a manner analogous to  $V_{mn}$  and  $W_{mn}$  in the previous chapter (see Eqs. (8.8) and (8.9)) although now the wave functions are more involved and the integration has been extended to all coordinates except  $r_1$ . That is,

$$\mathcal{V}_{mn}(r_1) = \int \frac{X_{(1),m}^*}{F_m(r_1)} \left[ \sum_{j \neq 1} \frac{1}{r_{1j}} \right] \frac{X_{(1),n}}{F_n(r_1)} r_1^2 dr_1^{-1} \quad (9.6)$$

$$\mathcal{W}_{mn}(r_1) = N \int \frac{X_{(1),m}^*}{F_m(r_1)} [H - E] X_{(2),n} r_1 dr_1^{-1}. \quad (9.7)$$

As has already been discussed, either the post- or prior-interaction

may be selected in the further reduction of Eq. (9.7). Hereafter, for convenience in writing, the subscript 1 will be omitted in Eq. (9.4) and its related definitions, and the radial variable of 1-electron will be denoted simply as  $r$ .

The advantage of choosing the complicated expansion, Eq. (9.2), in lieu of the far-simpler form, Eq. (8.6), becomes apparent when Eqs. (9.6) and (9.7) have been evaluated and the set, Eqs. (9.4), written out in full. In this composite representation, the Hamiltonian operator is diagonal in the  $J_T$  and  $M_T$  quantum numbers and independent of  $M_T$ . Hence Eqs. (9.4) have a block structure, each block representing a particular value of  $J_T$  and  $M_T$  with no coupling matrix elements between equations having different values for these quantum numbers. A particular value of  $J_T$  and  $M_T$  may be selected, and this subset of equations may be solved independent of the remainder of the set.

The evaluation of the matrix elements in Eqs. (9.6) and (9.7) is a most difficult and time-consuming task. At the outset, it is necessary to evaluate these integrals for the basic determinantal functions which comprise the atomic states. (See Eqs. I-5 in Appendix I.) The fundamental potential integrals are of a standard type, and their simplification can be accomplished with formulas discussed by Condon and Shortley, Chapter VI.<sup>53</sup> The corresponding exchange integrals are extremely more involved, and reference should be made to the original paper on OI by Seaton<sup>40</sup> for the appropriate formulas. With these fundamental integrals available, it is still necessary to carry through the several stages of vector-coupling to arrive at the final desired

matrix elements. These elements are tabulated in the following chapters after the appropriate notation and significant approximations have been discussed.

TABLE XI

SELECTED COMPOSITE STATE WAVE FUNCTIONS FOR  $M_T = J_T$ 

$\ell$	$J_T$	State Designation <sup>(a)</sup>	Wave Function <sup>(b)</sup>	$J$
0	1/2	a	$\frac{1}{\sqrt{3}} [ \sqrt{2} \psi_1^1 \Phi_{1/2}^{-1/2}(0) - \psi_1^0 \Phi_{1/2}^{1/2}(0) ]$	1
		b	$\psi_0^0 \Phi_{1/2}^{1/2}(0)$	0
0	3/2	1	$\frac{1}{\sqrt{5}} [ 2 \psi_2^2 \Phi_{1/2}^{-1/2}(0) - \psi_2^1 \Phi_{1/2}^{1/2}(0) ]$	2
		2	$\psi_1^1 \Phi_{1/2}^{1/2}(0)$	1
1	1/2	c	$\frac{1}{\sqrt{5}} [ \sqrt{2} \psi_2^2 \Phi_{3/2}^{-3/2}(1) - \frac{\sqrt{3}}{\sqrt{2}} \psi_2^1 \Phi_{3/2}^{-1/2}(1) + \psi_2^0 \Phi_{3/2}^{1/2}(1) - \frac{1}{\sqrt{2}} \psi_2^{-1} \Phi_{3/2}^{3/2}(1) ]$	2
		d	$\frac{1}{\sqrt{6}} [ \psi_1^1 \Phi_{3/2}^{-1/2}(1) - \sqrt{2} \psi_1^0 \Phi_{3/2}^{1/2}(1) + \sqrt{3} \psi_1^{-1} \Phi_{3/2}^{3/2}(1) ]$	1
		e	$\frac{1}{\sqrt{3}} [ \sqrt{2} \psi_1^1 \Phi_{1/2}^{-1/2}(1) - \psi_1^0 \Phi_{1/2}^{1/2}(1) ]$	1
		f	$\psi_0^0 \Phi_{1/2}^{1/2}(1)$	0

TABLE XI--Continued

$\ell$	$J_T$	State Designation <sup>(a)</sup>	Wave Function <sup>(b)</sup>	$J$
1	3/2	3	$\frac{1}{\sqrt{5}} [ \sqrt{2} \psi_2^2 \Phi_{3/2}^{-1/2}(1) - \sqrt{2} \psi_2^1 \Phi_{3/2}^{1/2}(1) + \psi_2^0 \Phi_{3/2}^{3/2}(1) ]$	2
		4	$\frac{1}{\sqrt{5}} [ \sqrt{2} \psi_1^1 \Phi_{3/2}^{1/2}(1) - \sqrt{3} \psi_1^0 \Phi_{3/2}^{3/2}(1) ]$	1
		5	$\psi_0^0 \Phi_{3/2}^{3/2}(1)$	0
		6	$\frac{1}{\sqrt{5}} [ 2 \psi_2^2 \Phi_{1/2}^{-1/2}(1) - \psi_2^1 \Phi_{1/2}^{1/2}(1) ]$	2
		7	$\psi_1^1 \Phi_{1/2}^{1/2}(1)$	1
		B	$\frac{1}{\sqrt{7}} [ 2 \psi_2^2 \Phi_{3/2}^{1/2}(1) - \sqrt{3} \psi_2^1 \Phi_{3/2}^{3/2}(1) ]$	2
		C	$\psi_1^1 \Phi_{3/2}^{3/2}(1)$	1
1	5/2	D	$\psi_2^2 \Phi_{1/2}^{1/2}(1)$	2
		g	$\frac{1}{\sqrt{15}} [ \psi_2^2 \Phi_{5/2}^{-3/2}(2) - \sqrt{2} \psi_2^1 \Phi_{5/2}^{-1/2}(2) + \sqrt{3} \psi_2^0 \Phi_{5/2}^{1/2}(2) - 2 \psi_2^{-1} \Phi_{5/2}^{3/2}(2) + \sqrt{5} \psi_2^{-2} \Phi_{5/2}^{5/2}(2) ]$	2

TABLE XI--Continued

$\ell$	$J_T$	State Designation <sup>(a)</sup>	Wave Function <sup>(b)</sup>	$J$
2	1/2	h	$\frac{1}{\sqrt{5}} \left[ \sqrt{2} \psi_2^2 \Phi_{3/2}^{-3/2}(2) - \frac{\sqrt{3}}{\sqrt{2}} \psi_2^1 \Phi_{3/2}^{-1/2}(2) \right.$ $\left. + \psi_2^0 \Phi_{3/2}^{1/2}(2) - \frac{1}{\sqrt{2}} \psi_2^{-1} \Phi_{3/2}^{3/2}(2) \right]$	2
		p	$\frac{1}{\sqrt{6}} \left[ \psi_1^1 \Phi_{3/2}^{-1/2}(2) - \sqrt{2} \psi_1^0 \Phi_{3/2}^{1/2}(2) \right.$ $\left. + \sqrt{3} \psi_1^{-1} \Phi_{3/2}^{3/2}(2) \right]$	1
2	3/2	8	$\frac{1}{\sqrt{35}} \left[ 2 \psi_2^2 \Phi_{5/2}^{-1/2}(2) - 3 \psi_2^1 \Phi_{5/2}^{1/2}(2) \right.$ $\left. + 2 \sqrt{3} \psi_2^0 \Phi_{5/2}^{3/2}(2) - \sqrt{10} \psi_2^{-1} \Phi_{5/2}^{5/2}(2) \right]$	2
		9	$\frac{1}{\sqrt{15}} \left[ \psi_1^1 \Phi_{5/2}^{1/2}(2) - 2 \psi_1^0 \Phi_{5/2}^{3/2}(2) \right.$ $\left. + \sqrt{10} \psi_1^{-1} \Phi_{5/2}^{5/2}(2) \right]$	1
		10	$\frac{1}{\sqrt{5}} \left[ \sqrt{2} \psi_2^2 \Phi_{3/2}^{-1/2}(2) - \sqrt{2} \psi_2^1 \Phi_{3/2}^{1/2}(2) \right.$ $\left. + \psi_2^0 \Phi_{3/2}^{3/2}(2) \right]$	2
		11	$\frac{1}{\sqrt{5}} \left[ \sqrt{2} \psi_1^1 \Phi_{3/2}^{1/2}(2) - \sqrt{3} \psi_1^0 \Phi_{3/2}^{3/2}(2) \right]$	1
		12	$\psi_0^0 \Phi_{3/2}^{3/2}(2)$	0

TABLE XI--Continued

$\ell$	$J_T$	State Designation <sup>(a)</sup>	Wave Function <sup>(b)</sup>	$J$
2	5/2	E	$\frac{1}{\sqrt{14}} [ \sqrt{3} \psi_2^2 \Phi_{5/2}^{1/2}(2) - \sqrt{6} \psi_2^1 \Phi_{5/2}^{3/2}(2) + \sqrt{5} \psi_2^0 \Phi_{5/2}^{5/2}(2) ]$	2
		F	$\frac{1}{\sqrt{7}} [ \sqrt{2} \psi_1^1 \Phi_{5/2}^{3/2}(2) - \sqrt{5} \psi_1^0 \Phi_{5/2}^{5/2}(2) ]$	1
		G	$\psi_0^0 \Phi_{5/2}^{5/2}(2)$	0
		H	$\frac{1}{\sqrt{7}} [ 2 \psi_2^2 \Phi_{3/2}^{1/2}(2) - \sqrt{3} \psi_2^1 \Phi_{3/2}^{3/2}(2) ]$	2
		P	$\psi_1^1 \Phi_{3/2}^{3/2}(2)$	1
2	7/2	II	$\frac{1}{3} [ 2 \psi_2^2 \Phi_{5/2}^{3/2}(2) - \sqrt{5} \psi_2^1 \Phi_{5/2}^{5/2}(2) ]$	2
		III	$\psi_1^1 \Phi_{5/2}^{5/2}(2)$	1
		IV	$\psi_2^2 \Phi_{3/2}^{3/2}(2)$	2

(a) See Table X.

(b) See discussion for explanation of the notation, and Appendix I for the component functions.

## CHAPTER X

### SPECIAL APPROXIMATIONS AND PROCEDURES

This chapter has been inserted as a digression from the normal development to discuss certain approximations which are necessary in solving the scattering equations, to introduce general notation which is to be involved in later chapters, and to present certain calculations which are found to be better performed preliminary to the principal solutions. In this manner, the general discussions can be made more compact, be better organized, and be made to concentrate more fully on the basic aspects of the special techniques involved.

The expansion indicated in Eq. (8.13) results essentially in a decomposition of the excitation cross sections into contributions from electrons with different values of relative orbital angular momentum (represented through the quantum number  $\ell$ ). It is a practical necessity that the series be terminated after a finite number of terms. For a neutral atom, the interaction is of sufficiently short range that only very close encounters are expected to contribute significantly to the cross sections. Distant encounters are effected by particles of large  $\ell$ , hence the series is expected to converge with reasonable rapidity and the cut-off has theoretical justification.

In the prior work on atomic oxygen,<sup>40,41,42</sup> the contributions from  $\ell = 1$  have been found to dominate the cross sections (in part



due to the previously-mentioned strong symmetrical exchange effects), with  $\ell = 2$  of only minor importance. Hence, as for the majority of electron-neutral atom collisions, the expansion cut-off was made near this point. In contrast, for OIII and similar ions with long-range Coulomb interactions, the effects of  $\ell = 3$  and  $4$  should perhaps be also considered. However, in view of other limitations upon the expected accuracy of the calculation and the increased complexity of the wave function angular dependence, an extension of the analysis to these higher- $\ell$  values is thought to be of minor importance in the majority of cases of current interest. In the present investigation, only contributions for  $\ell \leq 2$  have been considered.

In the majority of calculations for electron-neutral atom collisions, it has been deemed an acceptable approximation to ignore interaction matrix elements which are non-diagonal in the  $\ell$  quantum number. In other words, transitions for which there is no change in the relative orbital angular momentum of the colliding electron are assumed extremely more probable than those for which there is a change in the  $\ell$ -value, and only the former are included in the final analysis. This approximation was introduced in earlier work on OI, has been generally applied in this type of collision problem in the past, and is often adopted in preliminary investigations upon more complex systems (such as atom-molecule and molecule-molecule collisions).

The transitions of interest for OI are optically forbidden; an expansion of the interaction shows that  $\Delta \ell = 0, \pm 2$ . Rough estimates indicate that any interaction matrix element is dependent upon the amount of overlap for the wave functions of the incident and

scattered electrons. For small values of  $\ell$ , it is to be expected that the overlap for wave functions with  $\Delta \ell = \pm 2$  is small compared with that for which  $\Delta \ell = 0$ , and the corresponding matrix elements for the former are thought to be of minor relative importance. This approximation has been employed in the present work, with the resulting error believed to be well within the limits imposed by other phases of the calculation.

A minor difficulty in the present calculation has been the non-availability of bound radial wave functions for the spin-multiplet states of the  $^3P$  multiplet for neutral atomic oxygen. Accurate analytic SCF functions for  $^3P$  of OI have been calculated by Clementi, Roothaan and Yoshimine<sup>54</sup> and are summarized in Appendix II. It is believed to be well within the present order of approximation to ignore the differences between the true radial wave functions for the various J-states, and to substitute for them the above-described analytic functions. Accordingly, the radial functions for the various occupied orbitals are denoted simply by  $S_1$ ,  $S_2$ , and  $P$ , for the (1s), (2s), and (2p) orbitals respectively, and imply the use of the radial functions discussed in Appendix II. Seaton<sup>40,41,42</sup> has performed a similar approximation in situations where individual radial functions for the involved states were available; the approximation is believed to result in insignificant error and certainly simplifies the numerical procedures to a degree sufficient to warrant its use.

Before presenting the scattering equations in detail in the following chapters, it is appropriate at this point to summarize

the notation which has been adopted for the individual contributions to the potential and exchange matrix elements. The notation is equivalent to that employed by Seaton,<sup>40</sup> and is consistent with the work of Hartree<sup>55</sup> on atomic calculations. In the following, the capital letters A, B, C, . . . denote radial functions:

$$\Delta(A, B) = \int_0^{\infty} A(r_1) B(r_1) dr_1 \quad (10.1)$$

$$\begin{aligned} y_t(A, B | r_1) = & \frac{1}{r_1^{t+1}} \int_0^{r_1} A(r_2) B(r_2) r_2^t dr_2 \\ & + r_1^t \int_{r_1}^{\infty} \frac{A(r_2) B(r_2)}{r_2^{t+1}} dr_2 \end{aligned} \quad (10.2)$$

$$\begin{aligned} R_t(A, B, C, D) = & \int_0^{\infty} A(r_1) C(r_1) y_t(B, D | r_1) dr_1 \\ = & \int_0^{\infty} B(r_1) D(r_1) y_t(A, C | r_1) dr_1 \end{aligned} \quad (10.3)$$

$$\begin{aligned} \mathcal{H}_1^l(A, B) = & \int_0^{\infty} A(r_1) \left[ -\frac{1}{2} \left( \frac{d^2}{dr_1^2} - \frac{l(l+1)}{r_1^2} \right) - \frac{Z}{r_1} \right] \\ & \times B(r_1) dr_1 \end{aligned} \quad (10.4)$$

### Radial Potential Functions

Before commencing a formal solution for the set of radial differential equations, it was found very convenient for numerical reasons to perform a preliminary determination of the contributions to the interaction potential from the (1s), (2s) and (2p) bound electronic orbitals. It will be seen that the spherically-symmetric components,  $y_0(S_1S_1)$ ,  $y_0(S_2S_2)$ , and  $y_0(PP)$ , contribute only to the diagonal potential matrix elements and hence essentially provide only distortion of the free electron wave functions. On the other hand, the  $y_2(PP)$  terms also provide entries to the potential coupling elements, and have a more direct influence upon the magnitude of the cross section. It is worthwhile in any detailed investigation of the interaction potential, and necessary in all numerical computational procedures, that the far-field behaviors and small- $r$  expansions for these functions be thoroughly examined.

If the analytic form for the bound wave functions (see Appendix II) is used, the above functions can be represented in closed form. These expressions are lengthy, and are discussed briefly in Appendix III. For the numerical work, it was found desirable to exhibit these functions in forms which indicate explicitly their far-field behaviors. Accordingly:

$$y_0(S_1S_1) = Y1S + \frac{1}{r}, \text{ etc.}, \quad (10.5)$$

$$y_2(PP) = Y22P + \frac{1.974}{r^3}. \quad (10.6)$$

The functions,  $Y22P$ ,  $Y1S$ , etc., were evaluated numerically as functions of  $r$  from the formulas given in Appendix III, and inserted in tabular

form into the various computer programs. It was found that these latter functions yield insignificant contributions beyond  $r = 12.0$  au. and hence the above procedure proved to be very practical.

As the terms of the form, Eq. (10.5), appear only with the diagonal matrix elements, the  $1/r$  components explicitly cancel the  $Z/r$  contributions from the nuclear charge which appear through Eq. (9.5). The net result is a direct dependence of the potential distortion upon the  $Y_{1S}$ , etc., functions. The spherically-symmetric Coulomb potential which will appear on the diagonal of the potential matrix and which will represent the average potential of an electron in the field of a neutral oxygen atom may be defined in the following manner:

$$\begin{aligned} U(r) &= 2 y_0(S_1 S_1) + 2 y_0(S_2 S_2) + 4 y_0(PP) - \frac{8}{r} \\ &= 2 (Y_{1S} + Y_{2S} + 2 Y_{2P}) . \end{aligned} \quad (10.7)$$

This function was utilized in the calculation of the effective potentials which were illustrated in Chapter VII.

The small-value expansions for  $y_2(PP)$ ,  $y_0(S_1 S_1)$ , etc. are of importance in determining the starting solutions for the numerical integration of the radial differential equations. Special difficulties are encountered with the  $y_2(PP)$  function;  $Y_{2P}$  is a large negative number near the origin, and is meant to subtract from the long-range  $1/r^3$  term. However, with the limited computing accuracy available, this cancellation is not complete and results in an extremely large remainder. Thus,  $y_2(PP)$  as calculated from Eq. (10.6) diverges near the origin whereas in fact it should approach zero as  $r^2$ . This error for small  $r$  must be corrected in advance with a special expansion

valid near the origin; the neglect of this correction appears most significantly in various integrals which have  $y_2(\text{PP})$  as part of their integrand. The appropriate expansions are also discussed in Appendix III.

## CHAPTER XI

### CROSS SECTIONS FOR EXCITATION

#### The Scattering and Related Matrices

In time-independent theory, the peculiar properties of a collision problem are identified through the specification of the boundary conditions imposed upon the system. In such a theoretical development, the system consists of the target atom of interest, with a continuous stream of particles (electrons) incident along the space  $\hat{z}$  axis and being scattered by the atom. The incident particle stream is represented by a plane wave, and the scattered particles are described by a superposition of outgoing waves emerging from the origin at the atomic nucleus. The current analysis utilizes the partial wave technique; the incident plane wave is further decomposed into a sum of partial waves, each characteristic of a certain relative orbital angular momentum. The individual terms of this sum are then coupled with other angular momenta of the system to form the basis functions for the composite representation.

In formal scattering theory,<sup>12,56,45</sup> the essential features of the collision problem are most elegantly developed through the formalism of the scattering matrix. A particular set of quantum numbers which describes the state of the system at infinite separation of the

two major constituents defines a unique reaction channel. If "n" specifies a certain initial channel, the probability that after collision the system will have outgoing waves in channel "m" is described by the element,  $S(m,n)$ , of the Scattering (or S-) Matrix.  $S(m,n)$  is, in reality, the ratio of the amplitude of the outgoing wave in channel "m" to that of the incoming wave in channel "n". The cross section for this particular transition,  $n \rightarrow m$ , is proportional to  $|S(m,n)|^2$ .

The entire matrix which takes into account all possible channels available at the given total energy is sufficient to describe completely the observable properties of the scattering process. For an electron-atom collision, the cross section,  $Q(v, v')$ , for a transition from the atomic state,  $v'$ , to the state,  $v$ , may be found by considering the S-matrix elements connecting all channels which have the particular atomic states represented, summing the contributions to the cross section from the final channels, and averaging over the respective initial channels.

Instead of determining  $Q(v, v')$  directly, it has been found more convenient to express the results of the calculations in terms of  $\Omega(v, v')$ , a dimensionless parameter referred to as the "collision parameter" or "collision strength." The corresponding cross section can be readily obtained from this parameter:

$$Q(v, v') = \frac{\pi \Omega(v, v')}{\omega_{v'} k_{v'}^2}, \quad (11.1)$$

where  $\omega_{v'}$  is the degeneracy of the initial atomic state. Detailed balancing requires the collision strength to be symmetric:



$$\Omega(v, v') = \Omega(v', v). \quad (11.2)$$

Approximate atomic bound-state wave functions and post-prior discrepancies can cause this parameter to deviate from perfect symmetry; the latter degree of asymmetry may be viewed as an indication of the approximate error introduced into the calculation by these effects.

The atomic transitions of concern in the present work are between the  $J = 0, 1, 2$  levels of the  $^3P$  multiplet of OI. In the representation characteristic of  $J_T$  and  $M_T$ , the collision strength for a transition  $J' \rightarrow J$  is given by:

$$\Omega(J, J') = \sum_l \Omega_l(J, J') \quad (11.3)$$

$$\Omega_l(J, J') = \frac{1}{2} \sum_{j, j', J_T} (2J_T + 1) |T(\alpha' J j J_T, \alpha' J' j' J_T)|^2 \quad (11.4)$$

wherein the approximation of diagonality in the quantum number,  $l$ , has been assumed valid, and  $\alpha'$  is intended to represent the remainder of the array of quantum numbers specifying the composite state. The Transmission (or T-) Matrix utilized in Eq. (11.4) is simply related to the S-matrix through the unit matrix,  $\underline{1}$ ,:

$$\underline{T} = \underline{1} - \underline{S}. \quad (11.5)$$

The present calculation requires, in part, the numerical solution of a system of coupled radial differential equations. In general,  $S(m, n)$  and  $T(m, n)$  are complex, and a solution in terms of these quantities would require special techniques not readily available

on most computers. It is possible to limit the analysis to real functions by considering the collision strengths as expressed in terms of a third matrix, the Reactance (or R-) Matrix:

$$\underline{T} = \frac{-2i\underline{R}}{\underline{1} - i\underline{R}} \quad (11.6)$$

The R-matrix can be shown to be both real and symmetric, and its elements are evaluated by imposing the following boundary conditions on the system of equations:

$$F^R(m,n \mid r = 0) = 0 \quad (11.7)$$

$$F^R(m,n \mid r) \underset{r \rightarrow \infty}{\sim} \frac{1}{\sqrt{k_m}} \left[ \sin(k_n r - \frac{l_n \pi}{2}) \delta_{m,n} + R(m,n) \cos(k_m r - \frac{l_m \pi}{2}) \right] \quad (11.8)$$

The notation in Eqs. (11.7) and (11.8) implies that "m" is the final state and "n" is the initial state of the system, and  $\delta_{m,n}$  refers to the Kronecker delta.

In actual practice, the boundary conditions are applied by requiring the radial solutions to have the asymptotic form:

$$F^R(m,n \mid r) \underset{r \rightarrow \infty}{\sim} A \left[ \cos \eta P_{l_m + \frac{1}{2}}(k_m r) + (-1)^{l_m} \sin \eta P_{-(l_m + \frac{1}{2})}(k_m r) \right], \quad (11.9)$$

where

$$P_{l + \frac{1}{2}}(kr) = \sqrt{\frac{\pi kr}{2}} J_{l + \frac{1}{2}}(kr), \text{ etc., } \quad (11.10)$$

In the above expression,  $J_{\ell+\frac{1}{2}}(kr)$  is the well-known Bessel function of half-an-odd-integer order, and has the asymptotic behavior demanded by Eq. (11.8). The required R-matrix elements are thus evaluated in terms of the two parameters,  $A$ , corresponding to an amplitude which must be normalized in accordance with the incoming particle flux, and  $\eta$ , a phase shift of the function from the normal free-particle solution. The desired collision strengths then readily follow from Eqs. (11.3), (11.4) and (11.6). In the actual numerical work, the  $F_m$  functions are generally considered as linear combinations of other functions (to be denoted by  $G_i$ ), and the asymptotic conditions specified by Eq. (11.9) are applied to the latter functions. The transformation can then be utilized to insure the satisfaction of Eq. (11.8).

#### Born Approximation

Under certain special circumstances when the potential and exchange matrix elements are small, it is possible to arrive at a reliable estimate for the cross section without a detailed solution of the system of differential equations. These weak-coupling approximations are valuable tools where applicable, but extreme care must be observed that the required criteria for their validity is satisfied. There exist certain cases (an important example being transitions between the ground configuration  $^3P$ ,  $^1D$  and  $^1S$  levels of  $OI$ )<sup>40</sup> where exchange coupling dominates the cross sections, where the cross sections are determined primarily from the interaction over a small range of  $r$  and in this interval the weak-coupling approximations greatly over-estimate them, exceeding the conservation limit by several orders of magnitude.

The simplest and most widely used of the weak-coupling approximations is that due to Born. For this technique to be of value, the potential distortion,  $\mathcal{U}_{mm}$ , must be small, the potential coupling,  $\mathcal{V}_{mn}$ , must be weak, and all exchange terms,  $\mathcal{W}_{mn}$ , must be negligible relative to the  $\mathcal{V}_{mn}$ . Under the Born approximation, one can ignore all  $\mathcal{V}_{mn}$  elements except those directly connecting the two states of interest. The formalism establishes the cross section through an integration of this potential coupling term times the product of the initial and final wave functions for the projectile electron. In addition, the latter wave functions are chosen as those of a free particle (neglecting the potential distortion). This approximation (as well as the other weak-coupling approximations) violates the conservation conditions, but this is not serious if  $\underline{T} \ll \underline{1}$ .

Under the Born approximation, the required collision strengths may be evaluated from the formulas presented earlier in this chapter by the substitution:

$$\underline{T} = -2i \underline{B} \quad (11.11)$$

where the elements of  $\underline{B}$  are the Born integrals:

$$\begin{aligned} & B(J_{T'M_T} J j \ell \dots, J_{T'M_T} J' j' \ell' \dots) = \\ & -\pi \int_0^\infty J_{\ell+\frac{1}{2}}(kr) \mathcal{V}(J_{T'M_T} J j \ell \dots, J_{T'M_T} J' j' \ell' \dots) J_{\ell'+\frac{1}{2}}(k'r) r dr. \end{aligned} \quad (11.12)$$

For electron neutral-atom collisions, the above approximation can generally be applied for partial waves of large  $\ell$  where the electron remains sufficiently removed from the scattering center that the

excitation probability is small. In such cases, the short-range exchange forces are ineffective and there is insignificant distortion in the projectile electron's wave function compared to that of a free particle. For OI transitions, the contributions to the collision strengths for  $\ell = 2$  were evaluated with this simple approximation.

### Distorted Wave Approximation

An essential feature of the Born approximation is that the incident and scattered waves are taken to be plane waves. The next degree of refinement would be to retain the weak-coupling form for the collision strengths, but to consider the incident and scattered waves to be distorted by the fields of the scattering center. This correction to the Born approximation could be highly significant when the major contributions to the cross sections arise from regions close to the neutral atom where the distortion would be more pronounced. Yamanouchi, et al.,<sup>38</sup> applied this approximation to the  $^3P$ ,  $^1D$ ,  $^1S$  transitions of OI, but the results were inconclusive because of errors regarding the orthogonality of the free and bound wave functions. Seaton<sup>40,41,42</sup> included exchange distortion in several calculations of OI, OII, and OIII transition probabilities with this method; however, other approximations introduced sufficient inconsistencies to cause doubt as to the overall accuracy achieved.

In the formal analysis, Eq. (11.11) may still be retained, but the integrals defined by Eq. (11.12) must be modified. In particular, allowance should be made for exchange as well as potential coupling between the two states involved. Let  $\mathcal{U}_{mn}$  represent the series of coupling terms between composite states  $m$  and  $n$  as given by the

general form, Eq. (9.4). For a plane wave, the  $l$ -partial wave radial component can be taken as that solution of

$$\left[ \frac{d^2}{dr^2} - \frac{l(l+1)}{r^2} + k^2 \right] F(l) = 0 \quad (11.13)$$

which behaves asymptotically as

$$F(l) \sim \frac{1}{\sqrt{k}} \sin(kr + \eta). \quad (11.14)$$

These requirements are fulfilled by the function,

$$F(l) = \sqrt{\frac{\pi r}{2}} J_{l+\frac{1}{2}}(kr), \quad (11.15)$$

which appears in Eq. (11.12). If  $\mathcal{Y}(r)$  is a solution of an equation of the form, Eq. (11.13), with exchange and/or potential distortion terms added, and if  $\mathcal{Y}(r)$  is normalized for the asymptotic behavior specified by Eq. (11.14), it is possible to determine the improved collision strengths by replacing Eq. (11.12) with

$$B(m,n) = -2 \int_0^\infty \mathcal{Y}_m(k_m r) \mathcal{U}(m,n) \mathcal{Y}_n(k_n r) dr \quad (11.16)$$

where  $m$  and  $n$  represent the arrays of quantum numbers for the two states of interest.

The approximation just described is referred to in the literature by a variety of names, depending upon the nature of the distortion and coupling terms being considered. In the present work, it will be

designated simply by the "Distorted Wave Approximation," although, in reality, the refinements that have been incorporated into the present analysis extend beyond the original concept of such a labeling. This approximation has been utilized in phases of the numerical work concerning the p-wave interactions.

## CHAPTER XII

### COLLISION STRENGTHS FOR S-WAVE

The set of equations expressing the contributions to the cross section from the s-wave (the incident partial wave with  $\ell = 0$ ) has a simple form. Only  $J_T = 1/2$  and  $3/2$  blocks have coupling for this quantum number between the  $J = 0, 1, 2$  atomic levels, and each of these blocks consists of only two equations. The basic radial equations written in a general notation are:

$$\mathcal{L}_m^o F_m + \sum_n [\mathcal{V}_{mn} F_n - r \mathcal{W}_{mn}] = 0 \quad (12.1)$$

$$\mathcal{V}_{mn} = \rho_{mn} [4 y_o(\text{PP}) + 2 y_o(s_1 s_1) + 2 y_o(s_2 s_2)] \quad (12.2)$$

$$\begin{aligned} r \mathcal{W}_{mn} = & \alpha_{mn} [y_1(\text{PF}_n)P - R_1(s_1 \text{PPF}_n)s_1 - R_1(s_2 \text{PPF}_n)s_2] \\ & + \rho_{mn} \left\{ [y_o(s_1 F_n) + \lambda_{mn}^{(1)}(s_1 F_n)] s_1 \right. \\ & \left. + [y_o(s_2 F_n) + \lambda_{mn}^{(2)}(s_2 F_n)] s_2 \right\}, \end{aligned} \quad (12.3)$$

with



$$\begin{aligned}
\lambda_{mn}^{(1)}(S_1 F_n) &= \mathcal{H}_2^0(S_1 F_n) - \frac{k_n^2}{2} \Delta(S_1 F_n) + 4 R_o(PS_1 PF_n) \\
&+ R_o(S_1 S_1 S_1 F_n) + 2 R_o(S_2 S_1 S_2 F_n) - R_o(S_1 S_2 S_2 F_n)
\end{aligned}
\tag{12.4}$$

$$\begin{aligned}
\lambda_{mn}^{(2)}(S_2 F_n) &= \mathcal{H}_2^0(S_2 F_n) - \frac{k_n^2}{2} \Delta(S_2 F_n) + 4 R_o(PS_2 PF_n) \\
&+ R_o(S_2 S_2 S_2 F_n) + 2 R_o(S_1 S_2 S_1 F_n) - R_o(S_2 S_1 S_1 F_n).
\end{aligned}
\tag{12.5}$$

The various coefficients are summarized in Table XII. It should be noted that within a  $J_T$  block there is only exchange coupling, with the potential elements providing only distortion. Hence, the coupling interactions are of very short range, and good numerical results can be achieved with a reasonably low limit on the radial variable.

A preliminary approximation was invoked whereby the energy difference between the incident and scattered electron is neglected, and the  $J = 0, 1, 2$  atomic states are assumed to have equal energies. Under this Exact Resonance (or simply E. R. ) approximation,  $k_m^2 = k_n^2 = k^2$ . Then, in a particular  $J_T$  block, a simple transformation of dependent variables allows a complete de-coupling of the two equations and permits greater ease in obtaining a numerical solution. The respective transformations are:

$$J_T = 1/2:$$

$$\begin{aligned}
F_a &= -\sqrt{2} \ n_1 G_1 + \quad \quad n_2 G_2 \\
F_b &= \quad \quad n_1 G_1 + \sqrt{2} \ n_2 G_2
\end{aligned}
\tag{12.6}$$

TABLE XII  
 COEFFICIENTS IN THE POTENTIAL AND EXCHANGE MATRIX ELEMENTS FOR S-WAVE  
 ( $M_T = J_T$ )

$J_T$	$m,n$	$\rho_{mn}$	$\alpha_{mn}$
$1/2$	a,a	1	$1/3$
	a,b	0	$\sqrt{2}/3$
	b,a	0	$\sqrt{2}/3$
	b,b	1	$2/3$
$3/2$	1,1	1	$1/6$
	1,2	0	$\sqrt{5}/6$
	2,1	0	$\sqrt{5}/6$
	2,2	1	$5/6$

$$J_T = 3/2:$$

$$F_1 = -\sqrt{5} \, n_3 G_1 + n_4 G_2 \quad (12.7)$$

$$F_2 = n_3 G_1 + \sqrt{5} \, n_4 G_2$$

where  $G_1$  and  $G_2$  are the solutions of

$$\begin{aligned} [\mathcal{L}^0 + 4 y_0(\text{PP}) + 2 y_0(S_1 S_1) + 2 y_0(S_2 S_2)] G_1 &= [y_0(S_1 G_1) \\ &+ \lambda^{(1)}(S_1 G_1)] S_1 + [y_0(S_2 G_1) + \lambda^{(2)}(S_2 G_1)] S_2 \end{aligned} \quad (12.8)$$

$$\begin{aligned} [\mathcal{L}^0 + 4 y_0(\text{PP}) + 2 y_0(S_1 S_1) + 2 y_0(S_2 S_2)] G_2 &= [y_0(S_1 G_2) \\ &+ \lambda^{(1)}(S_1 G_2)] S_1 + [y_0(S_2 G_2) + \lambda^{(2)}(S_2 G_2)] S_2 + y_1(\text{PG}_2)P. \end{aligned} \quad (12.9)$$

In Eq. (12.8),  $\lambda^{(1)}$  and  $\lambda^{(2)}$  are as defined by Eqs. (12.4) and (12.5) with the "m" subscript now redundant. The  $\lambda^{(1)}$  and  $\lambda^{(2)}$  in Eq. (12.9) have been conveniently modified:

$$\lambda^{(1)}(S_1 G_2) = \lambda^{(1)}(S_1 G_2) - R_1(S_1 \text{PPG}_2) \quad (12.10)$$

$$\lambda^{(2)}(S_2 G_2) = \lambda^{(2)}(S_2 G_2) - R_1(S_2 \text{PPG}_2).$$

The parameters,  $n_1$ , etc., determine the amplitudes of the  $G$  functions and are dependent upon the boundary conditions; that is, they are specified through the imposition of Eq. (11.8) to the  $F_m$  functions.

Care should be taken not to confuse the above  $n_i$  parameters and  $G_i$  functions with similar notation (adopted for convenience in writing) employed in the equivalent transformations for the p-wave equations.

The methods used in the solution of Eqs. (12.8) and (12.9) are straight-forward numerical iteration procedures, and rapid convergence was attained with the special techniques described in Chapter XVI. The application of the boundary conditions yields the amplitudes and phases for the two functions,  $G_1$  and  $G_2$ ; these will be referred to as  $A_1$ ,  $\eta_1$ ,  $A_2$ , and  $\eta_2$  in the discussion presented in this chapter.

There is one aspect of the numerical procedures that deserves special emphasis at this point, and that is the treatment of the  $\lambda$  parameters. If the terms in Eq. (12.8) are multiplied on the left by  $S_1$ , and an integration performed over the radial variable, it is found that, as far as this differential equation is concerned, the particular value of  $\lambda^{(1)}(S_1 G_1)$  is arbitrary and indeterminant. A similar conclusion can be drawn for  $\lambda^{(2)}(S_2 G_1)$ ; likewise for  $\lambda^{(1)}(S_1 G_2)$  and  $\lambda^{(2)}(S_2 G_2)$  in Eq. (12.9). Consider now the Hartree-Fock radial differential equations for  $S_1$  and  $S_2$  as discussed in Appendix IV. By multiplying this  $S_1$  equation through by  $G_1$  on the left and integrating as above, an alternative expression for  $\lambda^{(1)}(S_1 G_1)$  can be obtained. The other parameters may also be evaluated in like manner, yielding the following:

$$\begin{aligned}
\lambda^{(1)}(S_1 G_1) &= (2/3)R_1(S_1 PPG_1) - (1/2)(\epsilon_{1s} + k^2) \Delta(S_1 G_1) \\
\lambda^{(2)}(S_2 G_1) &= (2/3)R_1(S_2 PPG_1) - (1/2)(\epsilon_{2s} + k^2) \Delta(S_2 G_1) \\
&\hspace{25em} (12.11) \\
\lambda^{(1)}(S_1 G_2) &= -(1/3)R_1(S_1 PPG_2) - (1/2)(\epsilon_{1s} + k^2) \Delta(S_1 G_2) \\
\lambda^{(2)}(S_2 G_2) &= -(1/3)R_1(S_2 PPG_2) - (1/2)(\epsilon_{2s} + k^2) \Delta(S_2 G_2).
\end{aligned}$$

Eqs. (12.11) can be used to uniquely determine the  $\lambda$ 's, however, being arbitrary in the respective scattering differential equations, there remains a degree of freedom available for each parameter. By imposing the side conditions that the  $G_1$  and  $G_2$  functions should be made orthogonal to the  $S_1$  and  $S_2$  bound radial functions, i. e.,

$$\begin{aligned}
\Delta(S_1 G_1) &= 0 & \Delta(S_2 G_1) &= 0 \\
\Delta(S_1 G_2) &= 0 & \Delta(S_2 G_2) &= 0,
\end{aligned}
\tag{12.12}$$

the values for these parameters become:

$$\begin{aligned}
\lambda^{(1)}(S_1 G_1) &= (2/3)R_1(S_1 PPG_1) & \lambda^{(1)}(S_1 G_2) &= -(1/3)R_1(S_1 PPG_2) \\
\lambda^{(2)}(S_2 G_1) &= (2/3)R_1(S_2 PPG_1) & \lambda^{(2)}(S_2 G_2) &= -(1/3)R_1(S_2 PPG_2).
\end{aligned}
\tag{12.13}$$

As described in the chapter which discusses the numerical procedures, the imposition of the conditions given by Eqs. (12.12) at each stage of the iterative process greatly facilitates the rapidity of convergence.

Having obtained the solutions of Eqs. (12.8) and (12.9) in terms of amplitudes and phases at large  $r$ , the elements of the R-matrix must be calculated, and the matrix manipulations implied by Eq. (11.6) performed to yield the ultimate collision strengths. For s-wave, the blocks representing  $J_T = 1/2$  and  $3/2$  involve only a pair of equations each, hence these calculations can be performed analytically without undue labor. For the special case of exact resonance now being considered, the results can be written in a very simple form whereby only the respective phases of  $G_1$  and  $G_2$  are of importance. The R-matrix elements for this special case are listed in Table XIII.

As a brief example of how the elements in Table XIII have been obtained, consider the  $J_T = 1/2$  set of equations with state "a" given as the initial state of the system. The boundary conditions expressed by Eq. (11.8) are established through the choice of  $n_1$  and  $n_2$  in the transformation, Eq. (12.6).

The requirements upon the coefficients of  $\sin(kr)$  become:

$$\begin{aligned} -\sqrt{2} A_1 \cos \mu_1 n_1 + A_2 \cos \mu_2 n_2 &= k^{-1/2} \\ A_1 \cos \mu_1 n_1 + \sqrt{2} A_2 \cos \mu_2 n_2 &= 0, \end{aligned} \quad (12.14)$$

from which  $n_1$  and  $n_2$  can be readily determined. The elements of the R-matrix for this choice of initial state are obtainable from the corresponding coefficients of  $\cos(kr)$ :

$$\begin{aligned} R(a,a) &= \sqrt{k} \left[ -\sqrt{2} n_1 A_1 \sin \mu_1 + n_2 A_2 \sin \mu_2 \right] \\ R(b,a) &= \sqrt{k} \left[ n_1 A_1 \sin \mu_1 + \sqrt{2} n_2 A_2 \sin \mu_2 \right] \end{aligned} \quad (12.15)$$

TABLE XIII

R-MATRIX ELEMENTS FOR S-WAVE WITH THE EXACT RESONANCE APPROXIMATION

$J_T$	Element	$R(m,n)^{(a)}$
1/2	R(a,a)	$(1/3) [ 2 \tan \eta_1 + \tan \eta_2 ]$
	R(b,a)	$(\sqrt{2}/3) [ \tan \eta_2 - \tan \eta_1 ]$
	R(a,b)	$(\sqrt{2}/3) [ \tan \eta_2 - \tan \eta_1 ]$
	R(b,b)	$(1/3) [ \tan \eta_1 + 2 \tan \eta_2 ]$
3/2	R(1,1)	$(1/6) [ 5 \tan \eta_1 + \tan \eta_2 ]$
	R(2,1)	$(\sqrt{5}/6) [ \tan \eta_2 - \tan \eta_1 ]$
	R(1,2)	$(\sqrt{5}/6) [ \tan \eta_2 - \tan \eta_1 ]$
	R(2,2)	$(1/6) [ \tan \eta_1 + 5 \tan \eta_2 ]$

(a) The phases,  $\eta_1$ , and  $\eta_2$ , are the respective asymptotic parameters obtained for  $G_1$  and  $G_2$  in the solution of Eqs. (12.8) and (12.9).

Eqs. (12.15) simplify to yield the first two entries in Table XIII. The remaining elements in the table have been evaluated by extending this procedure to other choices for the initial state of the system.

The final expressions for the collision strengths are best represented in a form which explicitly emphasizes the importance of the difference in phase of the  $G_1$  and  $G_2$  functions:

$$\begin{aligned}\Omega_s(1,2) &= (10/9) \sin^2(\eta_1 - \eta_2) \\ \Omega_s(0,1) &= (8/9) \sin^2(\eta_1 - \eta_2) \\ \Omega_s(0,2) &= 0\end{aligned}\tag{12.16}$$

Here the basic factors which control the cross sections are made apparent. The collision strengths depend heavily upon the asymptotic difference in phase between the  $G_1$  and  $G_2$  solutions; this difference in phase is dictated solely by the effect of the terms,  $y_1(PG_2)P$ ,  $R_1(S_1PPG_2)S_1$  and  $R_1(S_2PPG_2)S_2$ , which appear on the right side of Eq. (12.9). These terms add a particular solution to that obtained by Eq. (12.8), and this particular solution effects the difference in phase and the resulting cross sections. These additional terms in the  $G_2$  differential equation are short-range exchange terms, and depend upon the degree of overlap of the  $G_2$ ,  $P$ ,  $S_1$ , and  $S_2$  functions. This overlap must occur at small distances near where the bound functions peak, and hence is very sensitive to the precise form of the  $G_2$  function in this region. The latter, in turn, is influenced by the short-range exchange- and potential-distortion terms which, although having the same effect upon both the  $G_1$  and  $G_2$  functions, can control in an indirect, but definite, manner the magnitude of the above additional terms and hence the resulting final cross sections.



The results of the numerical work are summarized in Tables XIV and XV; the latter presents the collision strengths  $\Omega_s(1,2)$  and  $\Omega_s(0,1)$  for selected energies of interest. It should be noted that  $\Omega(0,2)$  has no contribution from the s-wave interactions. It is also worthwhile at this point to emphasize the importance of the  $S_1$  and  $S_2$  exchange terms and the related conditions imposed by Eqs. (12.12). As discussed in a previous paragraph, the amount of overlap of the  $G_2$  and  $P$  functions essentially determines the transition probabilities. Requiring orthogonality of  $G_2$  and  $S_2$  effectively requires portions of the  $S_2 G_2$  product in a given interval of  $r$  to cancel corresponding products over some other interval; these products are, of course, more significant in the regions where  $S_2$  has its peaks. It is well-known (and readily verified by plotting the wave functions) that the (2s) and (2p) atomic orbitals have a considerable amount of overlap, hence the above cancellation will, to some degree, extend to integrals which are dependent upon  $G_2$  and  $P$  overlap. The  $S_1$  wave function which peaks at a very small distance from the nucleus is not as important in this respect as the  $S_2$  function. These considerations have proven to be correct in the actual numerical work. Preliminary determinations were made of the collision strengths ignoring the  $S_1$  and  $S_2$  exchange terms and the associated orthogonality conditions. The results exceed those listed in Table XV by over a factor of 5. Hence, a failure to properly consider the effects of the  $(1s)^2 (2s)^2$  inner atomic core could result in an over-estimation of the s-wave collision strengths.

TABLE XIV

COMPUTED PHASES FOR S-WAVE FUNCTIONS UNDER EXACT RESONANCE

Energy (°K)	$\eta_1$	$\eta_2$
10,000	-0.4186	-0.3315
5,000	-0.2974	-0.2335
1,000	-0.1323	-0.1029
500	-0.0945	-0.0737

TABLE XV  
COLLISION STRENGTHS FOR S-WAVE<sup>(a)</sup>

Energy of Scattered Electron (°K)	Exact Resonance		Allowance for Energy Differences	
	$\Omega_s(1,2)$	$\Omega_s(0,1)$	$\Omega_s(1,2)$	$\Omega_s(0,1)$
10,000	0.0084	0.0067	0.0085	0.0067
5,000	0.0045	0.0036	0.0046	0.0037
1,000	0.00096	0.00077	0.00106	0.00081
500	0.00048	0.00038	0.00058	0.00042

(a) The parameter,  $\Omega_s(0,2)$ , is zero and does not contribute to the corresponding cross section.

Effect of Energy Differences

The Exact Resonance approximation which has been used to obtain Eqs. (12.8) and (12.9) can be corrected to allow for energy differences between the various bound atomic states with a technique suggested by Seaton.<sup>40,41</sup> The method is particularly applicable to the current s-wave interactions where only short-range exchange terms contribute to the coupling between states. In the following paragraphs, the subscript on " $k^2$ " refers to the  $J = 0, 1, 2$  specification of the bound atomic state. The suggested procedure is to apply the following transformations to the sets of coupled equations, in lieu of those described by Eqs. (12.6) and (12.7):

$$J_T = 1/2:$$

$$\begin{aligned} F_a(k_1^2) &= -\sqrt{2} n_1 G_1(k_1^2) + n_2 G_2(k_1^2) \\ F_b(k_0^2) &= n_1 G_1(k_0^2) + \sqrt{2} n_2 G_2(k_0^2) \end{aligned} \quad (12.17)$$

$$J_T = 3/2:$$

$$\begin{aligned} F_1(k_2^2) &= -\sqrt{5} n_3 G_1(k_2^2) + n_4 G_2(k_2^2) \\ F_2(k_1^2) &= n_3 G_1(k_1^2) + \sqrt{5} n_4 G_2(k_1^2) . \end{aligned} \quad (12.18)$$

In the above equations,  $G_1(k_0^2)$  implies a solution of Eq. (12.8) with  $k^2 = k_0^2$ , etc.

For the functions defined through Eqs. (12.17) and (12.18) to be valid solutions for the original coupled scattering equations, there is the requirement that the terms appearing on the right sides of Eqs. (12.8) and (12.9) be approximately independent of small variations in

the value of  $k^2$ . (The limit of the magnitude of these variations depends upon the maximum energy difference between the bound atomic states being considered.) The terms in question result from short-range exchange interactions; their magnitudes depend rather heavily upon the behavior of the  $G$  functions near the origin. The necessary conditions for the validity of the approximation can be satisfied by normalizing these functions such that they are independent of  $k^2$  in the vicinity of the origin. Such a restriction is, in reality, a condition upon the small-value expansions for the starting solutions of the  $G$  functions. In practice, this can be accomplished by adopting the same choice of  $A_0$  in Eq. (16.8) for all of the functions, and keeping only the first two terms in this expansion. Two terms have been found sufficient for accurate solutions provided the increment used in the numerical integration is chosen sufficiently small. It should be emphasized that these conditions are generally insufficient in cases where longer-range potential coupling terms are important and significant contributions to the cross sections arise from regions exterior to the atom.

The above procedures were adopted in the numerical solutions for  $G_1$  and  $G_2$ . The resulting functions which appear on the right sides of Eqs. (12.8) and (12.9) were examined for sensitivity to small variations of  $k^2$ , and were found to be unaffected to at least 3 significant figures. With the revised transformations, Eqs. (12.17) and (12.18), the elements of the R-matrix have a more complicated form, but are still capable of analytic manipulation in the subsequent determination of the collision strengths. The results have been included in

Table XV to facilitate comparison with the earlier approximation.

Deviations from the corresponding exact-resonance values should be important only at the lower end of the energy range being considered, and this has proven to be generally true. Calculated collision strengths were found to satisfy detailed balance within the accuracy of the numerical work. However, as is evident from the table, the corrections for energy differences are very small, and could probably be ignored without increasing the margin of error in the analysis.

## CHAPTER XIII

### COLLISION STRENGTHS FOR D-WAVE

The effects of the d-wave interactions (the incident partial wave with  $\ell = 2$ ) can be readily ascertained without undue difficulties. For a neutral atom, these partial cross sections are expected to be small. The interactions are weak, and of relatively short range (as compared, for instance, with collisions of electrons with ions or systems with a permanent dipole moment). The electron having an angular momentum corresponding to  $\ell = 2$  does not directly encounter the atomic force field, but always remains some distance away from the scattering center. For the present situation, this is found sufficient to make the short-range exchange forces ineffective, and significant interactions are to be expected only from the longer-range potential terms. For a neutral atom, even these terms decrease rather rapidly with increase of interparticle separation, behaving asymptotically as  $r^{-3}$ . It is thus sufficient to neglect all coupling interactions except those arising from the potential matrix elements, to assume the validity of the weak-coupling techniques, and to calculate the respective collision strengths by adopting the Born approximation. This approximation was discussed briefly in Chapter XI, and incorporates an additional assumption that diagonal potential and exchange distortion terms are unimportant in altering the form of the d-wave function from the

corresponding wave function for a free particle. This latter point has been checked and verified by Seaton<sup>42</sup> in his investigations of transitions in OI.

Hence, only the potential matrix elements which directly connect the two atomic states of interest need be considered; these elements are found to be proportional to  $y_2(\text{PP})$ . As this is the only  $r$ -dependence appearing in the  $\mathcal{V}_{mn}$ , it is convenient to write the array of matrix elements in a form which explicitly demonstrates this dependence. After defining

$$\mathcal{V}_{mn} = a_{mn} y_2(\text{PP}) , \quad (13.1)$$

the coefficients of interest are listed in Table XVI. Eq. (11.12) can be rewritten in the form:

$$B(m,n) = - a_{mn} \Gamma(m,n) , \quad (13.2)$$

where

$$\Gamma(m,n) = \pi \int_0^{\infty} J_{5/2}(k_m r) y_2(\text{PP}) J_{5/2}(k_n r) r dr, \quad (13.3)$$

and depends only upon the energies of the respective incident and scattered electrons. Hence, for a given total system energy, Eq. (13.3) is completely defined by a specification of the two  $J$  quantum numbers.

After the required summations and algebraic simplifications, the required collision strengths are expressible as follows:



TABLE XVI  
MATRIX ELEMENT COEFFICIENTS FOR POTENTIAL COUPLING TERMS, D-WAVE  
( $M_T = J_T$ )

$J_T$	$m, n$	$a_{mn} = a_{nm}^{(a)}$	$J_T$	$m, n$	$a_{mn} = a_{nm}^{(a)}$
1/2	g,p	$\sqrt{30}/50$	5/2	E,F,	$6\sqrt{6}/175$
	h,p	$3\sqrt{5}/50$		E,G	$4\sqrt{35}/175$
				E,P	$-3\sqrt{21}/175$
3/2	8,9	$6\sqrt{21}/175$		H,F	$-11\sqrt{6}/350$
	8,11	$\sqrt{21}/350$		H,G	$-2\sqrt{35}/175$
	8,12	$\sqrt{210}/175$		H,P	$-\sqrt{21}/50$
	10,9	$-3/50$			
	10,11	$3/25$	7/2	II,III	$-9\sqrt{5}/175$
	10,12	$\sqrt{10}/25$		IV,III	$3\sqrt{5}/175$

(a) Elements connecting the  $J = 0$  and  $J = 1$  atomic states are zero, and are not included in the listing.

$$\begin{aligned}
\Omega_d(1,2) &= (144/35) \quad |\Gamma(1,2)|^2 \\
\Omega_d(0,2) &= (64/35) \quad |\Gamma(0,2)|^2 \\
\Omega_d(0,1) &= 0 \quad .
\end{aligned}
\tag{13.4}$$

Detailed balance immediately follows from the symmetry of the  $a_{mn}$  coefficients and the  $\Gamma(m,n)$  integrals. The non-existence of a contribution from  $\Omega_d(0,1)$  results from a vanishing of the angular factors in the potential coupling elements between these two  $J$  levels.

The  $\Gamma(m,n)$  in Eq. (13.3) must be evaluated by numerical integration, but the procedures are direct and no important difficulties are encountered. Care must be taken to use the small-value expansion of  $y_2(\text{PP})$  near the origin, and simplification of the procedure can be increased with the corresponding asymptotic  $r^{-3}$  form above  $r = 12.0$  au. These considerations, along with a presentation of the associated formulas for  $y_2(\text{PP})$ , are discussed in Chapter X and Appendix III. It was found that allowance could be made for the differences in energy between the atomic states without an increase in the complexity of the analysis, hence these refinements were included in the numerical work. Final values obtained for the collision strengths are summarized in Table XVII. The results are seen to be sufficiently small to justify the validity of the chosen weak-coupling approximation.

TABLE XVII  
COLLISION STRENGTHS FOR D-WAVE, BORN APPROXIMATION<sup>(a)</sup>

Energy of Scattered Electron ( <sup>o</sup> K) <sup>(b)</sup>	$\Omega_d(0,2)$	$\Omega_d(1,2)$
10,000	0.00316	0.00708
5,000	0.00159	0.00358
1,000	0.000291	0.000683
500	0.000122	0.000307

(a) The parameter,  $\Omega_d(0,1)$ , is zero and does not contribute to the corresponding total cross section.

(b) Energy differences were allowed for, i.e.,  $k^2/2$  for the incident electron is greater than this value by the energy difference between the final and initial atomic states.

## CHAPTER XIV

### COLLISION STRENGTHS FOR P-WAVE, STRONG COUPLING METHODS

For the p-wave (the incident partial wave with  $l = 1$ ), there are three values of  $J_T$  which lead to transitions between the  $J = 0, 1$  and  $2$  levels of the  $^3P$  multiplet of  $OI$ , namely  $J_T = 1/2, 3/2$  and  $5/2$ . (See Table X). Each of these sets of coupled equations can be treated separately in the numerical work; for each block the resulting reduced radial differential equations may be expressed in the following compact form:

$$\mathcal{L}_m^1 F_m + \sum_n [\mathcal{V}_{mn} F_n - r \mathcal{W}_{mn}] = 0 \quad (14.1)$$

$$\mathcal{V}_{mn} = \rho_{mn} [4 y_0(PP) + 2 y_0(S_1 S_1) + 2 y_0(S_2 S_2)] + \sigma_{mn} y_2(PP) \quad (14.2)$$

$$\begin{aligned} r \mathcal{W}_{mn} = & [\alpha_{mn} \{ \rho_{mn} y_0(PF_n) + \lambda_{mn}(PF_n) \} + \delta_{mn} y_2(PF_n)] P \\ & + \frac{\rho_{mn}}{3} [y_1(S_1 F_n) S_1 + y_1(S_2 F_n) S_2] \end{aligned} \quad (14.3)$$

where

$$\begin{aligned}
\lambda_{mn}(PF_n) = & \theta_{mn} \left[ \cancel{R}_2^1(PF_n) - \frac{k_n^2}{2} \Delta(PF_n) + 3 R_0(PPPF_n) + 2 R_0(S_1 PS_1 F_n) \right. \\
& + 2 R_0(S_2 PS_2 F_n) - \frac{1}{3} R_1(PS_1 S_1 F_n) - \frac{1}{3} R_1(PS_2 S_2 F_n) \left. \right] \\
& + K_{mn} R_2(PPPF_n). \tag{14.4}
\end{aligned}$$

The values of the various coefficients for the respective  $J_T$  blocks are listed in Table XVIII.

It will be shown that the p-wave interaction is the most significant in establishing the total cross sections. However, these equations are also the most complex, with both exchange and potential coupling of comparable importance. It has been found desirable to employ an assortment of techniques to best evaluate the effects of the different types of coupling terms; at the same time the validity of these methods must also be examined. Due to the length and complexity of the calculations which pertain to the p-wave, a brief outline of the plan of presentation should be most beneficial. The essential features of the discussion in the present and following chapters are as follows:

- (1) First, a transformation is to be described which uncouples the p-wave equations with respect to the important spherically-symmetric exchange terms.
- (2) This transformation is then utilized in obtaining the contributions to the cross sections from states connected under this form of interaction.

TABLE XVIII

COEFFICIENTS IN THE POTENTIAL AND EXCHANGE MATRIX ELEMENTS FOR P-WAVE

$$(M_T = J_T)$$

$J_T$	$m, n$	$\rho_{mn}$	$\sigma_{mn}$	$\alpha_{mn}$	$\beta_{mn}$	$\delta_{mn}$	$\kappa_{mn}$
1/2	c, c	1	7/50	1/6	1	19/60	-3/50
	c, d	0	$3\sqrt{5}/50$	$\sqrt{5}/2$	1	$\sqrt{5}/20$	-9/50
	c, e	0	$3\sqrt{10}/50$	1	0	0	$3\sqrt{10}/50$
	c, f	0	$2\sqrt{5}/25$	$\sqrt{5}/3$	1	$\sqrt{5}/30$	-3/50
	d, c	0	$3\sqrt{5}/50$	$\sqrt{5}/2$	1	$\sqrt{5}/20$	-9/50
	d, d	1	-1/10	-1/2	1	1/4	1/10
	d, e	0	$\sqrt{2}/10$	1	0	0	$\sqrt{2}/10$
	d, f	0	0	-1	1	-1/10	-3/10
	e, c	0	$3\sqrt{10}/50$	1	0	0	$3\sqrt{10}/50$
	e, d	0	$\sqrt{2}/10$	1	0	0	$\sqrt{2}/10$
	e, e	1	0	1	1	2/5	-2/5
	e, f	0	0	1	0	0	0
	f, c	0	$2\sqrt{5}/25$	$\sqrt{5}/3$	1	$\sqrt{5}/30$	-3/50
	f, d	0	0	-1	1	-1/10	-3/10
	f, e	0	0	1	0	0	0
	f, f	1	0	1/3	1	1/3	-3/5

TABLE XVIII--Continued

$J_T$	$m, n$	$\rho_{mn}$	$\sigma_{mn}$	$\alpha_{mn}$	$\beta_{mn}$	$\delta_{mn}$	$\kappa_{mn}$
3/2	3,3	1	0	-2/3	1	13/75	-6/25
	3,4	0	3/25	1	0	3/25	0
	3,5	0	$\sqrt{10}/25$	$\sqrt{10}/6$	1	$-\sqrt{10}/75$	3/25
	3,6	0	-7/50	-5/6	1	-17/150	-21/125
	3,7	0	$-3\sqrt{5}/50$	$-\sqrt{5}/2$	1	$-\sqrt{5}/50$	-3/25
	4,3	0	3/25	1	0	3/25	0
	4,4	1	2/25	1	1	4/25	-2/25
	4,5	0	0	1	0	$3\sqrt{10}/50$	$-3\sqrt{10}/50$
	4,6	0	-9/50	1	0	3/50	-6/25
	4,7	0	$-\sqrt{5}/50$	1	0	$-3\sqrt{5}/50$	$\sqrt{5}/25$
	5,3	0	$\sqrt{10}/25$	$\sqrt{10}/6$	1	$-\sqrt{10}/75$	3/25
	5,4	0	0	1	0	$3\sqrt{10}/50$	$-3\sqrt{10}/50$
	5,5	1	0	5/6	1	7/30	-6/25
	5,6	0	$-\sqrt{10}/25$	$\sqrt{10}/12$	1	$-\sqrt{10}/150$	-3/5
	5,7	0	0	$\sqrt{2}/4$	1	$\sqrt{2}/10$	-3/5
	6,3	0	-7/50	-5/6	1	-17/150	-21/125
	6,4	0	-9/50	1	0	3/50	-6/25
	6,5	0	$-\sqrt{10}/25$	$\sqrt{10}/12$	1	$-\sqrt{10}/150$	-3/5
	6,6	1	0	7/12	1	103/300	-156/350
	6,7	0	0	$-\sqrt{5}/4$	1	$-\sqrt{5}/100$	-6/25

TABLE XVIII--Continued

$J_T$	$m, n$	$\rho_{mn}$	$\sigma_{mn}$	$\alpha_{mn}$	$\theta_{mn}$	$\delta_{mn}$	$\kappa_{mn}$
3/2	7,3	0	$-3\sqrt{5}/50$	$-\sqrt{5}/2$	1	$-\sqrt{5}/50$	$-3/25$
	7,4	0	$-\sqrt{5}/50$	1	0	$-3\sqrt{5}/50$	$\sqrt{5}/25$
	7,5	0	0	$\sqrt{2}/4$	1	$\sqrt{2}/10$	$-3/5$
	7,6	0	0	$-\sqrt{5}/4$	1	$-\sqrt{5}/100$	$-6/25$
	7,7	1	0	$1/4$	1	$1/4$	$-2/5$
5/2	B,B	1	$-1/10$	1	1	$19/100$	$-29/100$
	B,C	0	$-\sqrt{21}/50$	1	0	$3\sqrt{21}/100$	$-\sqrt{21}/20$
	B,D	0	$\sqrt{14}/50$	1	0	$-3\sqrt{14}/50$	$2\sqrt{14}/25$
	C,B	0	$-\sqrt{21}/50$	1	0	$3\sqrt{21}/100$	$-\sqrt{21}/20$
	C,C	1	$-1/50$	1	1	$31/100$	$-33/100$
	C,D	0	$\sqrt{6}/50$	1	0	$3\sqrt{6}/50$	$-\sqrt{6}/25$
	D,B	0	$\sqrt{14}/50$	1	0	$-3\sqrt{14}/50$	$2\sqrt{14}/25$
	D,C	0	$\sqrt{6}/50$	1	0	$3\sqrt{6}/50$	$-\sqrt{6}/25$
	D,D	1	0	1	1	$4/25$	$-4/25$



- (3) The discussion in Chapter XV begins with a description of the special transformation employed to obtain "exact" solutions for the  $J_T = 5/2$  set of equations. (The transformation as described in (1) and (2) above reduces to the identity transformation as far as these equations are concerned.) The validity of the Distorted Wave approximation as applicable to this set of equations is also investigated.
- (4) The method of distorted waves is used to estimate the corrections needed for the states of  $J_T = 1/2$  and  $3/2$  which were neglected in steps (1) and (2) above.
- (5) The validity of the special approach taken for the solution of the  $J_T = 1/2$  and  $3/2$  sets of equations is established. This work consolidates the detailed analyses of steps (1), (2) and (4).
- (6) Finally, the effects of allowing for the differences in energy for the different atomic states are estimated.

#### The Basic Transformation

In advance of the presentation of a formal solution for the sets of differential equations for the p-wave, it is thought appropriate to digress somewhat, and to discuss in some detail a set of transformations which have considerable importance in the numerical methods chosen for obtaining reliable cross sections. These transformations are to be defined by the following relationships:

$$J_T = 1/2:$$

$$\begin{aligned}
 F_c &= -2 n_a G_a && - \sqrt{5} n_d G_d \\
 F_d &= && -2 n_b G_b + 3 n_d G_d \\
 F_e &= n_c G_c \\
 F_f &= -\sqrt{5} n_a G_a + 3 n_b G_b + 2 n_d G_d
 \end{aligned} \tag{14.5}$$

$$J_T = 3/2:$$

$$\begin{aligned}
 F_3 &= && n_4 G_4 + 2 \sqrt{5} n_5 G_5 \\
 F_4 &= n_2 G_2 \\
 F_5 &= && + 3 n_3 G_3 && - \sqrt{2} n_5 G_5 \\
 F_6 &= -3 n_1 G_1 && - 2 n_4 G_4 + \sqrt{5} n_5 G_5 \\
 F_7 &= \sqrt{5} n_1 G_1 + \sqrt{2} n_3 G_3 && + 3 n_5 G_5.
 \end{aligned} \tag{14.6}$$

The various coefficients,  $n_i$ , establish the amplitudes of the functions, and are determined through a specification of the boundary conditions, Eq. (11.8). It should be noted that these boundary conditions differ depending upon which state is selected as the initial state, hence the  $n_i$  and the resulting transformations will differ for different choices of initial states. The  $G$ 's and  $n$ 's defining Eqs. (14.5) and (14.6) are not to be confused with those bearing similar numerical subscripts in the s-wave analysis. The comparable quantities are not related, and are never directly associated in the course of these discussions.

Consider now the following approximations as applied to the equations for p-wave interactions:

1. The atomic states of interest are to be given equal energies; this, in effect, is the Exact Resonance approximation, and results in  $k_m^2 = k_n^2 = k^2$ .

2. All  $y_2$  and  $R_2$  potential and exchange terms are to be omitted. The  $y_1$  and  $R_1$  terms involving exchange with the  $(1s)^2 (2s)^2$  atomic core may be omitted or retained, the particular choice will not alter the characteristic features of the transformations. For the current discussion, these latter terms are retained in the equations.

Under these special conditions, the transformations given by Eqs. (14.5) and (14.6) effect a de-coupling of the respective systems of equations. Under similar conditions, the equations for  $J_T = 5/2$  are separated without need of transformation. The corresponding solutions for the systems of equations may be derived from the following:

$$\begin{aligned}
 G_a &= G_b = G_c = \mathcal{J}' \\
 G_1 &= G_2 = G_3 = G_4 = \mathcal{J}' \\
 F_B &= F_C = F_D = \mathcal{J}' \\
 G_d &= G_5 = \mathcal{J}
 \end{aligned} \tag{14.7}$$

where  $\mathcal{J}'$  and  $\mathcal{J}$  are radial wave functions which satisfy the differential equations:

$$\begin{aligned}
 [\mathcal{L}^1 + 4 y_0(PP) + 2 y_0(S_1 S_1) + 2 y_0(S_2 S_2)] \mathcal{J}' &= [y_0(P \mathcal{J}) \\
 + \lambda^0(P \mathcal{J})] P + \frac{1}{3} y_1(S_1 \mathcal{J}) S_1 + \frac{1}{3} y_1(S_2 \mathcal{J}) S_2
 \end{aligned} \tag{14.8}$$

$$[\mathcal{L}^1 + 4 y_0(\text{PP}) + 2 y_0(\text{S}_1\text{S}_1) + 2 y_0(\text{S}_2\text{S}_2)] \mathcal{H} = -2 [y_0(\text{P}\mathcal{H}) + \lambda^0(\text{P}\mathcal{H})] \text{P} + \frac{1}{3} y_1(\text{S}_1\mathcal{H})\text{S}_1 + \frac{1}{3} y_1(\text{S}_2\mathcal{H})\text{S}_2 \quad (14.9)$$

with

$$\begin{aligned} \lambda^0(\text{P}\mathcal{H}) = & \mathcal{H}_2^1(\text{P}\mathcal{H}) - \frac{k^2}{2} \Delta(\text{P}\mathcal{H}) + 3 R_0(\text{PPP}\mathcal{H}) + 2 R_0(\text{S}_1\text{PS}_1\mathcal{H}) \\ & + 2 R_0(\text{S}_2\text{PS}_2\mathcal{H}) - \frac{1}{3} R_1(\text{PS}_1\text{S}_1\mathcal{H}) - \frac{1}{3} R_1(\text{PS}_2\text{S}_2\mathcal{H}). \end{aligned} \quad (14.10)$$

A similar expression holds for  $\lambda^0(\text{P}\mathcal{H})$ .

The details related to the solutions of Eqs. (14.8) and (14.9), the application of the boundary conditions, and the calculation of the collision strengths are not presented at this time. This information can be obtained as a special case of the corresponding discussions on the more refined equations which are to follow. However, it is worthwhile to point out here that the  $\mathcal{H}$  and  $\mathcal{H}$  functions each have a special distinct characteristic. As will be demonstrated later, the  $\mathcal{H}$  function may be made orthogonal to the bound atomic P wave function, while the  $\mathcal{H}$  function is already uniquely determined by Eq. (14.9) and cannot be so adjusted. The several functions which are obtained later as components of the solutions to the original complete coupled equations are found to maintain these characteristic features and to reduce to either  $\mathcal{H}$  or  $\mathcal{H}$  when the above-described approximations are applied. Hence, the description,  $\mathcal{H}$ -type or  $\mathcal{H}$ -type function, refers to the corresponding property regarding orthogonality.

The transformation that has been described above is an important method of taking into account the strong coupling contributed by the spherically-symmetric  $y_0(\text{PF})$  terms. Seaton<sup>40</sup> has found these coupling terms to completely dominate the transition probabilities between the  $^3\text{P}$ ,  $^1\text{D}$  and  $^1\text{S}$  ground configuration states of OI. Hence, as a zero-order approximation, he made the assumptions of exact resonance and non-importance of the asymmetric potential and exchange terms as described earlier in this chapter, and proceeded with a transformation similar to Eqs. (14.5) and (14.6). In later work, a correction was made for the omitted coupling terms with perturbation methods.

At first glance one would be tempted to follow this same scheme of calculation. However, the above calculations of Seaton were at energies much higher than those of concern here; at these higher energies, the special effects for p-wave as described in Chapter VII prove to increase the importance of exchange and orthogonality considerations, and to so dominate the cross sections that the treatment used by Seaton was both necessary and desirable. The present work has been done for energies quite below those of Seaton, and correspondingly below the energy region for which those effects mentioned in Chapter VII should be important. The longer-range potential coupling terms also appear to be of more significance here. In some instances, these latter terms with asymptotic  $r^{-3}$  dependence even tend to contribute more to the cross sections than the above exchange terms. For certain coupling terms, the situation becomes more acute; the  $y_2(\text{PP})$  potential terms appear with sign opposite to the exchange terms. Being of about the same magnitude, a cancellation occurs between two quantities of about equal

size, and leads to an extreme sensitivity of the resulting cross sections upon the distortion elements. Hence, a consideration of the symmetric exchange terms alone is certainly not sufficient, and the usual treatment of the potential coupling terms by simple perturbation is of doubtful value.

However, in precise numerical calculations, the transformation described by Eqs. (14.5) and (14.6) can be effectively used to initiate an iteration procedure, and once a solution has been obtained for the  $G$  functions, to establish a mechanism for evaluating the cross sections. This, in effect, is the essential feature of the development to be discussed in the remaining portion of this chapter. Hereafter, for purposes of convenience, the transformations defined by Eqs. (14.5) and (14.6) are to be referred to as the "Basic Transformations."

If the approximations which were outlined earlier in this chapter are retained throughout the calculation, the "Basic Transformations" lead to a comparatively simple pair of differential equations (see Eqs. (14.8) and (14.9)). The solution of these equations is by no means easy, but the numerical techniques are straight-forward and convergence of the iteration is rapid if the side conditions are properly established. The algebraic manipulations required to convert these solutions into values for the cross sections can be performed analytically. The algebra is quite lengthy and "messy" (requiring, among other things, the inversion of a  $4 \times 4$  complex matrix), but the results unfold into a very familiar form:

$$\begin{aligned}
\Omega_p(1,2) &= \frac{35}{18} \sin^2(\xi_1 - \xi_2) \\
\Omega_p(0,2) &= \frac{5}{9} \sin^2(\xi_1 - \xi_2) \\
\Omega_p(0,1) &= \frac{5}{9} \sin^2(\xi_1 - \xi_2)
\end{aligned} \tag{14.11}$$

where  $\xi_1$  and  $\xi_2$  are the asymptotic phases of  $\mathcal{P}$  and  $\mathcal{H}$ , respectively.

Although results calculated with the above formulas are expected to be in considerable error because of the neglect of the  $y_2(\text{PP})$  potential coupling terms, it is worthwhile to note the simple ratios that exist between the different collision strengths (ratios which are independent of  $\mathcal{P}$  and  $\mathcal{H}$ ). After more exact results have been obtained, the deviations of the corresponding "true" ratios from the simple ones calculated in the above manner can be considered an indication of the relative importance of the asymmetric terms as compared with the spherically-symmetric ones in establishing the cross sections.

#### Application of Basic Transformation to Equations for $J_T = 1/2, 3/2$

The transformation specified by Eqs. (14.5) and (14.6) will be shown to have a special importance because of the ease and directness with which the orthogonality restrictions can be introduced into the analysis. However, if this change of variables is applied to the complete  $J_T = 1/2$  and  $3/2$  systems of equations, with only the assumption of exact resonance retained, the  $G$  differential equations are not fully decoupled. In particular, coupling between equations will remain for the important  $y_2(\text{PP})$  terms.

Numerical iteration can, in general, provide a means of bypassing such an obstacle. However, it should be strongly emphasized at this point that Eqs. (14.5) and (14.6) are a very restricted transformation in the sense of the special treatment given to the  $F_e$  and  $F_d$  functions. For purposes of illustration, assume that the relevant "Basic Transformation" has been applied to the  $J_T = 1/2$  functions. The resulting equations for  $G_a, \dots, G_d$  remain coupled (except for the  $y_0(\text{PG})$  exchange terms). When the boundary conditions, Eqs. (11.8), are applied to determine the  $n_i$  amplitude coefficients, it is found that  $n_c = 0$  when "c", "d", or "f" is chosen for the initial state. Likewise, when the initial state is taken to be that described by "e", the equations for  $n_a, n_b$  and  $n_d$  are found to be linearly-dependent and not capable of a unique solution.

It is possible to circumvent this apparent difficulty with the following special approximation. Let all coupling terms between  $F_e$  and the remaining  $F$  functions be ignored in the original  $J_T = 1/2$  set, and let Eqs. (14.5) be applied only to  $F_c, F_d$  and  $F_f$ . In essence,  $F_e$  (and  $G_c$ ) is assumed to be completely decoupled from the other functions, and the contributions to the collision strengths from  $F_c, F_d$  and  $F_f$  are to be determined as if these functions were the only members of  $J_T = 1/2$ . Of course, some additional provision must eventually be made for including the contributions from the omitted "e" state.

At first, one might tend to disregard this approach as being too artificial. The method essentially assumes that, for example, the results for  $F_c, F_d$  and  $F_f$  are completely unaffected by the existence



of the "e" state. On the other hand, it should be noted that the principal coupling to this "e" state is of the  $y_2(PP)$  form (a potential term having a range considerably longer than the exchange terms), and in general the weak-coupling approximations have been found to be valid for this type of interaction (assuming, of course, that the resulting cross sections remain small). Hence, the basic assumption here is one of weak coupling between "e" and the remaining states. The troublesome strong short-range exchange coupling can be properly considered by obtaining "exact" iterative solutions for  $G_a$ ,  $G_b$  and  $G_d$ . A similar procedure would apply to  $F_4$  of  $J_T = 3/2$ .

The above-described technique was applied in the determination of the contributions to the p-wave collision strengths arising from  $J_T = 1/2$  and  $3/2$ . The Exact Resonance approximation was assumed to remain valid, all coupling terms to the "e" and "4" states were omitted, and Eqs. (14.5) and (14.6) were used to transform variables. The ultimate validity of this special approximation will be established at the conclusion of the next chapter after the numerical procedures have been described in greater detail. After transformation, the following equations result:

$$\underline{J_{\Gamma} = 1/2:}$$

$$\begin{aligned} [\mathcal{H}^1 + 4Y_o(\text{PP}) + 2Y_o(S_1S_1) + 2Y_o(S_2S_2)] G_a &= [Y_o(PG_a) + \bigwedge_a(PG_a)] P - \frac{17}{50} Y_2(\text{PP}) G_a \\ &+ \frac{2}{5} Y_2(PG_a) P + \frac{1}{3} Y_1(S_1G_a) S_1 + \frac{1}{3} Y_1(S_2G_a) S_2 + \frac{3\sqrt{5}}{50} \left[ \frac{n_b}{n_a} \right] Y_2(\text{PP}) G_b \end{aligned}$$

$$\begin{aligned} [\mathcal{H}^1 + 4Y_o(\text{PP}) + 2Y_o(S_1S_1) + 2Y_o(S_2S_2)] G_b &= [Y_o(PG_b) + \bigwedge_b(PG_b)] P + \frac{1}{10} Y_2(\text{PP}) G_b \\ &+ \frac{2}{5} Y_2(PG_b) P + \frac{1}{3} Y_1(S_1G_b) S_1 + \frac{1}{3} Y_1(S_2G_b) S_2 - \frac{2\sqrt{5}}{50} \left[ \frac{n_a}{n_b} \right] Y_2(\text{PP}) G_a \quad (14.12) \end{aligned}$$

13

$$\begin{aligned} [\mathcal{H}^1 + 4Y_o(\text{PP}) + 2Y_o(S_1S_1) + 2Y_o(S_2S_2)] G_a &= -2[Y_o(PG_a) + \bigwedge_a(PG_a)] P + \frac{1}{5} Y_2(\text{PP}) G_a \\ &+ \frac{1}{10} Y_2(PG_a) P + \frac{1}{3} Y_1(S_1G_a) S_1 + \frac{1}{3} Y_1(S_2G_a) S_2 \end{aligned} \quad (14.13)$$

$$\frac{J_T}{2} = 3/2:$$

$$\begin{aligned} [f_1^1 + 4Y_o(PF) + 2Y_o(S_1S_1) + 2Y_o(S_2S_2)]G_1 &= [Y_o(PG_1) + \Lambda_1(PG_1)]P + \frac{1}{3}Y_1(S_1G_1)S_1 \\ &+ \frac{1}{3}Y_1(S_2G_1)S_2 + \frac{2}{25}Y_2(PF)G_1 + \frac{1}{5}Y_2(PG_1)P + \frac{\sqrt{10}}{20}\left[\frac{n_3}{n_1}\right]Y_2(PG_3)P \\ &+ \frac{7}{50}\left[\frac{n_4}{n_1}\right]Y_2(PF)G_4 \end{aligned}$$

$$\begin{aligned} [f_1^1 + 4Y_o(PF) + 2Y_o(S_1S_1) + 2Y_o(S_2S_2)]G_3 &= [Y_o(PG_3) + \Lambda_3(PG_3)]P + \frac{1}{3}Y_1(S_1G_3)S_1 \\ &+ \frac{1}{3}Y_1(S_2G_3)S_2 + \frac{3}{10}Y_2(PG_3)P - \frac{\sqrt{10}}{25}\left[\frac{n_1}{n_3}\right][Y_2(PF)G_1 - Y_2(PG_1)P] \\ &- \frac{\sqrt{10}}{25}\left[\frac{n_4}{n_3}\right]Y_2(PF)G_4 \end{aligned} \tag{14.14}$$

$$\underline{J_T = 3/2:}$$

$$\begin{aligned}
 [\mathcal{L}^1 + 4Y_O(\text{PP}) + 2Y_O(S_1S_1) + 2Y_O(S_2S_2)] G_4 = & [Y_O(\text{PG}_4) + \wedge_4(\text{PG}_4)] P + \frac{1}{3} Y_1(S_1G_4)S_1 \\
 & + \frac{1}{3} Y_1(S_2G_4)S_2 - \frac{7}{25} Y_2(\text{PP})G_4 + \frac{2}{5} Y_2(\text{PG}_4)P - \frac{3}{25} \left[ \frac{n_1}{n_4} \right] [Y_2(\text{PP})G_1 \\
 & - 2Y_2(\text{PG}_1)P] - \frac{3\sqrt{10}}{50} \left[ \frac{n_3}{n_4} \right] [Y_2(\text{PP})G_3 + Y_2(\text{PG}_3)P]
 \end{aligned}$$

(14.14)  
(Continued)

$$\begin{aligned}
 [\mathcal{L}^1 + 4Y_O(\text{PP}) + 2Y_O(S_1S_1) + 2Y_O(S_2S_2)] G_5 = & -2 [Y_O(\text{PG}_5) + \wedge_5(\text{PG}_5)] P + \frac{1}{3} Y_1(S_1G_5)S_1 \\
 & + \frac{1}{3} Y_1(S_2G_5)S_2 + \frac{1}{5} Y_2(\text{PP})G_5 + \frac{1}{10} Y_2(\text{PG}_5)P
 \end{aligned}$$

(14.15)

The  $\Lambda$ 's have definition similar to the  $\lambda_{mn}$  of Eq. (14.4), with the addition of certain coupling terms. The appropriate coefficients and additional terms are given in Table XIX.

The functions denoted by  $G_4$  and  $G_5$  are seen to be equal, and are completely decoupled from the remaining functions in their respective set. Furthermore, these two functions will be shown to possess the properties of  $\mathcal{L}$ -type functions. The remainder of the  $G$  functions in a particular set (Eqs. (14.12) or (14.14)) are  $\mathcal{O}$ -type and are not uncoupled by the "Basic Transformation." The coupling terms for the latter functions are proportional to ratios of the form  $(n_i/n_j)$ ; hence the coupling is dependent upon the boundary conditions and the initial state of the system.

Assume for the moment that the coupling terms in Eqs. (14.12) and (14.14) are known; each equation is then non-homogeneous in only one unknown dependent variable. The solution of such an equation is accomplished by numerical iteration, and is discussed in detail in Chapter XVI. The chief concern here is the treatment of the  $\Lambda$  parameter. Consider, for example, the equation for  $G_a$ . Upon multiplication of each term of this equation on the left by  $P$ , and integration, the  $\Lambda_a(PG_a)$  parameter is found to be indeterminant, and its numerical value is arbitrary as far as the differential equation is concerned. However, an expression for  $\Lambda_a(PG_a)$  can be obtained by a similar manipulation of the Hartree-Fock differential equation for the bound  $P$  function (see Appendix IV). For this example, the latter results in the following expression:

TABLE XIX

COEFFICIENTS AND COUPLING TERMS FOR  $\wedge_i(\text{PG}_i)$  PARAMETERS

$J_T$	Parameter	$\vartheta$	$\kappa$	Coupling terms, $\wedge_i - \lambda_i$
1/2	$\wedge_a$	1	-3/50	$-\frac{3\sqrt{5}}{50} \left[ \frac{n_b}{n_a} \right] R_2(\text{PPPG}_b)$
	$\wedge_b$	1	-1/2	$\frac{3\sqrt{5}}{50} \left[ \frac{n_a}{n_b} \right] R_2(\text{PPPG}_a)$
	$\wedge_d$	1	-3/20	
3/2	$\wedge_1$	1	-7/25	$-\frac{\sqrt{10}}{20} \left[ \frac{n_3}{n_1} \right] R_2(\text{PPPG}_3) - \frac{7}{50} \left[ \frac{n_4}{n_1} \right] R_2(\text{PPPG}_4)$
	$\wedge_3$	1	-3/10	$\frac{\sqrt{10}}{25} \left[ \frac{n_4}{n_3} \right] R_2(\text{PPPG}_4)$
	$\wedge_4$	1	-3/25	$-\frac{3}{25} \left[ \frac{n_1}{n_4} \right] R_2(\text{PPPG}_1) + \frac{3\sqrt{10}}{25} \left[ \frac{n_3}{n_4} \right] R_2(\text{PPPG}_3)$
	$\wedge_5$	1	-3/20	
5/2	$\wedge_B$	1	-9/20	$-\frac{9\sqrt{21}}{100} \left[ \frac{n_C}{n_B} \right] R_2(\text{PPPG}_C)$
	$\wedge_C$	1	27/100	$\frac{3\sqrt{21}}{100} \left[ \frac{n_B}{n_C} \right] R_2(\text{PPPG}_B)$
	$\wedge_D$	1	-3/5	

$$\Lambda_a(PG_a) = \frac{6}{25} R_2(PPPG_a) - \frac{3\sqrt{5}}{50} \left[ \frac{n_b}{n_a} \right] R_2(PPPG_b) - \frac{1}{2} (\epsilon_{2p} + k^2) \Delta(PG_a). \quad (14.16)$$

With the single degree of freedom available, the  $G_a$  function can be restricted to be orthogonal to the bound-state  $P$  function, i.e., the side condition can be imposed upon  $G_a$  such that:

$$\Delta(PG_a) = 0. \quad (14.17)$$

Hence  $G_a$  is an  $\mathcal{P}$ -type function and its solution follows readily from the treatment presented in Chapter XVI. The remaining functions in the coupled sets have similar properties, and hence can be evaluated once the coupling terms are known.

Consider now a set of coupled differential equations, for example the two coupled equations for  $G_a$  and  $G_b$ . If the  $(n_i/n_j)$  ratio can be assumed to be known, the set can be solved by iteration. In this procedure, the two homogeneous equations (the right sides of Eqs. (14.12) being replaced by zero) are solved; these solutions are then used to evaluate the right sides of the two full equations and the resulting non-homogeneous equations are solved for the improved functions. This process should be continued until convergence is achieved within the desired level of accuracy. Side conditions similar to Eq. (14.17) were satisfied after each successive stage of the iteration in the manner discussed in Chapter XVI. The set of 3 equations for  $J_T = 3/2$  were treated in a similar fashion, and although the more elaborate coupling decreases the rate of convergence, the computing requirements were not excessive.

The final fallacy in the above description concerns the  $(n_i/n_j)$  ratios. Theoretically, these are not known until the final  $G$  functions have been computed, hence it is necessary to apply another iteration routine on the complete set of functions to evaluate these parameters. The set of homogeneous solutions provide at least a starting guess for these ratios. The coupled equations can then be solved with these crude estimates in the manner of the preceding paragraph. From these results, better values are available for  $(n_i/n_j)$ , and the process can be repeated until consistent ratios are achieved. Hence, the basic approach has been one of iteration on the  $(n_i/n_j)$  ratios, each stage of this iteration being a full iteration on the complete set of coupled differential equations. No major difficulties were encountered in obtaining accurate consistent results in a reasonable amount of machine time.

Although the  $G_d$  differential equation (and hence the  $G_5$  equation also) is free of coupling with the other equations in the set, a different type of problem is encountered in the evaluation of  $\Lambda_d(PG_d)$ . By following a procedure equivalent to that described for the  $G_a$  function, it is found that this parameter is not arbitrary in the scattering differential equation. The differential equation for  $G_d$  specifies that

$$\Lambda_d(PG_d) = -R_0(PPPG_d) + \frac{1}{20} R_2(PPPG_d). \quad (14.18)$$

However, to be consistent with the Hartree-Fock differential equation for the bound-state  $P$  function,



$$\Lambda_d(PG_d) = \frac{2}{20} R_2(PPPG_d) - \frac{1}{2} (\epsilon_{2p} + k^2) \Delta(PG_d). \quad (14.19)$$

The side condition imposed on the  $G_d$  solution is that these two values be made equal, that is

$$\frac{1}{2} (\epsilon_{2p} + k^2) \Delta(PG_d) = R_0(PPPG_d) + \frac{1}{10} R_2(PPPG_d). \quad (14.20)$$

This requirement is believed to lead to minimum error in the computational work. Eq. (14.20) can be satisfied after each step of the iteration process by the method suggested in Chapter XVI.

Eqs. (14.12), (14.13), (14.14), and (14.15) were solved in terms of their asymptotic amplitudes and phases for a selected set of incident electron energies. For the special case of exact resonance, only the various phases are needed in evaluating the elements of the R-matrices, however, the amplitudes are involved in establishing the  $(n_i/n_j)$  ratios. The latter parameters enter into the coupled  $G$  differential equations, and as these ratios are dependent upon the initial state, the final phase for a particular  $G$  function must carry a label to denote the state so chosen. Accordingly,  $\alpha_{a,c}$  implies the phase for  $G_a$  when  $F_c$  describes the initial state of the system. The elements of the R-matrices for  $J_T = 1/2$  and  $3/2$  under exact resonance are summarized in Table XX. The computed numerical values for the required phases are listed in Tables XXI and XXII. In the numerical work, the respective matrices were found to have the required symmetry within three figures of accuracy.

TABLE XX

ELEMENTS OF R-MATRIX FOR STATES CONNECTED UNDER THE

"BASIC TRANSFORMATION"

$J_T$	$m,n^{(a)}$	$R(m,n)^{(b)}$
1/2	c,c	$(1/18) [13 \tan \eta_{a,c} + 5 \tan \eta_{d,c}]$
	d,c	$(\sqrt{5}/6) [\tan \eta_{b,c} - \tan \eta_{d,c}]$
	f,c	$(\sqrt{5}/36)[13 \tan \eta_{a,c} - 9 \tan \eta_{b,c} - 4 \tan \eta_{d,c}]$
	c,d	$(\sqrt{5}/6) [\tan \eta_{a,d} - \tan \eta_{d,d}]$
	d,d	$(1/2) [\tan \eta_{b,d} + \tan \eta_{d,d}]$
	f,d	$(1/12) [5 \tan \eta_{a,d} - 9 \tan \eta_{b,d} + 4 \tan \eta_{d,d}]$
	c,f	$(\sqrt{5}/9) [\tan \eta_{a,f} - \tan \eta_{d,f}]$
	d,f	$(-1/3) [\tan \eta_{b,f} - \tan \eta_{d,f}]$
	f,f	$(1/18) [5 \tan \eta_{a,f} + 9 \tan \eta_{b,f} + 4 \tan \eta_{d,f}]$
	3,3	$(1/9) [4 \tan \eta_{4,3} + 5 \tan \eta_{5,3}]$
	5,3	$(\sqrt{10}/18) [\tan \eta_{3,3} - \tan \eta_{5,3}]$
	6,3	$(1/18) [11 \tan \eta_{1,3} - 16 \tan \eta_{4,3} + 5 \tan \eta_{5,3}]$
3/2	7,3	$(\sqrt{5}/54)[-11 \tan \eta_{1,3} + 2 \tan \eta_{3,3} + 9 \tan \eta_{5,3}]$

TABLE XX--Continued

$J_T$	$m,n^{(a)}$	$R(m,n)^{(b)}$
3/2	3,5	$(\sqrt{10}/18) [\tan \eta_{4,5} - \tan \eta_{5,5}]$
	5,5	$(1/18) [17 \tan \eta_{3,5} + \tan \eta_{5,5}]$
	6,5	$(\sqrt{10}/36) [5 \tan \eta_{1,5} - 4 \tan \eta_{4,5} - \tan \eta_{5,5}]$
	7,5	$(\sqrt{2}/108) [-25 \tan \eta_{1,5} + 34 \tan \eta_{3,5} - 9 \tan \eta_{5,5}]$
	3,6	$(5/18) [-\tan \eta_{4,6} + \tan \eta_{5,6}]$
	5,6	$(\sqrt{10}/36) [\tan \eta_{3,6} - \tan \eta_{5,6}]$
	6,6	$(1/36) [11 \tan \eta_{1,6} + 20 \tan \eta_{4,6} + 5 \tan \eta_{5,6}]$
	7,6	$(\sqrt{5}/108) [-11 \tan \eta_{1,6} + 2 \tan \eta_{3,6} + 9 \tan \eta_{5,6}]$
	3,7	$(\sqrt{5}/6) [\tan \eta_{5,7} - \tan \eta_{4,7}]$
	5,7	$(\sqrt{2}/12) [\tan \eta_{3,7} - \tan \eta_{5,7}]$
	6,7	$(\sqrt{5}/12) [-5 \tan \eta_{1,7} + 4 \tan \eta_{4,7} + \tan \eta_{5,7}]$
	7,7	$(1/36) [25 \tan \eta_{1,7} + 2 \tan \eta_{3,7} + 9 \tan \eta_{5,7}]$

(a) These indices refer to the labeling of the F states.

(b) The phase,  $\eta_{a,c}$ , is that of  $G_a$  when the initial state of the system is described by  $F_c$ .

TABLE XXI

COMPUTED PHASES FOR MODIFIED EQUATIONS OF  $J_T = 1/2$ 

G Function	Initial State	Phase			
		500°K	1,000°K	5,000°K	10,000°K
a	c	-0.0150	-0.0216	-0.0550	-0.0886
b	c	-0.0090	-0.0132	-0.0372	-0.0648
d	c	-0.0329	-0.0745	-0.2787	-0.4222
a	d	-0.0090	-0.0132	-0.0372	-0.0648
b	d	-0.00036	-0.0010	-0.0115	-0.0304
d	d	-0.0329	-0.0745	-0.2787	-0.4222
a	f	-0.0284	-0.0405	-0.0949	-0.1417
b	f	+0.0104	+0.0141	+0.0207	+0.0128
d	f	-0.0329	-0.0745	-0.2787	-0.4222

TABLE XXII

COMPUTED PHASES FOR MODIFIED EQUATIONS OF  $J_T = 3/2$ 

G Function	Initial State	Phase			
		500°K	1,000°K	5,000°K	10,000°K
1	3	-0.0126	-0.0185	-0.0509	-0.0866
3	3	-0.0285	-0.0410	-0.1000	-0.1552
4	3	-0.0139	-0.0202	-0.0538	-0.0892
5	3	-0.0329	-0.0745	-0.2787	-0.4222
1	5	-0.0052	-0.0081	-0.0308	-0.0627
3	5	-0.0010	-0.0021	-0.0155	-0.0383
4	5	-0.0285	-0.0410	-0.0999	-0.1551
5	5	-0.0329	-0.0745	-0.2787	-0.4222
1	6	+0.0244	+0.0335	+0.0584	+0.0584
3	6	+0.0892	+0.1235	+0.2458	+0.3030
4	6	-0.0169	-0.0243	-0.0606	-0.0950
5	6	-0.0329	-0.0745	-0.2787	-0.4222
1	7	-0.0053	-0.0081	-0.0287	-0.0566
3	7	+0.0104	+0.0144	+0.0263	+0.0285
4	7	-0.0091	-0.0135	-0.0400	-0.0715
5	7	-0.0329	-0.0745	-0.2787	-0.4222

The different states that are coupled under the spherically-symmetric exchange interaction are also those which are affected by the modified "Basic Transformation." Hence the elements in Tables XX, XXI and XXII can be used to evaluate the contributions from these selected states to the p-wave collision strengths. Other methods for estimating the effects of the remainder of the composite states are discussed in the following chapter. Table XXIX at the latter part of Chapter XV summarizes the individual contributions from these different sources and presents the final p-wave collision strengths under the Exact Resonance approximation.

## CHAPTER XV

### COLLISION STRENGTHS FOR P-WAVE, SPECIAL REFINEMENTS

#### Exact Solutions for $J_T = 5/2$ Equations

It has already been pointed out that the  $J_T = 5/2$  set of differential equations has no symmetric exchange ( $y_0(PF)$ , etc.) coupling terms, and hence a "Basic Transformation" for these equations is merely the identity transformation. Under such a technique, (which would be consistent with the methods of Chapter XIV), there would be no ready-made procedure available for evaluating exactly the contributions of these states to the total cross sections.

However, these states are coupled under the equally-important asymmetric potential interaction (terms of the form  $y_2(PP)F$ , etc.), and the methods of the preceding analysis can be extended an additional degree of refinement by de-coupling the equations with respect to these terms. This is possible only because the symmetric exchange distortion terms are the same in each of the equations of this  $J_T = 5/2$  set. The necessary transformation is:

$$\begin{aligned} F_B &= \sqrt{2} n_C G_C + \sqrt{7} n_D G_D \\ F_C &= \sqrt{2} n_B G_B + \sqrt{3} n_D G_D \\ F_D &= \sqrt{3} n_B G_B + \sqrt{7} n_C G_C - \sqrt{2} n_D G_D \end{aligned} \quad (15.1)$$

The resulting equations are:

$$\begin{aligned} [\mathcal{L}^1 + 4y_o(\text{PP}) + 2y_o(S_1S_1) + 2y_o(S_2S_2)] G_B &= [y_o(\text{PG}_B) + \wedge_B(\text{PG}_B)]P + \frac{1}{3} y_1(S_1G_B)S_1 \\ &+ \frac{1}{3} y_1(S_2G_B)S_2 - \frac{1}{25} y_2(\text{PP})G_B + \frac{49}{100} y_2(\text{PG}_B)P + \frac{9\sqrt{21}}{100} \left[ \frac{n_C}{n_B} \right] y_2(\text{PG}_C)P \end{aligned}$$

$$\begin{aligned} [\mathcal{L}^1 + 4y_o(\text{PP}) + 2y_o(S_1S_1) + 2y_o(S_2S_2)] G_C &= [y_o(\text{PG}_C) + \wedge_C(\text{PG}_C)]P + \frac{1}{3} y_1(S_1G_C)S_1 \\ &+ \frac{1}{3} y_1(S_2G_C)S_2 - \frac{1}{25} y_2(\text{PP})G_C - \frac{23}{100} y_2(\text{PG}_C)P - \frac{3\sqrt{21}}{100} \left[ \frac{n_B}{n_C} \right] y_2(\text{PG}_B)P \end{aligned}$$

$$\begin{aligned} [\mathcal{L}^1 + 4y_o(\text{PP}) + 2y_o(S_1S_1) + 2y_o(S_2S_2)] G_D &= [y_o(\text{PG}_D) + \wedge_D(\text{PG}_D)]P + \frac{1}{3} y_1(S_1G_D)S_1 \\ &+ \frac{1}{3} y_1(S_2G_D)S_2 + \frac{1}{5} y_2(\text{PP})G_D + \frac{2}{5} y_2(\text{PG}_D)P \end{aligned} \tag{15.2}$$



The equations for  $G_B$  and  $G_C$  are still coupled by terms proportional to  $(n_C/n_B)$  and  $(n_B/n_C)$  which depend upon the boundary conditions.

The  $\Lambda$  parameters are defined analogous to Eq. (14.4) with an additional allowance being made for the coupling terms between  $G_B$  and  $G_C$ . The coefficients and correction terms are given as a part of Table XIX. The similarity between Eqs. (15.2) and those for  $J_T = 1/2$  (See Eqs. (14.12) and (14.13)) is readily apparent; the method of solution is sufficiently similar to forego a restatement of those procedures. Eqs. (15.2) are found to be  $\mathcal{P}$ -type equations, and the orthogonality condition given by Eq. (14.17) can be readily imposed upon the solutions. Iteration on  $(n_B/n_C)$  must be included as a basic part of the numerical procedures.

The elements of the R-matrix for  $J_T = 5/2$  under exact resonance and the procedure just described are given in Table XXIII. The notation is similar to that employed in Table XX. The numerical values for the various phases are listed in Table XXIV. R-matrix symmetry was achieved to within 3 significant figures. The interaction for total angular momentum of  $5/2$  can lead to transitions between the  $J = 2$  and  $J = 1$  atomic levels only, and hence will provide a correction only to  $\Omega_p(1,2)$  and  $\Omega_p(2,1)$ . These additions are included in Table XXIX.

#### Application of the Method of Distorted Waves

As emphasized in Chapter XIV, the "e" and "4" states of  $J_T = 1/2$  and  $3/2$ , respectively, were isolated from the remaining states in the calculations concerning the latter. It was also stated at that time that refined weak-coupling approximations should be applicable in

TABLE XXIII  
ELEMENTS OF R-MATRIX FOR  $J_T = 5/2$

$J_T$	$m, n^{(a)}$	$R(m, n)^{(b)}$
5/2	B, B	$\frac{1}{12} [5 \tan \eta_{C,B} + 7 \tan \eta_{D,B}]$
	C, B	$\frac{\sqrt{21}}{12} [-\tan \eta_{B,B} + \tan \eta_{D,B}]$
	D, B	$\frac{\sqrt{14}}{24} [-3 \tan \eta_{B,B} + 5 \tan \eta_{C,B} - 2 \tan \eta_{D,B}]$
	B, C	$\frac{\sqrt{21}}{12} [-\tan \eta_{C,C} + \tan \eta_{D,C}]$
	C, C	$\frac{1}{4} [3 \tan \eta_{B,C} + \tan \eta_{D,C}]$
	D, C	$\frac{\sqrt{6}}{24} [9 \tan \eta_{B,C} - 7 \tan \eta_{C,C} - 2 \tan \eta_{D,C}]$
	B, D	$\frac{\sqrt{14}}{12} [\tan \eta_{C,D} - \tan \eta_{D,D}]$
	C, D	$\frac{\sqrt{6}}{12} [\tan \eta_{B,D} - \tan \eta_{D,D}]$
	D, D	$\frac{1}{12} [3 \tan \eta_{B,D} + 7 \tan \eta_{C,D} + 2 \tan \eta_{D,D}]$

(a) These indices refer to the labeling of the F states.

(b) The phase,  $\eta_{B,C}$ , is that of  $G_B$  when the initial state of the system is described by  $F_C$ .

TABLE XXIV  
COMPUTED PHASES FOR  $J_T = 5/2$

G Function	Initial State	Phase			
		500°K	1,000°K	5,000°K	10,000°K
B	B	-0.00272	-0.00456	-0.0218	-0.0479
C	B	-0.00277	-0.00470	-0.0231	-0.0511
D	B	+0.01069	+0.01460	+0.0225	+0.0157
B	C	-0.00264	-0.00434	-0.0196	-0.0425
C	C	-0.00272	-0.00456	-0.0218	-0.0479
D	C	+0.01069	+0.01460	+0.0225	+0.0157
B	D	-0.00235	-0.00356	-0.0119	-0.0237
C	D	-0.00284	-0.00490	-0.0251	-0.0559
D	D	+0.01069	+0.01460	+0.0225	+0.0157

estimating the contributions of these omitted states to the various collision strengths. The formulas related to the method of distorted waves have been discussed in Chapter XI; the principal numerical difficulty is found to be the evaluation of Eq. (11.16). In evaluating these integrals, an important problem is the type and amount of distortion that should be included for the  $\mathcal{Y}$  functions. Other phases of this analysis have emphasized the importance of the short-range exchange distortion terms and the requirements pertaining to orthogonality. As these effects can be included in the numerical procedures with a minimum of effort, they have comprised the major source of distortion in computing the  $\mathcal{Y}$  functions. As the coupling to the "e" and "4" states is of the longer-range potential type (proportional to  $y_2(\text{PP})$ ), the required integrals should not display much sensitivity to other forms of distortion.

If the above convention regarding distortion is followed, the  $\mathcal{Y}$  functions are essentially the appropriate combinations of the  $\mathcal{S}$  and  $\mathcal{H}$  functions (the solutions of Eqs. (14.8) and (14.9)) as specified by the "Basic Transformation" (Eqs. (14.5) and (14.6)). For example,

$$\mathcal{Y}_c = -2 n_a \mathcal{S} - \sqrt{5} n_d \mathcal{H} \quad (15.3)$$

$$\mathcal{Y}_e = n_c \mathcal{S} \quad , \text{ etc.}$$

The approximation of exact resonance has been extended to these calculations, and the asymptotic behavior of the  $\mathcal{Y}$  functions as demanded by Eq. (11.14) helps to determine the  $n_i$  coefficients.

Technically speaking, this form of the Distorted Wave method should be valid for the  $J_T = 5/2$  set of equations as these states display the same type of coupling as the aforementioned "e" and "4" states. Such a check-out was performed for the  $\Omega_p(1,2)$  contribution from  $J_T = 5/2$ , and the results are presented in Table XXV for comparison with the more exact calculations described earlier in this chapter. The only significant difference between the two methods appears at the higher energy limit, and this discrepancy should not be sufficient to invalidate the reliability of the Distorted Wave method for other similar applications.

There are four basic integrals of the form, Eq. (11.16), required in the application of the Distorted Wave method to the "e" and "4" states. The constituents of these integrals for the excitation transitions are listed in Table XXVI. De-excitation cross sections can be evaluated by interchanging the subscripts on the initial and final  $F$  functions. It has been found that, for the transitions of concern here, the requirement of detailed balance is not satisfied. Algebraic simplification of the integrals demonstrates that this discrepancy is proportional to  $\Delta(P\&)$ , a quantity that is non-zero because of the limitations prohibiting the orthogonality of  $\&$  and  $P$ . Table XXVII illustrates the amount of error involved, and, as these are the only contributions to the final collision strengths that exhibit such discrepancies, the geometric mean of the two related parameters has been extended into the final summary. In general, the error at the higher energies is insignificant in establishing the final total collision strengths for the p-wave interaction.

TABLE XXV  
COMPARISON OF DISTORTED WAVE AND "EXACT" COLLISION STRENGTHS

$$J_T = 5/2$$

Exact Resonance Energy ( $^{\circ}\text{K}$ )	$\Omega_p(1,2) = \Omega_p(2,1)$	
	Distorted Wave Approximation	"Exact" Method
10,000	0.0069	0.0078
5,000	0.0037	0.0040
1,000	0.00078	0.00081
500	0.00039	0.00040

TABLE XXVI  
COMPONENTS OF DISTORTED WAVE INTEGRALS

$J_T$	Atomic Transition $J' \rightarrow J$	$F_m^{(a)}$	Coupling Element with Initial State
1/2	$2 \rightarrow 1$	$F_e$	$\frac{3\sqrt{10}}{50} [R_2(PPPF_c)P - y_2(PP)F_c]$
3/2	$2 \rightarrow 1$	$F_4$	$\frac{3}{25} [y_2(PF_3)P - y_2(PP)F_3]$
3/2	$2 \rightarrow 1$	$F_4$	$\frac{1}{50} [9 y_2(PP)F_6 + 3 y_2(PF_6)P - 12 R_2(PPPF_6)P]$
3/2	$1 \rightarrow 0$	$F_5$	$\frac{3\sqrt{10}}{50} [y_2(PF_4)P - R_2(PPPF_4)P]$

(a) This function specifies the final state of the system.

TABLE XXVII  
POST-PRIOR DISCREPANCIES UNDER DISTORTED WAVE METHOD<sup>(a)</sup>

Energy (°K)	$\Omega_p(1,2)$	$\Omega_p(2,1)$	$\Omega_p(0,1)$	$\Omega_p(1,0)$	Geometric Mean	
					$\Omega_p(1,2)$	$\Omega_p(0,1)$
10,000	0.019	0.016	0.00010	0.00017	0.017	0.00013 <sup>(c)</sup>
5,000	0.011	0.0092	(b)	(b)	0.010	(b)
1,000	0.0026	0.0024	(b)	(b)	0.0025	(b)
500	0.0014	0.0013	(b)	(b)	0.0013	(b)

- (a) These are contributions to p-wave collision strengths due to interactions with the "e" and "4" states.
- (b) Results are too small to be of significance in establishing the final total p-wave collision strength.
- (c) Error is insignificant in the final total p-wave collision strength.



Validity of Approximations

It was found desirable to check the validity of the special treatment that has been given to the "e" and "4" states in the current and preceding chapters. For purposes of illustration, the discussion will center around the "e" state of  $J_T = 1/2$ . The net effect of the assumptions that have been made has been an isolation of this state from the remaining states of the set, the belief being that the presence of the "e" state does not significantly influence the calculated results for the others. Weak-coupling approximations have also been regarded as valid for transitions which involve this special state.

If the transformation, Eqs. (14.5), is applied to the complete set of differential equations for  $J_T = 1/2$ , with the presence of the "e" state retained, the following additions must be made to the right sides of Eqs. (14.12):

$$\begin{aligned}
 G_a: & \quad + \frac{3\sqrt{10}}{100} \left[ \frac{n_c}{n_a} \right] [y_2(PP)G_c - R_2(PPPG_c)P] \\
 G_b: & \quad + \frac{\sqrt{2}}{20} \left[ \frac{n_c}{n_b} \right] [y_2(PP)G_c - R_2(PPPG_c)P]
 \end{aligned} \tag{15.4}$$

The following additional equation must be added to the coupled set, Eqs. (14.12):

$$\begin{aligned}
[\mathcal{L}^1 + 4y_0(\text{PP}) + 2y_0(S_1S_1) + 2y_0(S_2S_2)] G_c &= [y_0(\text{PG}_c) + \Lambda_c(\text{PG}_c)]P \\
&+ \frac{1}{3} y_1(S_1G_c)S_1 + \frac{1}{3} y_1(S_2G_c)S_2 + \frac{2}{5} y_2(\text{PG}_c)P \\
&+ \frac{3\sqrt{10}}{25} \left[ \frac{n_a}{n_c} \right] y_2(\text{PP})G_a + \frac{\sqrt{2}}{5} \left[ \frac{n_b}{n_c} \right] y_2(\text{PP})G_b, \quad (15.5)
\end{aligned}$$

with  $\Lambda_c(\text{PG}_c)$  having coefficients of  $\vartheta = 1$ ,  $\kappa = -(2/5)$  in Eq. (14.4), and coupling terms of  $-(3\sqrt{10}/25)(n_a/n_c) R_2(\text{PPPG}_a) - (\sqrt{2}/5)(n_b/n_c) R_2(\text{PPPG}_b)$ .

The resulting set of three coupled equations can be solved by the techniques described in Chapters XIV and XVI; however, a difficulty is encountered in the evaluation of the  $n_c$  coefficient from the boundary conditions. With the restricted transformation, Eqs. (14.5), and "e" not the initial state, the absence of the sine term in Eq. (11.8) demands that  $n_c = 0$ . Hence there would be an effective uncoupling of  $G_c$  from the remainder of set. However, the defects of the chosen transformation can be remedied by the following series of procedures.

Select an arbitrary value for  $n_c$ , say  $n_c = n_c^{(1)}$ , in the set of coupled equations. Best results are obtained for  $n_c^{(1)}$  having an order of magnitude comparable with  $n_a$  and  $n_b$ . Choosing "c" as the initial state, the three equations (Eqs. (14.12) with (15.4), and (15.5)) are solved in the manner prescribed in Chapters XIV and XVI. The  $n_a$  and  $n_b$  coefficients are chosen to satisfy the same boundary conditions as would have been imposed had the "e" state not been considered. This establishes the correct asymptotic behavior for  $F_c$ ,  $F_d$  and  $F_f$ . The

final solutions and coefficients so obtained are to be denoted by the superscript (1).

Another arbitrary value,  $n_c = n_c^{(2)}$ , may be selected and the above routine repeated. ( $n_c^{(2)}$  should be chosen sufficiently different from  $n_c^{(1)}$  to insure different results for the set of equations; in practice  $n_c^{(2)} = 5 n_c^{(1)}$  was found satisfactory.) The superscript (2) serves to distinguish these solutions. As a linear combination of the two independent sets of solutions is also a solution, the final  $F$  functions can be chosen as follows:

$$\begin{aligned} F_c &= q_1 F_c^{(1)} + q_2 F_c^{(2)} \\ &\vdots \\ F_f &= q_1 F_f^{(1)} + q_2 F_f^{(2)}, \end{aligned} \tag{15.6}$$

where  $q_1$  and  $q_2$  are to be adjusted to satisfy Eq. (11.8). In particular, since "c" has been adopted here as the initial state, one requirement is that

$$q_1 + q_2 = 1. \tag{15.7}$$

The remaining parameter is selected to establish the correct boundary condition on  $F_c$ ; that is, to cause the coefficient of  $\sin(kr - \pi/2)$  to vanish. The resulting solutions as given by Eqs. (15.6) are thus uniquely specified and possess the required asymptotic behavior.

As the primary purpose of the above procedure has been to check the results of the earlier approximation, it is only necessary to compare the significant features which differ in the two alternative

methods. Algebraic manipulations show that for the method described above, the elements of the "refined" R-matrix which are associated with the initial "c" state can be obtained from those listed in Table XX by the following substitutions:

$$\begin{aligned}\tan \mathfrak{m}_{a,c} &\rightarrow q_1 \tan \mathfrak{m}_{a,c}^{(1)} + q_2 \tan \mathfrak{m}_{a,c}^{(2)} \\ \tan \mathfrak{m}_{b,c} &\rightarrow q_1 \tan \mathfrak{m}_{b,c}^{(1)} + q_2 \tan \mathfrak{m}_{b,c}^{(2)} .\end{aligned}\tag{15.8}$$

Hence, the extent of possible error can be ascertained by comparing these quantities directly. In addition, it can be shown that under the above method,

$$R_{e,c} = \sqrt{k} \left[ q_1 n_c^{(1)} A_{c,c}^{(1)} \sin \mathfrak{m}_{c,c}^{(1)} + q_2 n_c^{(2)} A_{c,c}^{(2)} \sin \mathfrak{m}_{c,c}^{(2)} \right] .\tag{15.9}$$

The notation is the same as that employed in Table XX. The magnitude of  $R_{e,c}$  above is directly comparable with the corresponding B-matrix element obtained with Eq. (11.16) under the Distorted Wave approximation.

Detailed calculations were performed on the system of coupled equations for  $J_T = 1/2$  which included the coupling to the "e" state. An energy of  $5,000^\circ\text{K}$  was chosen, the Exact Resonance approximation was retained, and "c" was considered as the initial state. The desired comparison with the associated quantities obtained under the approximate method is illustrated in Table XXVIII. The excellent agreement should be sufficient to validate the treatment that has been presented

TABLE XXVIII

## COMPARISON OF APPROXIMATE AND EXACT METHODS

(J<sub>T</sub> = 1/2, Initial State = "c", Energy = 5,000°K)

Element under Approximate Method		Corresponding Element under Exact Method	
$\tan \eta_{a,c} = -0.055$		$-0.054^{(a)}$	
$\tan \eta_{b,c} = -0.037$		$-0.036^{(a)}$	
$B(e,c)$	$= -0.028$	$R(e,c)$	$= -0.030$

(a) See Eqs. (15.8).

in this chapter and in Chapter XIV concerning the isolation of the "e" and "4" states.

Although computations are possible with the exact method that has just been described, and would certainly be more elegant for formal presentation, the corresponding increase in difficulty is sufficient to warrant thoughtful consideration before such an attempt is made. The addition of another equation to the coupled set for  $J_T = 3/2$  would impose considerable additional requirements concerning computer memory and running time. (The limited availability of the former has already been a major problem in the current calculations.) In view of the limits imposed upon the overall accuracy by approximations in other phases of the work, and upon consideration of the excellent comparison exhibited in Table XXVIII, such extended calculations are not thought necessary at the present time.

A detailed summary of the p-wave collision strengths under exact resonance is presented in Table XXIX. As adjustments have already been made for the slight lack of detailed balance in the distorted wave contributions, the exhibited parameters are symmetric (i.e.,  $\Omega_p(m,n) = \Omega_p(n,m)$ ).

#### Allowance for Energy Differences

In an attempt to extend the development for the p-wave collision strengths that comprises the current and preceding chapters, no direct method was found for relaxing the restrictions imposed by the Exact Resonance approximation. However, the introduction of different energies for the various bound atomic states should provide only minor corrections to the cross sections; these adjustments are expected

TABLE XXIX  
ANALYSIS AND SUMMARY OF COLLISION STRENGTHS FOR P-WAVE  
UNDER EXACT RESONANCE

Exact Resonance Energy (°K)	Contributions to $\Omega_p$			Total $\Omega_p$
	Modified Basic Transformation (Chapter XIV)	$J_T=5/2$	D. W. Corrections	
<u><math>\Omega_p(1,2):</math></u>				
10,000	0.246	0.0078	0.017	0.271
5,000	0.117	0.0040	0.010	0.131
1,000	0.0084	0.00081	0.0025	0.0117
500	0.0015	0.00040	0.0013	0.0032
<u><math>\Omega_p(0,2):</math></u>				
10,000	0.068			0.068
5,000	0.033			0.033
1,000	0.0030			0.0030
500	0.00092			0.00092
<u><math>\Omega_p(0,1):</math></u>				
10,000	0.101		0.00013	0.101
5,000	0.049		0.0	0.049
1,000	0.0044		0.0	0.0044
500	0.0010		0.0	0.0010

to be significant only near the lower end of the energy range being considered.

The portions of the p-wave collision strengths which are capable of being determined by the Distorted Wave approximation can be corrected in a very direct and simple manner. It is merely necessary to insert the proper wave functions (those calculated with the correct electron energies) into the integral of Eq. (11.16). New computational procedures are required and more wave functions must be evaluated, but the overall procedural aspects of the problem are unchanged, the validity of the approach is unquestionable, and the computer requirements remain reasonable. Table XXX displays a comparison of portions of these distorted wave calculations (for the states of  $J_T = 5/2$ ) with the associated results from the Exact Resonance approximation. No differences between the two methods were detected at 5,000 °K, and only minor deviations were found for even the lowest electron energy.

The correct treatment of the states which are connected under the strong coupling of the spherically-symmetric exchange terms poses much more of a problem. These are the portions of the  $J_T = 1/2$  and  $3/2$  sets of equations which were solved "exactly" under exact resonance with the methods described in Chapter XIV. Seaton<sup>40,41,42</sup> suggested a method of making an allowance for the differences in energy for the atomic states; this method has been discussed in detail in its application to the s-wave collision strengths in Chapter XII and is not to be repeated. However its usefulness with respect to the p-wave equations is highly questionable as the essential criterion for validity can no longer be satisfied. For the p-wave, the  $y_2(PP)$  long-range



TABLE XXX  
COMPARISON OF DIFFERENT METHODS OF ALLOWING FOR ENERGY  
DIFFERENCES,  $J_T = 5/2$

Energy <sup>(a)</sup> (°K)	$\Omega_p(1,2)^{(b)}$			
	Exact Resonance		Allowance for Energy Differences	
	Distorted Wave Approximation	"Exact" Method	Distorted Wave Approximation	Seaton <sup>(c)</sup> Method
5,000	0.0037	0.0040	0.0037	0.0041 $\pm$ 2.6%
1,000	0.00078	0.00081	0.00082	0.00089 $\pm$ 13%
500	0.00039	0.00040	0.00042	0.00048 $\pm$ 28%

(a) This value represents the electron energy when the atom is in the excited ( $J = 1$ ) state.

(b) The figures tabulated refer only to contributions from  $J_T = 5/2$ .

(c) Percent of error is the result of the asymmetry of the R-matrix.

potential coupling terms show a sensitivity to variations in  $k^2$  that cannot be compensated for by the normalization requirements proposed for s-wave. (In the latter case, the principal coupling terms were short-range exchange interactions whose magnitudes were sensitive to the wave function behavior near the origin.) On the other hand, it can be argued that the Seaton approach should be an improvement over the Exact Resonance approximation, and should provide better estimates of the collision strengths even though complete accuracy cannot be claimed. This is the extent of the refinement that has been performed in the current calculation to allow for energy differences.

An additional difficulty becomes apparent when the Seaton method is applied to the equations of  $J_T = 1/2$  and  $3/2$  which are evaluated with the modified "Basic Transformation." Of course the elements of the R-matrices no longer have the simple forms displayed in Table XX, and must be re-evaluated in terms of both amplitudes and phases. In addition, the inability of the new transformations to completely satisfy the original coupled scattering equations results in the R-matrices deviating from the required symmetry. This asymmetry is related to discrepancies between  $\Omega(m,n)$  and  $\Omega(n,m)$ ; in the work concerning the distorted wave applications, the latter differences were corrected by adopting the geometric mean of the two collision strengths. In lieu of this procedure, it appears more desirable to symmetrize the R-matrix (using the geometric mean of the corresponding elements), and to calculate the maximum error so introduced. This percentage error has been included with the final results, and in all cases has been within the limits of the overall accuracy expected.

It is possible to obtain an indication of the accuracy of the above method by comparing the results so obtained for the  $J_T = 5/2$  equations with the corresponding calculations performed with the Distorted Wave approximation. (The agreement was excellent for the case of exact resonance.) This comparison is exhibited in Table XXX, and the agreement can be viewed as acceptable.

A special examination was made of the  $J_T = 1/2$  contributions at 5,000 °K when energy differences were allowed for under the Seaton method. Deviations of the calculated results from comparable exact resonance values were found to be insignificant, thereby substantiating the argument that energy differences are unimportant at this electron energy. This is in agreement with conclusions derivable from the distorted wave calculations, and similar computations for s-wave (see Table XV). Hence the comprehensive numerical calculations related to energy differences were performed only at the two lower energies.

Table XXXI compares the exact-resonance collision strengths for p-wave with similar quantities evaluated under the methods suggested in this section. The latter numbers are extended into the final collision strength summary in Chapter XVIII. As Table XXXI well illustrates, the corrections for energy differences are not of major importance except perhaps for  $\Omega_p(1,2)$ , and for this parameter the associated percentage error is comparatively small.

TABLE XXXI

P-WAVE COLLISION STRENGTHS WITH ALLOWANCE FOR ENERGY DIFFERENCES

Electron Energy <sup>(a)</sup> (°K)	$\Omega_p$		
	Exact Resonance Approximation <sup>(b)</sup>	Allowance for Energy Differences <sup>(c)</sup>	Computed Error <sup>(d)</sup>
<u><math>\Omega_p(1,2):</math></u>			
10,000	0.271	0.271	
5,000	0.131	0.131	
1,000	0.0117	0.0160	<1%
500	0.0032	0.0055	4%
<u><math>\Omega_p(0,2):</math></u>			
10,000	0.068	0.068	
5,000	0.033	0.033	
1,000	0.0030	0.0032	2%
500	0.00092	0.00104	13%
<u><math>\Omega_p(0,1):</math></u>			
10,000	0.101	0.101	
5,000	0.049	0.049	
1,000	0.0044	0.0044	3%
500	0.0010	0.0012	5%

(a) This value represents the electron energy when the atom is in the respective excited state.

(b) See Table XXIX.

(c) See discussion for methods employed for the different contributions.

(d) This error arises because of the asymmetry of the R-matrix.

## CHAPTER XVI

### NUMERICAL METHODS

This chapter is to be devoted chiefly to a discussion of the numerical procedures involved in the solution of the various integro-differential equations that appear throughout the analysis, and of the special techniques of iteration that have been applied to achieve rapid convergence.

Under the scheme of iteration to be described, it has been found necessary to numerically solve a radial differential equation of the general form:

$$\frac{d^2G}{dr^2} = f(r)G + g(r). \quad (16.1)$$

This special equation is linear in the dependent variable and its derivatives and furthermore has no explicit dependence upon the first derivative,  $dG/dr$ . The functions,  $f(r)$  and  $g(r)$ , are assumed to be known and well-behaved. An efficient method for obtaining a numerical solution of Eq. (16.1) is the treatment ascribed to Numerov:<sup>57</sup>

$$\begin{aligned}
& \left[ 1 - \frac{1}{12} (\delta r)^2 f_n \right] G_n - 2 \left[ 1 - \frac{1}{12} (\delta r)^2 f_{n-1} \right] G_{n-1} \\
& + \left[ 1 - \frac{1}{12} (\delta r)^2 f_{n-2} \right] G_{n-2} \\
& = (\delta r)^2 \left[ f_{n-1} G_{n-1} + g_{n-1} + \frac{1}{12} \delta^2 g_{n-1} \right], \quad (16.2)
\end{aligned}$$

where  $\delta r$  is the radial increment of integration, and

$$\delta^2 g_k = g_{k+1} - 2g_k + g_{k-1}. \quad (16.3)$$

In application, the procedure is to start the integration process at one end of the interval, and to proceed step-by-step to the other boundary. The peculiar nature of the scattering problem suggests initiating the solution at  $r = 0$ , (where the  $G$  function is required to vanish), and to continue the integration until it is appropriate to apply the asymptotic boundary conditions (for instance, Eq. (11.9)). As seen by Eq. (16.2), it is necessary to know the function at a minimum of two consecutive values of  $r$  to be able to proceed with the solution, but these are easily obtained with a small-value expansion near the origin.

For convenience, a new form has been chosen for the radial differential operator (in lieu of that defined by Eq. (9.5)), namely

$$L = \frac{d^2}{dr^2} - \frac{l(l+1)}{r^2} - 2U + k^2 \quad (16.4)$$

with the spherically-symmetric potential function,  $U(r)$ , given by Eq. (10.7). Let the following general form be assumed for the basic

integro-differential equation of the scattering problem:

$$L G = \mathcal{A}(G). \quad (16.5)$$

The function,  $\mathcal{A}(G)$ , may include, among other terms, the exchange integrals  $y_t(PG)$ , etc., with the unknown function appearing as part of an integrand. The chosen method of approach is to solve the set of equations:

$$\begin{aligned} L G^{(0)} &= 0 \\ L G^{(1)} &= \mathcal{A}(G^{(0)}) \\ L G^{(2)} &= \mathcal{A}(G^{(1)}) \\ &\vdots \\ L G^{(n)} &= \mathcal{A}(G^{(n-1)}) \end{aligned} \quad (16.6)$$

These equations are of the special form specified by Eq. (16.1), and can be readily solved with Eq. (16.2).

The solution of Eq. (16.5) can be taken as

$$G = G^{(0)} + G^{(1)} + G^{(2)} + \dots + G^{(n)}. \quad (16.7)$$

The  $G^{(0)}$  function is essentially the complementary solution, and the remaining sum in Eq. (16.7) can be thought of as contributing the particular solution to the differential equation. The number of terms required depends upon the speed of convergence, that is, it is determined by how fast the  $\mathcal{A}(G^{(k)})$  functions approach zero and cease to contribute a significant particular solution to the sum in Eq. (16.7).

An important part of the numerical analysis is to establish the appropriate starting solutions near the origin for the constituents of the set, Eqs. (16.6). A Frobenius expansion of  $G$  is sufficient to determine the form of the power series solution valid for small  $r$ , with the coefficients determined from the associated differential equation. For  $OI$ , the  $y_0(PP)$ ,  $y_0(S_1S_1)$  and  $y_0(S_2S_2)$  terms in  $U(r)$  can be shown to approach constant values near the origin, and are unimportant if the validity of a two-term expansion can be established. The latter condition can be easily achieved by starting the solution sufficiently close to  $r = 0$ . Hence, for the complementary solution, sufficient accuracy has been obtained with

$$G^{(0)} = A_0 r^{\ell+1} \left[ 1 - \frac{Zr}{\ell+1} \right], \quad r \ll 1. \quad (16.8)$$

The constant,  $A_0$ , is arbitrarily set at a fixed value for the numerical work, and subsequently adjusted through the imposition of the asymptotic boundary conditions.

The starting functions for the particular solutions are somewhat more involved, and depend heavily upon the behavior of  $\mathcal{A}(G^{(k)})$  near the origin. Two separate situations were encountered in the course of the present work. It should be noted that  $\mathcal{A}(G^{(k)})$  in Eqs. (16.6) corresponds to  $g(r)$  in Eq. (16.1). Assume first that

$$g(r) = \alpha r^2 + \beta r^3, \quad r \ll 1. \quad (16.9)$$

In a general notation, the correct small-value expansion is



$$G^{(j)} = \frac{\alpha}{10} r^4 + \frac{(\beta - 1.6\alpha) r^5}{18}, \quad r \ll 1. \quad (16.10)$$

However, in the solution of the scattering equations for s-wave, it is found that

$$g(r) = d_1 r + d_2 r^2, \quad r \ll 1, \quad (16.11)$$

and

$$G^{(j)} = \frac{d_1}{6} r^3 + \frac{1}{12} \left[ d_2 - \frac{Zd_1}{3} \right] r^4, \quad r \ll 1. \quad (16.12)$$

In the formal iteration process, the appropriate coefficients,  $\alpha$  and  $\beta$ , or  $d_1$  and  $d_2$ , are dependent upon  $G^{(k)}$ , and hence upon the form and magnitude of  $G^{(k)}$ , and must be re-evaluated after each pass to provide the proper starting solution for the next iteration.

The procedures thus far outlined in this chapter have direct application to the radial differential equations which arise from the s- and p-wave interactions with the neutral atom. These methods have been applied in the solution of the various  $G$  functions; these functions were obtained by transformation as linear combinations of the original  $F$  functions. Exchange interactions play a very significant role in these equations, and are shown to make major contributions to the excitation cross sections. In addition, the presence of exchange introduces a very unique feature into the normal numerical procedures. This concerns the treatment and evaluation of the  $\lambda$  (or  $\Lambda$ ) parameters that appear in all of these equations. As discussed in Chapters XII, XIV, and XV, these parameters permit certain side conditions to be imposed upon the solutions either to insure orthogonality, or to

minimize the effects of non-orthogonality. These side conditions can be incorporated into the numerical procedures in such a manner as to both simplify the detailed labor and facilitate rapid convergence of the iteration. Seaton has applied the method to the p-wave equations for  $^3P$ ,  $^1D$ ,  $^1S$  transitions in OI, and obtained very rapid convergence.<sup>41</sup> Although the basic concepts are the same for both s-wave and p-wave interactions, there are sufficient small differences to warrant separate presentations.

For equations characteristic of the p-wave interaction, it is desirable to separate out the  $\lambda$  dependence, and write Eq. (16.5) in the form:

$$L G = g(G) + \tau \lambda (PG) P \quad (16.13)$$

where  $\tau$  is some numerical constant. The steps in the iteration process become the following:

$$\begin{aligned}
 (1): \quad & L \bar{G}^{(0)} = 0 \\
 & L u = -2 P \\
 & G^{(0)} = \bar{G}^{(0)} + \mu_0 u \\
 (2): \quad & L \bar{G}^{(1)} = g(G^{(0)}) \\
 & G^{(1)} = \bar{G}^{(1)} + \mu_1 u \\
 & \cdot \\
 & \cdot \\
 & \cdot \\
 (n+1): \quad & L \bar{G}^{(n)} = g(G^{(n-1)}) \\
 & G^{(n)} = \bar{G}^{(n)} + \mu_n u.
 \end{aligned} \quad (16.14)$$

The final solution of Eq. (16.13) is simply

$$G = G^{(0)} + G^{(1)} + \dots + G^{(n)}. \quad (16.15)$$

The parameters denoted by  $\mu_{i=1,n}$  are determined after each stage of the iteration to insure that the solution satisfies the required side conditions. For example, either Eq. (14.17) or Eq. (14.20) may be so selected. Convergence was found to be very rapid, even with the long-range potential terms present. Five stages of iteration were found to be more than sufficient for the  $\mathcal{P}$ -type equations, and eight passes were accomplished for the  $\mathcal{S}$ -type.

The approach to the s-wave equations is very similar to that described above, except that now, as shown by Eqs. (12.8) and (12.9), there are two parameters that need to be considered. Accordingly,

$$L G = Q(G) + \tau_1 \lambda (S_1 G) S_1 + \tau_2 \lambda (S_2 G) S_2. \quad (16.16)$$

The solution proceeds in the following manner:

$$\begin{aligned} (1): \quad & L \bar{G}^{(0)} = 0 \\ & L u_1 = -2 S_1 \\ & L u_2 = -2 S_2 \\ & G^{(0)} = \bar{G}^{(0)} + \mu_0^{(1)} u_1 + \mu_0^{(2)} u_2 \\ (2): \quad & L \bar{G}^{(1)} = Q(G^{(0)}) \\ & G^{(1)} = \bar{G}^{(1)} + \mu_1^{(1)} u_1 + \mu_1^{(2)} u_2 \\ & \text{etc.} \end{aligned} \quad (16.17)$$

with

$$G = G^{(0)} + G^{(1)} + G^{(2)} + \dots + G^{(n)}. \quad (16.18)$$

As noted in the discussion in Chapter XII, the side conditions for these solutions can be stated very explicitly, namely that  $G$  be made orthogonal to both the  $S_1$  and  $S_2$  bound radial wave functions. These requirements, as expressed through Eqs. (12.12), are sufficient to determine the various  $\mu^{(1)}$  and  $\mu^{(2)}$  parameters in the above outline of procedure. Five stages of iteration were found satisfactory for accurate solutions of the s-wave equations.

The discussion in Chapters XIV and XV centered around the solution of sets of coupled differential equations having  $l = 1$ . For a particular set, the individual equations are coupled together, and a solution for the group is possible only through numerical iteration. The iteration between different equations of a set is straight-forward and standard methods are readily applicable. The general approach taken has been briefly outlined in Chapter XIV. However, once the appropriate approximations have been inserted for the coupling functions, the individual equations reduce to the form specified by Eq. (16.13) and can be solved with the corresponding special techniques that have been presented for such equations.

## CHAPTER XVII

### POLARIZATION INTERACTION

The discussion in Chapter VII expressed concern over the possible effects of polarization, in particular for the s-wave. If the major contribution from the polarization interaction arises from regions near the interior of the atom, the increase in the various collision strengths could be quite significant. Under such a situation, the effect would be most pronounced for s-wave (which implies a direct collision) because of the possible penetration of the bound electronic charge cloud. In addition, the negative-ion state mentioned in Chapter VII, if such exists, could establish this mechanism as the dominant one. However, if the principal influence of polarization exists in regions farther removed from the atom, the p-wave and d-wave would be more sensitive to its form and magnitude. In the latter case, the net overall corrections would be expected to be comparatively small. In spite of the known uncertainty concerning the correct treatment of the polarization potential, a brief examination of this interaction force has been undertaken for the s-wave component.

The form chosen for the polarization potential has been the empirical formula given by

$$V^P = - \frac{\alpha_P}{2 r^4} \left[ 1 - e^{-(r/a)^8} \right] \quad (17.1)$$

where  $\alpha_P = 5.2$  au. is the experimental polarizability<sup>59</sup> for neutral atomic oxygen, and "a" is a cut-off parameter introduced to prevent divergence difficulties at the origin and to adjust for proper behavior in the interior of the atom. The properties of this particular expression and prior successful applications have been discussed in detail in Part I of this dissertation, and are not to be repeated. The curve profile displays a peak around .95a, behaves asymptotically as  $r^{-4}$ , and approaches zero as  $r^4$ .

No correct procedure has yet been established for the proper selection of the cut-off parameter. In the principal applications of polarization, the policy has generally been to adjust the value of this parameter until good agreement is obtained with experimental data. Of the many treatments of the polarization interaction in atomic problems, there are two which deserve some discussion here. Jackson and Garrett<sup>26</sup> have recently determined theoretically the photo-detachment and elastic cross sections for  $O^-$  and  $OI$  respectively. In the process of the calculation, a polarization potential was developed for the distortion of the neutral atom by the external electron. First-order perturbation theory was employed in conjunction with the usual adiabatic approximation. The resulting curve has a profile very similar to that obtained with Eq. (17.1) with a calculated polarizability of 5.149 au. The peak occurs around 1 au., near the approximate location of the peak in the (2p) bound-state wave function. (The latter criterion has often been used in atomic problems to establish the polarization cut-off

parameter). However, the dipole approximation introduced into the calculation of the polarized orbitals is not valid for regions interior to the atom, and can result in a reduction of the accuracy expected for the lower part of the potential curve. Hence, although satisfactory results were obtained, it is highly possible that the corresponding cut-off of 1 au. could result in large errors if the most significant contributions to the cross sections arise from  $r < a$ .

The elastic scattering of slow electrons by OI has also been recently considered by Lenander.<sup>23</sup> Polarization was treated as a surface effect only, with the interaction valid only in regions completely removed from the atom. A cut-off parameter of 5.9 au. was found to give results compatible with existing experimental data.

In the present analysis, the contributions from the s-wave arise solely from exchange interactions with the atomic (2p) orbitals. The value of  $a = 5.9$  au. as determined by Lenander should certainly provide at least a lower limit to the cross section contributed by polarization, with the 1.0 au. of Jackson and Garrett as a possible estimate for the corresponding upper limit.

If a spherically-symmetric interaction term such as Eq. (17.1) is included in the Hamiltonian, Eq. (8.1), this same term would appear in the scattering equations for s-wave, Eqs. (12.8) and (12.9), as an additive correction to the  $y_0(\text{PP})$ , etc., terms. For example, Eq. (12.8) will assume the form:

$$[\mathcal{L}^0 + 4y_0(\text{PP}) + 2y_0(S_1S_1) + 2y_0(S_2S_2) + V^P]G_1 = [y_0(S_1G_1) + \lambda_P^{(1)}(S_1G_1)]S_1 + [y_0(S_2G_1) + \lambda_P^{(2)}(S_2G_1)]S_2 \quad (17.2)$$

where

$$\lambda_P^{(1)}(S_1 G_1) = \lambda^{(1)}(S_1 G_1) + \int_0^\infty S_1 G_1 V^P dr, \text{ etc.} \quad (17.3)$$

The integral in Eq. (17.3) arises from the polarization exchange interaction, and is necessary if the orthogonality conditions, Eqs. (12.12), are to be properly applied. Other conditions and procedures for the solution of the s-wave equations and the calculation of the collision strengths remain as outlined in Chapter XII.

The polarization interaction term given by Eq. (17.1) was included in the scattering equations for s-wave, and a series of calculations were performed for selected values of the cut-off parameter between the limits of 5.9 and 1.0 au. Under exact resonance, the collision strengths for s-wave are proportional to  $\sin^2(m_1 - m_2)$ . (See, for example, Eqs. (12.16).) The results for the latter quantity have been plotted in Figure 7 to illustrate its sensitivity to the choice of cut-off parameter, and to compare its magnitude and behavior with the corresponding polarization-free value.

The curves in Figure 7 show a high sensitivity to the value of the cut-off parameter in the region  $a \leq 1.5$  au., while above this number the variation is not so severe. Theoretically this behavior is to be expected from the nature of the coupling interaction. For s-wave the transitions arise from the short-range exchange forces with the (2p) bound electrons; these coupling terms are largest around  $r = 1.0$  au. near where the  $P$  function peaks, and hence should show considerable sensitivity to distortion in this region. As a cut-off of 5.9 au. results in only minor corrections to the polarization-free



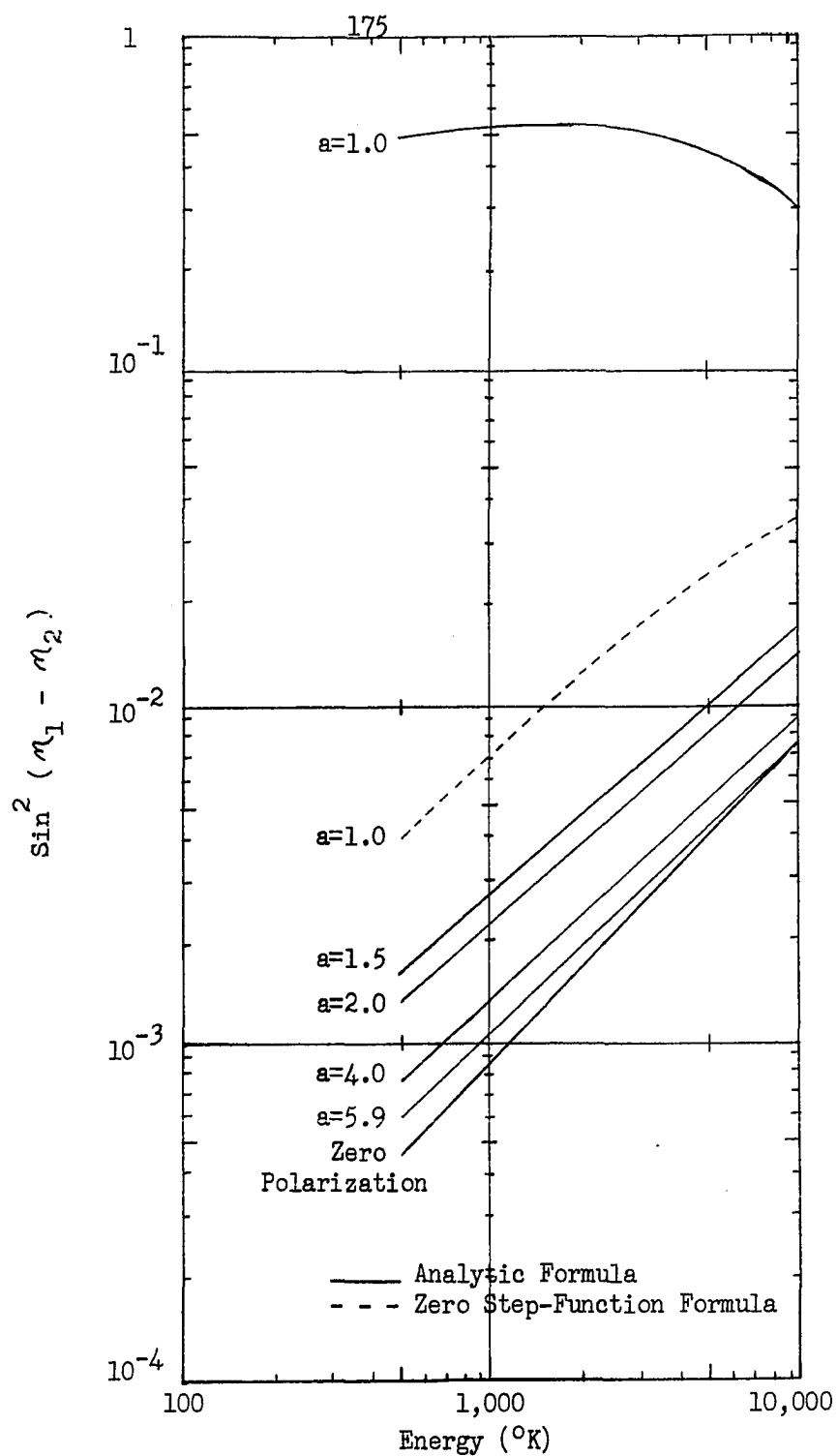


Figure 7. Effect of Different Polarization Cut-Off Parameters upon S-wave Cross Sections.

collision strengths, the major problem is whether a choice of  $a < 1.5$  au. can be justified.

Since the dominant contribution of the polarization potential appears to originate from regions interior to the atomic charge cloud, it is necessary to investigate the role played by the lower tail of the polarization curve. As has already been discussed, the function, Eq. (17.1), peaks around  $r = a$  and then rapidly goes to zero at the origin. The latter part of this curve is most inaccurate, hence separate calculations were performed with the following modified form:

$$\begin{aligned} V^P &= \text{Eq. (17.1)} & a \leq r \\ V^P &= 0 & r < a \end{aligned} \quad (17.4)$$

This function is equivalent to the Zero Step-Function formula discussed in Part I. For  $a > 4.0$  au., the results are practically identical to those obtained with Eq. (17.1). Deviations begin near  $a \simeq 1.5$  au. where the above modified potential yielded cross sections which are equivalent to choosing  $a = 2.0$  au. in Eq. (17.1).

Finally, for  $a = 1.0$  au., the effects of the lower tail are well emphasized by the two curves plotted in Figure 7. The discrepancies between the two results are seen to exceed an order of magnitude. The collision strengths for s-wave are thus found to depend heavily upon the specific form chosen for the polarization interaction in the near-field, and the lack of a rigorous model thereof contributes to the uncertainties related to this form of interaction. In view of these developments, it is almost impossible to place any real reliance upon the magnitudes of these collision strengths at the present time.

As a result of the above uncertainties, the final collision strengths for the OI spin-multiplet transitions are to be summarized in the next chapter for two special cases. The first neglects the polarization interaction completely, while the second should be considered only as a compromise designed to demonstrate the possible effects of polarization. The latter have been calculated with Eq. (17.4) adopting  $a = 1.0$  au., and serve to illustrate the increase in the cross sections that can be effected by these forces. Final conclusions as to the correct magnitudes of these collision strengths must be withheld until more information can be obtained regarding the correct treatment of polarization, and no claim will be made as to the ultimate accuracy of the results presented here. However, the tabulated collision strengths which neglect polarization can certainly be regarded as possible lower limits to the correct magnitudes, and as such are still of significant importance in astrophysical calculations.

## CHAPTER XVIII

### SUMMARY OF COLLISION STRENGTHS FOR THE SPIN-MULTIPLETS OF OI

Before presenting a final summary of the calculated collision strengths, a brief discussion should be presented of the method that has been used to estimate these parameters for astrophysical applications. The rough approximations used by Gershberg<sup>46</sup> emphasized comparative ratios with similar parameters for the associated OIII ion. Seaton<sup>41</sup> has found that for the first few electron volts above threshold, the energy variation of the  $\Omega$ 's (considering the  $^3P$ ,  $^1D$  and  $^1S$  levels of OIII) was very slow and could be neglected in most physical problems. For slow collisions between electrons and positive ions, the transition probabilities are considerably larger than for neutral atoms because of the attractive Coulomb field, and the related collision strengths tend to finite limits at the excitation thresholds. Hence, it is common practice to calculate and tabulate only the threshold values of the collision strengths for positive ions. Gershberg contends that there are deviations from this simple behavior near the excitation threshold. The statement is made that the cross section should be zero at the threshold energy  $E_0$ , should increase rapidly to a maximum at energy  $E_0 + \Delta E$ , and then drop off approximately as  $E^{-1}$ . For calculations concerning physical processes involving electrons and positive ions near threshold, a convenient formula can be

obtained for the total rate of excitation by considering  $\Omega$  to be constant (that is, accepting the tabulated threshold value,  $\Omega^0$ ) and adjusting for the above behavior with a correction factor,  $x(E_0, T_e)$ .

Gershberg gives

$$x = \frac{1}{(t + \Delta t) \Delta t} [t + 2 - e^{-\Delta t}(t + 2 + 2 \Delta t)] , \quad (18.1)$$

where

$$t = \frac{11,600 E_0}{T_e} , \quad \Delta t = \frac{11,600 \Delta E}{T_e} . \quad (18.2)$$

In the above expression,  $E_0$  and  $\Delta E$  are to be expressed in electron volts, and  $T_e$  is the electron temperature of the gas.

The OI neutral atom and OIII ion have a similar term structure. The ground configurations for the two systems are compared in Figure 8. The ratio  $\Omega(\text{OI}) / x \Omega^0(\text{OIII})$  was determined for selected energies from accepted values of the parameters for transitions between the  $^3P$ ,  $^1D$  and  $^1S$  terms. Table XXXII is a summary of the results obtained by Gershberg; the values for  $^3P - ^1D$  have been checked independently and can be considered to be reliable. The data in this table shows that the above ratio depends only slightly on  $T_e$ . The contention was made that this ratio should be the same for the transitions between the spin-multiplets of the  $^3P$  terms. Accordingly, a mechanism can be made available for estimating the unknown collision strengths of OI.

Using this approximate scheme, Gershberg proceeded to calculate the energy loss rates in the intermediate HI-HII zones due to excitation

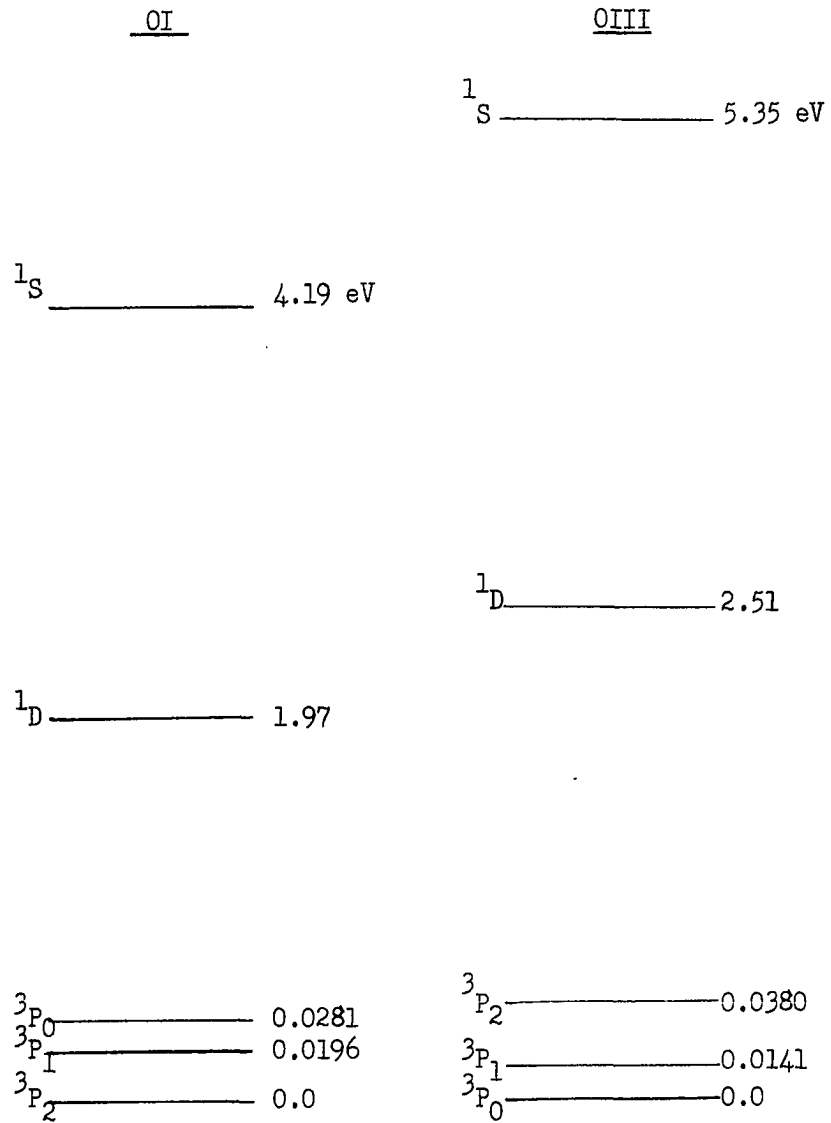


Figure 8. A Comparison of the Ground Configuration Energy Levels of OI and OIII. (The energy scale has been enlarged for the  $3P_J$  intervals.)

TABLE XXXII  
COMPARISON OF ASSOCIATED COLLISION STRENGTHS FOR OI AND OIII

$T_e$ (°K)	$\Omega(\text{OI}) / \times \Omega^0(\text{OIII})^{(a)}$	
	$3P - 1D$	$3P - 1S$
10,000	0.43	0.48
5,000	0.37	0.36
1,000	0.28	0.26
500	0.23	0.26

(a) Numerical values have been adopted from the work of Gershberg.<sup>46</sup>

of the  $^3P_J$  levels of neutral atomic oxygen. No collision strength data has been specifically tabulated, hence no direct comparison is possible between the values employed by Gershberg and the results of the current calculation. It appears that the above-described ratio was held fixed at 0.3 for all energies in the range considered, and  $E_0$  taken as approximately zero. It is difficult to state with certainty what value was given to  $\Delta E$ ; however, other calculations in the paper were performed with  $\Delta E = 1$  eV. The following threshold collision strengths for OIII have been calculated by Seaton:<sup>42</sup>

$$\begin{aligned}
 \Omega^{\circ}(^3P_1, ^3P_2) &= 0.96 \\
 \Omega^{\circ}(^3P_0, ^3P_2) &= 0.25 \\
 \Omega^{\circ}(^3P_0, ^3P_1) &= 0.31
 \end{aligned}
 \tag{18.3}$$

This information in conjunction with Eqs. (18.1) and (18.2) permits a crude estimate to be made of the corresponding spin-multiplet collision strengths for OI. The results of such a calculation are compared with the final, more rigorous, theoretical parameters in Table XXXIII.

The approximate method that has just been described should not be expected to yield more than order-of-magnitude accuracy. The chosen value of 0.3 for the  $\Omega(\text{OI}) / \times \Omega^{\circ}(\text{OIII})$  ratio is essentially a rough average of the numbers in Table XXXII. On the basis of this approximation alone, the collision strengths in Table XXXIII that have been calculated under this procedure can be expected to be underestimated by at least 60% for the highest electron energy considered, and considerably over-estimated for energies at the lower end of the range. Hence, accurate cross sections for the OI spin-multiplet transitions as calculated by the more rigorous methods of quantum mechanics have been considered necessary to substantiate the conclusions of Gershberg concerning the cooling of the interstellar media.

The calculated collision strengths for transitions between the spin-multiplets of OI are analyzed and summarized in Table XXXIII. The p, d and s (neglecting polarization) partial collision strengths originate from Tables XXXI, XVII, and XV, respectively. The analysis also includes results which are applicable when the polarization



TABLE XXXIII

FINAL SUMMARY OF THE COLLISION STRENGTHS FOR THE SPIN-MULTIPLETS OF OI

Electron Energy <sup>(a)</sup> (°K)	$\Omega_p$	$\Omega_d$	$\Omega_s$		$\Omega$		Estimated From [ $\frac{\Omega(OI)}{x \Omega^o(OIII)}$ ]
			No Polarization	With Polarization <sup>(b)</sup>	No Polarization	With Polarization <sup>(b)</sup>	
<u><math>\Omega(1,2):</math></u>							
10,000	0.271	0.0071	0.0085	0.040	0.287	0.318	0.138
5,000	0.131	0.0036	0.0046	0.028	0.139	0.163	0.072
1,000	0.0160	0.00068	0.00106	0.0085	0.0177	0.0252	0.0043
500	0.0055	0.00031	0.00058	0.0045	0.0064	0.0103	0.0011
<u><math>\Omega(0,2):</math></u>							
10,000	0.068	0.0032			0.071	0.071	0.036
5,000	0.033	0.0016			0.035	0.035	0.019
1,000	0.0032	0.00029			0.0035	0.0035	0.0011
500	0.00104	0.00012			0.0012	0.0012	0.0003
<u><math>\Omega(0,1):</math></u>							
10,000	0.101		0.0067	0.032	0.108	0.133	0.047
5,000	0.049		0.0037	0.022	0.053	0.071	0.023
1,000	0.0044		0.00081	0.0068	0.0052	0.0112	0.0014
500	0.0012		0.00042	0.0036	0.0016	0.0048	0.0003

(a) This value represents the electron energy when the atom is in the respective excited state.

(b) Presented for information and comparative purposes only. Refer to Chapter XVII for a discussion of the method of calculation and the expected accuracy.

interaction has been incorporated into the s-wave formalism in the manner described in Chapter XVII. For purposes of information and comparison only, the s-wave collision strengths calculated with the Zero Step-Function formula and a cut-off of 1.0 au. are included in the table. Reference should be made to Chapter XVII for the full details regarding the form of this correction, the sensitivity to the choice of the cut-off parameter, and remarks related to the reliability of the numbers presented. As has been specifically emphasized, a variation in the form of the polarization potential for regions interior to the atom can increase the tabulated s-wave collision strengths by over an order of magnitude, but no theoretical validity for a specific form has yet been established and it is difficult to justify a cut-off value less than 1.0 au. (approximately the peak in the wave function of the (2p) bound orbital for OI).

The comparison in Table XXXIII serves to illustrate that the influence of polarization is probably significant only at the lower part of the energy range considered where the final cross sections are sufficiently small to be of minor importance in physical applications. In the very extreme, the tabulated collision strengths should certainly display the correct orders of magnitude despite the inconsistencies of the treatment of polarization. In conclusion, despite the theoretical rigor, detail, thoroughness and numerical accuracy exhibited in the polarization-free calculations, it is impossible at the present time to substantiate any claim as to the final accuracy achieved for the entries in Table XXXIII. The latter must be delayed until more knowledge is acquired regarding the details of the polarization interaction.

A comparison of the final collision strengths with the values predicted by Gershberg<sup>46</sup> is also of considerable significance. In all cases considered, the parameters given in Table XXXIII exceed those estimated with the ratio method (although the correct orders of magnitude are correctly given by the approximate scheme). Hence, if other phases of the energy-loss calculations of Gershberg can be assumed to be correct, the present theoretical results certainly substantiate, and perhaps even strengthen, the conclusions derivable therefrom.

There is a slight inconsistency in Table XXXIII which deserves some comment at this point; this concerns the interpretation given to  $T_e(^{\circ}\text{K})$ . Throughout the detailed calculations,  $T_e$  has been taken as "(Electron Energy after Excitation) / (Boltzmann Constant)." However, Gershberg's quantity,  $\bar{\Omega}(\text{OIII})$  is meant to represent the corrected parameter after averaging over a Maxwellian distribution at  $T_e$ . Yet in the calculation of the given ratio, it appears that  $T_e$  of  $\Omega(\text{OI})$  was interpreted as in the present analysis. If such were the actual case, a direct comparison of the calculated and estimated collision strengths would be valid. On the other hand, if the ratio used in the approximate method is intended to imply an average for the OI parameter also, it would appear to be technically in error to derive quantitative conclusions from a comparison of the quantities presented in Table XXXIII. Assuming the latter to be true, if one further approximates the behavior of the calculated  $\Omega(\text{OI})$  collision strengths for the spin-multiplets in the neighborhood of a fixed  $T_e$  as essentially linear, the appropriate average reduces to  $\Omega(\text{OI})$  evaluated at  $T_e$ . As the curvature of  $\Omega$  vs Electron Energy is not excessive in this

portion of the spectrum, and in view of the other assumptions incorporated into the Gershberg estimate, further refinements are thought to be of limited usefulness, and the overall features of the comparison afforded by Table XXXIII should be considered as acceptable.

From a practical viewpoint, the increase in the OI cross sections due to polarization would be of doubtful value in this particular application, since the results for the other ions being considered also lack this correction. Hence, the role of neutral atomic oxygen in the cooling of the interstellar media (and perhaps in other astrophysical phenomena) is of sufficient comparable significance to warrant more than a mere casual consideration.

## APPENDIX I

### WAVE FUNCTIONS FOR THE ATOMIC SPIN-MULTIPLY STATES, AND FOR THE FREE ELECTRONS

The wave functions for atomic states within a  $(2p)^4$  configuration can be expressed in terms of basic antisymmetric determinantal functions of the form:

$$\frac{1}{\sqrt{4!}} \begin{vmatrix} u_1(1) & u_1(2) & \dots & u_1(4) \\ u_2(1) & & & \vdots \\ \vdots & & & \vdots \\ u_4(1) & \dots & & u_4(4) \end{vmatrix}, \quad (\text{I-1})$$

where  $u_i(j)$  is a one-electron orbital for the  $j$ -th electron. The present case is restricted to orbitals having the principal quantum number equal to 2,  $l = 1$ , and electron spin of  $1/2$ ; hence this labeling is unnecessary and the notation can be greatly simplified. Following Slater,<sup>58</sup> an example of such a determinantal function would be  $(1^+ 1^- 0^+ -1^+)$ , where  $1^+$  denotes an orbital for electron (1) having  $m_l = 1$ ,  $m_s = +1/2$ ; the position of the orbital in the sequence indicates the labeling of the associated electron.

For the  $^3P$  multiplet of the above configuration, Slater gives for the wave function having  $M_L = 0$ ,  $M_S = 0$ , the following

expression:

$$^3P = \frac{1}{\sqrt{2}} (\psi_1 + \psi_2) \quad (\text{I-2})$$

where

$$\begin{aligned} \psi_1 &= (1^- 0^+ 0^- -1^+) \\ \psi_2 &= (1^+ 0^+ 0^- -1^-). \end{aligned} \quad (\text{I-3})$$

The step-up and step-down operators can be applied to this  $M_L = 0$ ,  $M_S = 0$  wave function to yield the following wave functions for the different states of  $^3P$ :

$M_L$	$M_S$	Wave Function
1	1	$-(1^+ 1^- 0^+ -1^+)$
1	0	$-(1/\sqrt{2}) [(1^+ 1^- 0^- -1^+) + (1^+ 1^- 0^+ -1^-)]$
1	-1	$-(1^+ 1^- 0^- -1^-)$
0	1	$(1^+ 0^+ 0^- -1^+)$
0	0	$(1/\sqrt{2}) [(1^- 0^+ 0^- -1^+) + (1^+ 0^+ 0^- -1^-)]$
0	-1	$(1^- 0^+ 0^- -1^-)$
-1	1	$-(1^+ 0^+ -1^+ -1^-)$
-1	0	$-(1/\sqrt{2}) [(1^- 0^+ -1^+ -1^-) + (1^+ 0^- -1^+ -1^-)]$
-1	-1	$-(1^- 0^- -1^+ -1^-)$

(I-4)

The  $^3P$  multiplet of the  $(2p)^4$  configuration has  $L = 1$ ,  $S = 1$ . Under strong spin-orbit coupling (as is true for OI), the different states of this multiplet are better described by a representation in which the total atomic electronic angular momentum,  $\vec{J} = \vec{L} + \vec{S}$ , is diagonal. The basis functions for such a representation are formed

from linear combinations of the above functions using the Clebsch-Gordan (or vector-coupling) coefficients.<sup>53</sup> There are three spin-multiplets thus formed which correspond to  $J = 2, 1, 0$ ; the wave functions for the individual states are given below.

$\underline{J}$	$\underline{M}$	$\underline{\psi_J^M}$	
2	2	$-(1^+1^-0^+1^+)$	
	1	$(1/\sqrt{2}) \left[ (1^+0^+0^-1^+) - (1/\sqrt{2}) [(1^+1^-0^-1^+) + (1^+1^-0^+1^-)] \right]$	
	0	$(1/\sqrt{6}) \left[ -(1^+0^+1^+1^-) + \sqrt{2} [(1^-0^+0^-1^+) + (1^+0^+0^-1^-)] - (1^+1^-0^-1^-) \right]$	
	-1	$(1/\sqrt{2}) \left[ (1^-0^+0^-1^-) - (1/\sqrt{2}) [(1^-0^+1^+1^-) + (1^+0^-1^+1^-)] \right]$	
	-2	$-(1^-0^-1^+1^-)$	(I-5)
1	1	$-(1/\sqrt{2}) \left[ (1^+0^+0^-1^+) + (1/\sqrt{2}) [(1^+1^-0^-1^+) + (1^+1^-0^+1^-)] \right]$	
	0	$(1/\sqrt{2}) \left[ (1^+0^+1^+1^-) - (1^+1^-0^-1^-) \right]$	
	-1	$(1/\sqrt{2}) \left[ (1^-0^+0^-1^-) + (1/\sqrt{2}) [(1^-0^+1^+1^-) + (1^+0^-1^+1^-)] \right]$	
0	0	$-(1/\sqrt{3}) \left[ (1^+0^+1^+1^-) + (1^+1^-0^-1^-) + (1/\sqrt{2}) [(1^-0^+0^-1^+) + (1^+0^+0^-1^-)] \right]$	

It should be noted that the different states above are characterized by the complete set of quantum numbers ( $J, M, L = 1, S = 1, \ell_i = 1, s_i = 1/2$ ), with  $i = 1, \dots, 4$ .

The  $(1s)^2 (2s)^2$  electrons of OI are incorporated into the above formulas by the inclusion of 4 additional rows and columns in each of the basic determinants; the new entries for each of the determinants are the same throughout the listing. In the formal analysis of the scattering problem, these core electrons were originally omitted, and correction terms to the equations were included later in the work.

In the general formulation, the wave function which describes the motion of the free electron was expanded in terms of partial waves. A component partial wave may be written as a simple product of spatial and spin wave functions (for instance,  $\phi_l^{m_l}(+)$ , with the quantum numbers being the relative orbital angular momentum  $l$ , spin  $s = 1/2$ ,  $m_l$ ,  $m_s = +1/2$ ), or alternatively as a linear combination of these simple products formed with the Clebsch-Gordan coefficients under the vector-coupling scheme  $\vec{j} = \vec{l} + \vec{s}$ . The latter procedure has been adopted in the present work; the resultant basis functions have been denoted by  $\Phi_j^{mj}(l)$  and have the complete set of quantum numbers ( $j$ ,  $m_j$ ,  $l$ ,  $s = 1/2$ ). The members of this set which are of interest here are listed below:

$l = 0$ :

$$\Phi_{1/2}^{1/2}(0) = \phi_0^0(+)$$

$$\Phi_{1/2}^{-1/2}(0) = \phi_0^0(-)$$

$l = 1$ :

$$\Phi_{3/2}^{3/2}(1) = \phi_1^1(+)$$

$$\Phi_{3/2}^{1/2}(1) = (1/\sqrt{3}) [\phi_1^1(-) + \sqrt{2} \phi_1^0(+)]$$

$$\Phi_{3/2}^{-1/2}(1) = (1/\sqrt{3}) [\phi_1^{-1}(+) + \sqrt{2} \phi_1^0(-)]$$



$\ell = 1:$

$$\begin{aligned}\Phi_{3/2}^{-3/2}(1) &= \phi_1^{-1}(-) \\ \Phi_{1/2}^{1/2}(1) &= (1/\sqrt{3}) [\sqrt{2} \phi_1^1(-) - \phi_1^0(+)] \\ \Phi_{1/2}^{-1/2}(1) &= (1/\sqrt{3}) [\phi_1^0(-) - \sqrt{2} \phi_1^{-1}(+)]\end{aligned}$$

$\ell = 2:$

$$\begin{aligned}\Phi_{5/2}^{5/2}(2) &= \phi_2^2(+) \\ \Phi_{5/2}^{3/2}(2) &= (1/\sqrt{5}) [2 \phi_2^1(+) + \phi_2^2(-)] \\ \Phi_{5/2}^{1/2}(2) &= (1/\sqrt{5}) [\sqrt{3} \phi_2^0(+) + \sqrt{2} \phi_2^1(-)] \\ \Phi_{5/2}^{-1/2}(2) &= (1/\sqrt{5}) [\sqrt{2} \phi_2^{-1}(+) + \sqrt{3} \phi_2^0(-)] \\ \Phi_{5/2}^{-3/2}(2) &= (1/\sqrt{5}) [\phi_2^{-2}(+) + 2 \phi_2^{-1}(-)] \\ \Phi_{5/2}^{-5/2}(2) &= \phi_2^{-2}(-) \\ \Phi_{3/2}^{3/2}(2) &= (1/\sqrt{5}) [-\phi_2^1(+) + 2 \phi_2^2(-)] \\ \Phi_{3/2}^{1/2}(2) &= (1/\sqrt{5}) [-\sqrt{2} \phi_2^0(+) + \sqrt{3} \phi_2^1(-)] \\ \Phi_{3/2}^{-1/2}(2) &= (1/\sqrt{5}) [-\sqrt{3} \phi_2^{-1}(+) + \sqrt{2} \phi_2^0(-)] \\ \Phi_{3/2}^{-3/2}(2) &= (1/\sqrt{5}) [-2 \phi_2^{-2}(+) + \phi_2^{-1}(-)]\end{aligned}$$

## APPENDIX II

### ATOMIC RADIAL WAVE FUNCTIONS FOR OI

The atomic radial wave functions adopted for the numerical calculations were the Analytic SCF functions determined for OI by Clementi, Roothaan, and Yoshimine.<sup>54</sup> These authors performed an expansion in terms of Slater-Type-Orbitals with integer principal quantum numbers but flexible exponents, and with the variational principle have obtained functions which are believed to represent to at least three decimal places the solutions of the Hartree-Fock integro-differential equations. For an occupied orbital, ( $S_1$ ,  $S_2$ , or P), this expansion has the form:

$$\sum_k \frac{a_k (2\sigma_k)^{n_k+1/2}}{\sqrt{(2n_k)!}} r^{n_k} e^{-\sigma_k r} \quad (\text{II-1})$$

The coefficients required for the  $^3P$  ground state of OI are given below:

	<u>a</u>	<u><math>\sigma</math></u>	<u>n</u>	<u>Energy(a.u.)</u>
$S_1$	0.93835	7.6160	1	-20.66864
	0.03825	13.3243	1	
	-0.00097	1.7582	2	
	0.00439	2.5627	2	
	-0.00829	4.2832	2	
	0.04171	5.9445	2	
$S_2$	-0.21979	7.6160	1	-1.24428
	-0.00573	13.3243	1	
	0.42123	1.7582	2	
	0.54368	2.5627	2	
	0.23061	4.2832	2	
	-0.17856	5.9445	2	
P	0.16371	1.1536	2	-0.63186
	0.57600	1.7960	2	
	0.33392	3.4379	2	
	0.01495	7.9070	2	

The entry in the last column is the energy of an electron in the specified occupied orbital, and is related to  $\epsilon$  in the differential equations. (  $\epsilon = -2$  Energy.) The orthogonality of the  $S_1$  and  $S_2$  functions was verified by direct numerical integration.

In order to obtain solutions of the scattering radial differential equations, it is necessary to examine the behavior of the atomic wave functions for small values of  $r$ . These expansions near the origin

may be written:

$$P \sim \frac{2}{\sqrt{3}} \sum_k a_k \sigma_k^{5/2} [r^2 - \sigma_k r^3 + \dots] \quad (\text{II-2})$$

$$S(1 \text{ or } 2) \sim C_1 r + C_2 r^2 \quad (\text{II-3})$$

where

$$C_1 = 2 \sum_{k=1,2} a_k \sigma_k^{3/2} \quad (\text{II-4})$$

$$C_2 = -2 \sum_{k=1,2} a_k \sigma_k^{5/2} + \frac{2}{\sqrt{3}} \sum_{k=3}^6 a_k \sigma_k^{5/2}. \quad (\text{II-5})$$

The numerical values for the coefficients in the small value S-expansions were determined separately from the major programs and were inserted as constants. These numbers are:

$$S_1: C_1 = 43.1651$$

$$C_2 = -346.1498$$

$$S_2: C_1 = -9.7965$$

$$C_2 = 78.7317$$

# APPENDIX III

## POTENTIAL FUNCTIONS FOR OI

With the analytic wave functions described in Appendix II, the potential integrals are expressible in the following form:

$$y_0( , ) = \sum_{i,j} \frac{a_i a_j (2\sigma_i)^{n_i+1/2} (2\sigma_j)^{n_j+1/2}}{\sqrt{(2n_i)! (2n_j)!}} \left[ \frac{(m_{ij})!}{\alpha_{ij}^{m_{ij}+1}} \right] \times \left[ \frac{1}{r} - e^{-\alpha_{ij}r} \left[ \frac{1}{r} + \sum_{v=1}^{m_{ij}-1} \frac{(m_{ij}-v)}{m_{ij}} \alpha_{ij}^v \frac{r^{v-1}}{v!} \right] \right] \quad (\text{III-1})$$

$$y_2(\text{PP}) = \frac{4}{3} \sum_{ij} \frac{a_i a_j (\sigma_i \sigma_j)^{5/2}}{r^3 \alpha_{ij}^7} \left[ 720 - e^{-\alpha_{ij}r} [ 720 + 720 \alpha_{ij}r + 360 (\alpha_{ij}r)^2 + 120 (\alpha_{ij}r)^3 + 30 (\alpha_{ij}r)^4 + 5 (\alpha_{ij}r)^5 ] \right] \quad (\text{III-2})$$

where  $a_i$ ,  $\sigma_i$  and  $n_i$  refer to the constants in the appropriate wave function, and

$$m_{ij} = n_i + n_j, \quad \alpha_{ij} = (\sigma_i + \sigma_j). \quad (\text{III-3})$$

If the corresponding wave function has been properly normalized, the leading term in Eq. (III-1) should reduce to  $1/r$ . The only serious

discrepancy arose for the  $S_1$  wave function; the normalization yielded 1.0186 and corrections were applied to this potential function. The error was not regarded as serious since the (1s) electrons are believed to have an almost insignificant effect upon the calculated cross sections. Numerical calculations were performed for the above potential functions to allow their expression in the forms described in Chapter X.

The behavior of the functions,  $y_0(S_1S_1)$ ,  $y_0(S_2S_2)$  and  $y_0(PP)$ , near the origin was examined in greater detail. As  $r \rightarrow 0$ , these functions approach constant values; in initiating the solutions for the radial differential equations, the magnitudes of these constants were found to be of no importance as two terms of the scattering-function-small  $r$ -expansions were found sufficient for reliable results. In addition, at  $r = .001$  where the solution begins, accurate values for the potential can be obtained with the form described in Chapter X.

The  $y_2(PP)$  function has no effect upon the starting solution for the differential equation, however, where required in certain integrals, the form of this function as given by Eq. (10.6) is grossly inaccurate for small values of  $r$ . For  $r \leq .1$ , it was found necessary to adopt the following expansion (constants are for the  $^3P$  function):

$$y_2(PP) = 4.974 r^2 - 76.441 r^4 \quad (r \leq .1) \quad . \quad (III-4)$$

## APPENDIX IV

### HARTREE-FOCK DIFFERENTIAL EQUATIONS FOR BOUND-STATE FUNCTIONS OF OI

The following differential equations for the  $S_1$ ,  $S_2$  and  $P$  radial functions for the  $^3P$  multiplet in the  $(1s)^2 (2s)^2 (2p)^4$  ground configuration of OI are adopted from Slater,<sup>58</sup> with a slight change of the notation to conform with that chosen in this work. These equations are required for the evaluation of certain parameters which appear in the scattering equations for the  $s$ - and  $p$ -waves.

1.  $(1s)$  orbital:

$$\left[ -\frac{1}{2} \frac{d^2}{dr^2} - \frac{Z}{r} + y_0(S_1 S_1) + 2y_0(S_2 S_2) + 4y_0(PP) + \frac{\epsilon_{1s}}{2} \right] S_1$$

$$- y_0(S_1 S_2) S_2 - \frac{2}{3} y_1(S_1 P) P = 0. \quad (\text{IV-1})$$

2.  $(2s)$  orbital:

$$\left[ -\frac{1}{2} \frac{d^2}{dr^2} - \frac{Z}{r} + y_0(S_2 S_2) + 2y_0(S_1 S_1) + 4y_0(PP) + \frac{\epsilon_{2s}}{2} \right] S_2$$

$$- y_0(S_1 S_2) S_1 - \frac{2}{3} y_1(S_2 P) P = 0. \quad (\text{IV-2})$$

3. (2p) orbital:

$$\left[ -\frac{1}{2} \frac{d^2}{dr^2} - \frac{Z}{r} + \frac{1}{r^2} + 2y_0(S_1S_1) + 2y_0(S_2S_2) + 3y_0(PP) - \frac{3}{10} y_2(PP) + \frac{\epsilon_{2p}}{2} \right] P$$

$$-\frac{1}{3} y_1(S_1P)S_1 - \frac{1}{3} y_1(S_2P)S_2 = 0. \quad (IV-3)$$



## BIBLIOGRAPHY

1. H. Ramien, A. Physik 70, 353 (1931).
2. W. Harries, Z. Physik 42, 26 (1927).
3. G. J. Schulz, Phys. Rev. 135, A988 (1964).
4. G. J. Schulz, Phys. Rev. 116, 1141 (1959).
5. G. J. Schulz, Phys. Rev. 125, 229 (1962).
6. J. C. Y. Chen and J. L. Magee, J. Chem. Phys. 36, 1407 (1962).
7. A. G. Engelhardt and A. V. Phelps, Phys. Rev. 131, 2115 (1963).
8. A. G. Engelhardt, A. V. Phelps and C. G. Risk, Phys. Rev. 135, A1566 (1964).
9. Ta-You Wu, Phys. Rev. 71, 111 (1947).
10. P. M. Morse, Phys. Rev. 90, 51 (1953).
11. T. R. Carson, Proc. Phys. Soc. (London) A67, 909 (1954).
12. N. F. Mott and H. S. W. Massey, Theory of Atomic Collisions (Oxford University Press, London, England, 1949), 2nd ed.
13. E. Ishiguro, T. Arai, M. Mizushima and M. Kotani, Proc. Phys. Soc. (London) A65, 178 (1952).
14. W. Kolos and C. C. J. Roothaan, Rev. Mod. Phys. 32, 219 (1960).
15. D. R. Bates, Proc. Roy. Soc. (London) 188, 350 (1947).
16. B. H. Bransden, A. Dalgarno, T. L. John and M. J. Seaton, Proc. Phys. Soc. 71, 877 (1958).
17. L. B. Robinson, Phys. Rev. 127, 2076 (1962).
18. A. S. Douglas, Proc. Camb. Phil. Soc. 52, 687 (1956).
19. K. Takayanagi, J. Phys. Soc. Japan 20, 562 (1965).

20. K. Takayanagi and S. Geltman, Phys. Rev. 138, A1003 (1965).
21. E. Treffitz and L. Biermann, Z. Astrophys. 30, 275 (1952).
22. L. Biermann, Z. Astrophys. 22, 157 (1943).
23. C. J. Lenander, Phys. Rev. 142, 1 (1966).
24. W. R. Garrett and R. A. Mann, Phys. Rev. 130, 658 (1963).
25. W. R. Garrett and R. A. Mann, Phys. Rev. 135, A580 (1964).
26. H. T. Jackson, Jr. and W. R. Garrett, U of Alabama Res. Inst. Rept. 32, 1 (1965).
27. D. M. Golden and B. Crawford, Jr., J. Chem. Phys. 36, 1654 (1962).
28. N. F. Ramsey, Molecular Beams (Oxford University Press, Oxford, England, 1956), p. 230.
29. H. S. W. Massey and E. H. S. Burhop, Electronic and Ionic Impact Phenomena (Clarendon Press, Oxford, England, 1952), p. 206.
30. H. S. W. Massey, Trans. Faraday Soc. 31, 556 (1935).
31. R. Haas, Z. Physik 148, 177 (1957).
32. E. J. Stansbury, M. F. Crawford and H. L. Welsh, Can. J. Phys. 31, 954 (1953).
33. L. A. Gribov and V. N. Smirnov, Usp. Fiz. Nauk 75, 527 (1961) [English transl.: Soviet Phys. - Usp. 4, 919 (1961)] .
34. A. Temkin and J. C. Lamkin, Phys. Rev. 121, 788 (1961).
35. A. Temkin, Phys. Rev. 116, 358 (1959).
36. A. Temkin, Phys. Rev. 107, 1004 (1957).
37. J. N. Bardsley, A. Herzenberg and F. Mandl, IVth Intern. Conf. Phys. Electronic and Atomic Collisions, in Quebec, Canada, Aug. 2-6 (1965).
38. T. Yamanouchi, Y. Inui and A. Amemiya, Proc. Phys. Math. Soc. Japan 22, 847 (1940).
39. D. R. Bates, A. Fundaminsky, J. W. Leech and H. S. W. Massey, Phil. Trans. A243, 93 (1950).
40. M. J. Seaton, Phil. Trans. A245, 469 (1953).

41. M. J. Seaton, Proc. Roy. Soc. A218, 400 (1953).
42. M. J. Seaton, Proc. Roy. Soc. A231, 37 (1955).
43. M. H. Hebb and D. H. Menzel, Astrophys. J. 92, 408 (1940).
44. M. J. Seaton, Ann. d'Astrophys. 18, 188 (1955).
45. M. J. Seaton, Rev. Mod. Phys. 30, 979 (1958).
46. R. E. Gershberg, Repts. Crimean Astrophys. Obs. 26, 324 (1961)  
(Russian).
47. H. S. W. Massey, Negative Ions (Cambridge University Press,  
London, England, 1950), 2nd Ed.
48. D. R. Bates, Proc. R. Irish Acad. A51, 151 (1947).
49. D. R. Bates and H. S. W. Massey, Proc. Roy. Soc. A192, 1 (1947).
50. J. W. Cooper and J. B. Martin, Phys. Rev. 123, 1482 (1962).
51. M. M. Klein and K. A. Brueckner, Phys. Rev. 111, 1115 (1958).
52. L. B. Robinson, Phys. Rev. 105, 922 (1957).
53. E. U. Condon and G. H. Shortley, The Theory of Atomic Spectra  
(Cambridge University Press, London, England, 1957).
54. E. Clementi, C. C. J. Roothaan and M. Yoshimine, Phys. Rev.  
127, 1618 (1962).
55. D. R. Hartree, The Calculation of Atomic Structures (John Wiley  
and Sons, New York, 1957).
56. Ta-You Wu and T. Ohmura, The Quantum Theory of Scattering  
(Prentice-Hall Inc., New Jersey, 1962).
57. D. R. Hartree, Numerical Analysis (Clarendon Press, Oxford,  
England, 1952).
58. J. C. Slater, Quantum Theory of Atomic Structure II (McGraw-Hill,  
New York, 1960).
59. R. A. Alpher and D. R. White, Phys. Fluids 2, 153 (1959).